The 2014 stock assessment of paua (*Haliotis iris*) for Chalky and South Coast in PAU 5A

D. Fu

Contents

EXECUTIVE SUMMARY

Fu, D. (2015). The 2014 stock assessment of paua (*Haliotis iris*) for Chalky and South Coast in PAU 5A.

This report summarises the stock assessment for Chalky and South Coast in PAU 5A which includes fishery data up to the 2013–14 fishing year. The report describes the model structure and output, including current and projected stock status. The stock assessment is implemented as a length-based Bayesian estimation model, with point estimates of parameters based on the mode of the joint posterior distribution, and uncertainty of model estimates investigated using the marginal posterior distributions generated from Markov chain-Monte Carlo simulation.

The data fitted in the assessment model were: (1) a standardised CPUE series based on the early CELR data, (2) a standardised CPUE series based on recent PCELR data, (3) commercial catch sampling length frequency series (CSLF), (4) tag-recapture length increment data, and (5) maturity-at-length data. The research diver survey data was not included in the base case because there is concern that the data are not a reliable index of abundance.

The base case model (1.5) estimated that the spawning stock population in 2014 (B_{2014}) was 41% (33–50%) of B_0. The model projection made for three years assuming current catch levels and using recruitment re-sampled from the recent model estimates, suggested that the spawning stock biomass will increase to 43% (32–56%) B_0 over the next three years. The projection also indicated that the probability of the spawning stock biomass being above the target (40% B_0) will increase from 55% in 2014 to 67% in 2016, and that the stock status is very unlikely to be below the soft (20% B_0) and hard limits (10% B_0)

The assessment model indicated that the stock status was above the target level and that the estimated stock abundance has been increasing over recent years, corroborating the observed trend in the fishery. Most data sets used in the model were collected from a wide range of areas and are believed to be representative of the stock. However, the pre-2002 catch sampling length frequency data were considered to be unrepresentative of the fishery due to the small sample size and were not included in the base case. There is also large uncertainty in the estimates of commercial catch history before 1995–96. Estimated stock status was 34% and 46% B_0 respectively, when the lower bound and upper bound of the commercial catch history estimates were used.

1. INTRODUCTION

1.1 Overview

This report summarises the stock assessment for Chalky and South Coast in PAU 5A (Figure 1) with the inclusion of data to the end of 2013–14 fishing year. The report describes the model structure and output, including current and projected stock status. The stock assessment is conducted with the length-based Bayesian estimation model first used in 1999 for PAU 5B (Breen et al. 2000a) with revisions made for subsequent assessments in PAU 5B (Breen et al. 2000b, Breen & Smith 2008a, Fu 2014a), PAU 4 (Breen & Kim 2004a), PAU 5A (Breen & Kim 2004b, Breen & Kim 2007, Fu & Mackenzie 2010a, b), PAU 5D (Breen et al. 2000a, Breen & Kim 2007, Fu 2013), PAU 7 (Andrew et al. 2000, Breen et al. 2001, Breen & Kim 2003, 2005, McKenzie & Smith 2009a, Fu 2012), and PAU 3 (Fu 2014b). PAU 5A was last assessed in 2010 (Fu & Mackenzie 2010a, b). The model was published by Breen et al. (2003).

Earlier assessments for PAU 5A (Breen & Kim 2004b, 2007) were conducted assuming a homogeneous area covering the whole of PAU 5A. There were concerns about the applicability of the assessment to the entire QMA given the differences in exploitation histories between subareas, although there was a general agreement that biomass decline had occurred in the southern region of the stock over recent years. Before 2005–06 fishery-independent surveys were conducted only in the area from Dusky south, which has accounted for about 60% of the catch over the last four years. Recent studies suggested that trends in the changes of abundance may have varied between subareas within PAU 5A (Cordue 2009). Since 1 October 2006, a voluntary subdivision was agreed which divided PAU 5A into six fishing management zones, based on the research strata, and a proportion of the total annual catch entitlements (ACE) was allocated to each zone. Each of the management zones has a voluntary harvest cap and minimum harvest length in place.

Based on differences in exploitation histories and management initiatives, a decision was made in 2010 to split the QMA into a southern area including Chalky and South Coast, and a northern area, including Milford, George, Central, and Dusky, and to conduct separate assessments for the southern and northern areas (Fu et al. 2010).

This report summarises the stock assessment for the southern area of PAU 5A (Chalky and South Coast) and includes fishery data up to the 2013–14 fishing year. The five sets of data used in the assessment were: (1) a standardised CPUE series covering 1990–2001 based on CELR data (CPUE), (2) a standardised CPUE series covering 2002–2014 based on PCELR data (PCPUE), (3) a commercial catch sampling length frequency series (CSLF), (4) tag-recapture length increment data, and (5) maturity-at-length data. Catch history was an input to the model, encompassing commercial, recreational, customary, and illegal catch. Another document describes the datasets that are used in the stock assessment and the updates that were made for the previous assessment (Fu et al. 2015).

There have been concerns over the research diver survey methodology and its usefulness in providing relative abundance indices (Cordue 2009, Haist 2010). In the most recent stock assessments of PAU 5B (Fu 2014a) and PAU 5D (Fu 2013) the research diver survey indices (RDSI) and research diver survey length frequency (RDLF) data were not included in the base case. The same decision has been made here: the RDSI and RDLF were excluded from the base case but were included as a sensitivity trial.

The assessment was made in several steps. First, the model was fitted to the data with parameters estimated at the mode of their joint posterior distribution (MPD). Next, from the resulting fit, Markov chain-Monte Carlo (MCMC) simulations were made to obtain a large set of samples from the joint posterior distribution. From this set of samples, forward projections were made with a set of agreed

indicators obtained. Sensitivity trials were explored by comparing MPD fits made with alternative model assumptions.

This document describes the model structure and assumptions, the fits to the data, estimates of parameters and indicators, and projection results. This report fulfils part of Objective 1 "Undertake a stock assessment for PAU 5A, using a length-based Bayesian model" of the Ministry for Primary Industries Project PAU201401.

1.2 Description of the fishery

The paua fishery was summarised by Schiel (1992), and in numerous previous assessment documents (e.g., Schiel 1989, McShane et al. 1994, 1996, Breen et al. 2000a, 2000b, 2001, Breen & Kim 2003, 2004a, 2004b, 2007, Breen & Smith 2008b, McKenzie & Smith 2009b, Fu et al. 2010, 2012, 2013, 2014a,b). A summary of the PAU 5A fishery up to the 2013–14 fishing year is presented in Fu et al. (2015).

2. MODEL

This section gives an overview of the model used for the stock assessment of PAU 5A in 2014; for full description see Breen et al. (2003). The model was developed for use in PAU 5B in 1999 and has been revised each year for subsequent assessments, in many cases echoing changes made to the rock lobster assessment model (Kim et al. 2004), which is a similar but more complex length-based Bayesian model. The last revision made to the model was in 2013 for the assessment of PAU 5B (Fu 2014a).

2.1 Changes to the 2010 assessment model of PAU 5A

One minor change was made to allow an annual step change in selectivity, echoing the increase of minimum harvest size from 125 mm to 130 mm since 2007:

$$V_k^{t,s} = \frac{1}{1 + 19^{-\left(\left(l_k - D_{50} - D_t^a D^s\right)/D_{95-50}\right)}} \quad \text{(See Section 2.2.11)}$$

In addition, the 2010 assessment for PAU 5A, Fu & McKenzie (2010a, 2010b) reported B_{init}; the spawning stock biomass at the end of the initialisation phase (the equilibrium biomass assuming that recruitment is equal to base recruitment and with no fishing), and B_0; the equilibrium spawning stock biomass assuming that recruitment is equal to the average recruitment from the period for which recruitment deviations were estimated (B_0 normally differs from B_{init}). In this assessment a constraint was placed on the recruitment deviations so that their average is 1 for the period in which they are estimated, based on the parameterisation of Bull et al. (2012). This ensures that the average recruitment for the period in which they are estimated (e.g. 1990–2010) is close to R_0, and as a result B_{init} will be close to B_0.

2.2 Model description

The model partitioned the paua stock into a single sex population, with length classes from 70 mm to 170 mm, in groups of 2 mm (i.e., from 70 to under 72 mm, 72 mm to under 74 mm, etc.). The largest length bin is well above the maximum size observed. The stock was assumed to reside in a single,

homogeneous area. The partition accounted for numbers of paua by length class within an annual cycle, where movement between length classes was determined by the growth parameters. Paua entered the partition following recruitment and were removed by natural mortality and fishing mortality.

The model annual cycle was based on the fishing year. Note that model references to "year" within this paper refer to the fishing year, and are labelled as the most recent calendar year, i.e., the fishing year 1998–99 is referred to as "1999" throughout. References to calendar years are denoted specifically.

The models were run for the years 1965–2014. The model assumes one time step within an annual cycle. Catches were collated for 1974–2014, and were assumed to increase linearly between 1965 and 1973 from 0 to the 1974 catch level. Catches included commercial, recreational, customary, and illegal catch, and all catches occurred at the same time step.

Recruitment was assumed to take place at the beginning of the annual cycle, and length at recruitment was defined by a uniform distribution with a range between 70 and 80 mm. Recruitment deviations were assumed known and equal to 1 for the years up to 1980. This was ten years before the length data were available (loosely based on the approximate time taken for recruited paua to appear at the right hand end of the length distribution). The stock-recruitment relationship is unknown for paua, but is likely to be weak (Shepherd et al. 2001). A relationship may exist on small scales, but may not be apparent when large-scale data are modelled (Breen et al. 2003). No explicit stock-recruitment relationship has been modelled in previous assessments. The Shellfish Working Group suggested assuming a Beverton-Holt stock-recruitment relationship with a steepness of 0.75 for the base case.

Maturity does not feature in the population partition. The model estimated proportions mature with the inclusion of length-at-maturity data. Growth and natural mortalities were also estimated within the model.

The models used two selectivities: the commercial fishing selectivity and research diver survey selectivity — both assumed to follow a logistic curve (see later) and then remain constant.

The model is implemented in AD Model Builder™ (Otter Research Ltd., http://otter-rsch.com/admodel.htm) version 9.0.65, compiled with the MinGW 4.50 compiler.

The seven sets of data collated for the assessment model were: (1) a standardised CPUE series based on CELR data (2) a standardised CPUE series based on PCELR data (3) a standardised research diver survey index (RDSI) (4) a research diver survey proportions-at-lengths series (5) a commercial catch sampling length frequency series (6) tag-recapture length increment data and (7) maturity-at-length data (see Fu et al. 2015).

2.2.1 Estimated parameters

Parameters estimated by the model are as follows. The parameter vector is referred to collectively as θ.

$\ln(R0)$	natural logarithm of base recruitment
M	instantaneous rate of natural mortality
g_1	expected annual growth increment at length L_1
g_2	expected annual growth increment at length L_2
ϕ	CV of the expected growth increment
α	parameter that defines the variance as a function of growth increment

β	parameter that defines the variance as a function of growth increment
Δ_{max}	maximum growth increment
l_{50}^g	length at which the annual increment is half the maximum
l_{95}^g	length at which the annual increment is 95% of the maximum
l_{95-50}^g	difference between l_{50}^g and l_{95}^g
q^I	scalar between recruited biomass and CPUE
q^{I_2}	scalar between recruited biomass and PCPUE
q^J	scalar between numbers and the RDSI
L_{50}	length at which maturity is 50%
L_{95-50}	interval between L_{50} and L_{95}
T_{50}	length at which research diver selectivity is 50%
T_{95-50}	difference between T_{50} and T_{95}
D_{50}	length at which commercial diver selectivity is 50%
D_{95-50}	difference between D_{50} and D_{95}
D^s	change in commercial diver selectivity for one unit change of MHS
$\widetilde{\sigma}$	common component of error
h	shape of CPUE versus biomass relation
ε	vector of annual recruitment deviations, estimated from 1977 to 2013
H	steepness of the Beverton-Holt stock-recruitment relationship

2.2.2 Constants

l_k	length of a paua at the midpoint of the kth length class (l_k for class 1 is 71 mm, for class 2 is 73 mm and so on)
σ_{MIN}	minimum standard deviation of the expected growth increment (assumed to be 1 mm)
σ_{obs}	standard deviation of the observation error around the growth increment (assumed to be 0.25 mm)
MLS_t	minimum legal size in year t (assumed to be 125 mm for all years)
$P_{k,t}$	a switch based on whether abalone in the kth length class in year t are above the minimum legal size (MLS) ($P_{k,t} = 1$) or below ($P_{k,t} = 0$)
a, b	constants for the length-weight relation, taken from Schiel & Breen (1991) (2.592E-08 and 3.322 respectively, giving weight in kilograms)
w_k	the weight of an abalone at length l_k
ϖ^I	relative weight assigned to the CPUE dataset. This and the following relative weights were varied between runs to find a basecase with balanced residuals
ϖ^{I2}	relative weight assigned to the PCPUE dataset.
ϖ^J	relative weight assigned to the RDSI dataset
ϖ^r	relative weight assigned to RDLF dataset
ϖ^s	relative weight assigned to CSLF dataset
ϖ^{mat}	relative weight assigned to maturity-at-length data

ϖ^{tag}	relative weight assigned to tag-recapture data
κ_t^s	normalised square root of the number of paua measured greater than 113 mm in CSLF records for each year, normalised by the lowest year
κ_t^r	normalised square root of the number of paua measured greater than 89 mm in RDLF records for each year, normalised by the lowest year
U^{max}	exploitation rate above which a limiting function was invoked (0.80 for the base case)
μ_M	mean of the prior distribution for M, based on a literature review by Shepherd & Breen (1992)
σ_M	assumed standard deviation of the prior distribution for M
σ_ε	assumed standard deviation of recruitment deviations in log space (part of the prior for recruitment deviations)
n_ε	number of recruitment deviations
L_1	length associated with g_1 (75 mm)
L_2	length associated with g_2 (120 mm)
D_t^a	Change in Minimum Harvest Size (MHS) in year t, (exogenous variable associated with the change in commercial diver selectivity in year t)

2.2.3 Observations

C_t	observed catch in year t
I_t	standardised CPUE in year t
$I2_t$	standardised PCPUE in year t
σ_t^I	standard deviation of the estimate of observed CPUE in year t, obtained from the standardisation model
cv_t^I	CV of the estimate of observed CPUE in year t, obtained from the standardisation model
σ_t^{I2}	standard deviation of the estimate of observed PCPUE in year t, obtained from the standardisation model
cv_t^{I2}	CV of the estimate of observed PCPUE in year t, obtained from the standardisation model
J_t	standardised RDSI in year t
σ_t^J	the standard deviation of the estimate of RDSI in year t, obtained from the standardisation model
cv_t^J	CV of the estimate of observed RDSI in year t, obtained from the standardisation model
$p_{k,t}^r$	observed proportion in the kth length class in year t in RDLF
$p_{k,t}^s$	observed proportion in the kth length class in year t in CSLF
l_j	initial length for the jth tag-recapture record
d_j	observed length increment of the jth tag-recapture record
Δt_j	time at liberty for the jth tag-recapture record
p_k^{mat}	observed proportion mature in the kth length class in the maturity dataset

2.2.4 Derived variables

$R0$	base number of annual recruits
$N_{k,t}$	number of paua in the kth length class at the start of year t
$N_{k,t+0.5}$	number of paua in the kth length class in the mid-season of year t
$R_{k,t}$	recruits to the model in the kth length class in year t
g_k	expected annual growth increment for paua in the kth length class
σ^{g_k}	standard deviation of the expected growth increment for paua in the kth length class, used in calculating $\mathbf{G}$
$\mathbf{G}$	growth transition matrix
B_t	spawning stock biomass at the beginning of year t
$B_{t+0.5}$	spawning stock biomass in the mid-season of year t
B_0	equilibrium spawning stock biomass assuming no fishing and average recruitment from the period in which recruitment deviations were estimated.
B_{init}	spawning stock biomass at the end of initialisation phase (or B_{1964})
B_t^r	biomass of paua above the MLS at the beginning of year t
$B_{t+0.5}^r$	biomass of paua above the MLS in the mid-season of year t
B_0^r	equilibrium biomass of paua above the MLS assuming no fishing and average recruitment from the period in which recruitment deviations were estimated
B_{init}^r	biomass of paua above the MLS at the end of initialisation phase (or B_{1964}^r)
U_t	exploitation rate in year t
A_t	the complement of exploitation rate
$SF_{k,t}$	finite rate of survival from fishing for paua in the kth length class in year t
V_k^r	relative selectivity of research divers for paua in the kth length class
V_k^s	relative selectivity of commercial divers for paua in the kth length class
$\sigma_{k,t}^r$	error of the predicted proportion in the kth length class in year t in RDLF data
n_t^r	relative weight (effective sample size) of the RDLF data in year t
$\sigma_{k,t}^s$	error of the predicted proportion in the kth length class in year t in CSLF data
n_t^s	relative weight (effective sample size) of the CSLF data in year t
σ_j^d	standard deviation of the predicted length increment for the jth tag-recapture record
σ_j^{tag}	total error predicted for the jth tag-recapture record
σ_k^{mat}	error of the proportion mature-at-length for the kth length class
$-\ln(\mathbf{L})$	negative log-likelihood
f	total function value

2.2.5 Predictions

$\hat{I}_t$	predicted CPUE in year t
$\hat{I2}_t$	predicted PCPUE in year t

$\hat{J}_t$ predicted RDSI in year t

$\hat{p}_{k,t}^r$ predicted proportion in the kth length class in year t in research diver surveys

$\hat{p}_{k,t}^s$ predicted proportion in the kth length class in year t in commercial catch sampling

$\hat{d}_j$ predicted length increment of the jth tag-recapture record

$\hat{p}_k^{mat}$ predicted proportion mature in the kth length class

2.2.6 Initial conditions

The initial population is assumed to be in equilibrium with zero fishing mortality and the base recruitment. The model is run for 60 years with no fishing to obtain near-equilibrium in numbers-at-length. Recruitment is evenly divided among the first five length bins:

(1) $\qquad R_{k,t} = 0.2 R0 \qquad$ for $1 \le k \le 5$

(2) $\qquad R_{k,t} = 0 \qquad$ for $k > 5$

A growth transition matrix is calculated inside the model from the estimated growth parameters. If the growth model is linear, the expected annual growth increment for the kth length class is:

(3) $\qquad \Delta l_k = \left(\dfrac{L_2 g_1 - L_1 g_2}{g_1 - g_2} - l_k \right) \left[1 - \left(1 + \dfrac{g_1 - g_2}{L_1 - L_2} \right) \right]$

The model uses the AD Model Builder™ function *posfun*, with a dummy penalty, to ensure a positive expected increment at all lengths, using a smooth differentiable function. The *posfun* function is also used with a real penalty to force the quantity $\left(1 + \dfrac{g_1 - g_2}{L_1 - L_2} \right)$ to remain positive. If the growth model is exponential (used for the base case), the expected annual growth increment for the kth length class is:

(4) $\qquad \Delta l_k = g_1 \left(g_2 / g_1 \right)^{(l_k - L_1)/(L_2 - L_1)}$

again using posfun with a dummy penalty to ensure a positive expected increment at all lengths. If the inverse logistic growth model is used the expected annual growth increment for the kth length class is:

(5) $\qquad \Delta l_k = \dfrac{\Delta_{max}}{\left(1 + \exp \left(\ln(19) \left(\left(l_k - l_{50}^g \right) / \left(l_{95}^g - l_{50}^g \right) \right) \right) \right)}$

All the models were examined and the exponential growth model was chosen for fitting the tag-recapture data in the base case of the PAU 5A assessment.

The standard deviation of g_k is assumed to be proportional to g_k with minimum σ_{MIN}:

(6) $\qquad \sigma^{g_k} = \left(g_k \phi - \sigma_{MIN} \right) \left(\dfrac{1}{\pi} \tan^{-1} \left(10^6 \left(g_k \phi - \sigma_{MIN} \right) \right) + 0.5 \right) + \sigma_{MIN}$

Or a more complex functional form between the growth increment and its standard deviation can be defined as:

$$(7) \qquad \sigma^{g_k} = \left(\alpha(g_k)^\beta - \sigma_{MIN}\right)\left(\frac{1}{\pi}\tan^{-1}\left(10^6\left(\alpha(g_k)^\beta - \sigma_{MIN}\right)\right) + 0.5\right) + \sigma_{MIN}$$

From the expected increment and standard deviation for each length class, the probability distribution of growth increments for a paua of length l_k is calculated from the normal distribution and translated into the vector of probabilities of transition from the kth length bin to other length bins to form the growth transition matrix **G**. Zero and negative growth increments are permitted, i.e., the probability of staying in the same bin or moving to a smaller bin can be non-zero.

In the initialisation, the vector $\mathbf{N_t}$ of numbers-at-length is determined from numbers in the previous year, survival from natural mortality, the growth transition matrix **G**, and the vector of recruitment $\mathbf{R_t}$:

$$(8) \qquad \mathbf{N_t} = \left(\mathbf{N_{t\text{-}1}}\, e^{-M}\right) \bullet \mathbf{G} + \mathbf{R_t}$$

where the dot (•) denotes matrix multiplication.

2.2.7   Dynamics

2.2.7.1   Sequence of operations

After initialising, the first model year is 1965 and the model is run through to 2013. In the first nine years the model is run with an assumed catch vector, because it is unrealistic to assume that the fishery was in a virgin state when the first catch data became available in 1974. The assumed catch vector rises linearly from zero to the 1974 catch. These years can be thought of as an additional part of the initialisation, but they use the dynamics described in this section.

Model dynamics are sequenced as follows.

- Numbers at the beginning of year t-1 are subjected to fishing, then natural mortality, then growth to produce the numbers at the beginning of year t.

- Recruitment is added to the numbers at the beginning of year t.

- Biomass available to the fishery is calculated and, with catch, is used to calculate the exploitation rate, which is constrained if necessary.

- Half the exploitation rate (but no natural mortality) is applied to obtain mid-season numbers, from which the predicted abundance indices and proportions-at-length are calculated. Mid-season numbers are not used further.

2.2.7.2   Main dynamics

For each year t, the model calculates the start-of-the-year biomass available to the commercial fishery. Biomass available to the commercial fishery is:

$$(9) \qquad B_t = \sum_k N_{k,t} V_k^s w_k$$

$$(10) \qquad V_k^{t,s} = \cfrac{1}{1+19^{-\left(\left(l_k - D_{50}\right)/D_{95-50}\right)}} \qquad \text{for } t < 2007$$

$$(11) \qquad V_k^{t,s} = \cfrac{1}{1+19^{-\left(\left(l_k - D_{50} - D_t^a D^s\right)/D_{95-50}\right)}} \qquad \text{for } t \geq 2007$$

The observed catch is then used to calculate the exploitation rate, constrained for all values above U^{max} with the *posfun* function of AD Model Builder™. If the ratio of catch to available biomass exceeds U^{max}, then exploitation rate is constrained and a penalty is added to the total negative log-likelihood function. Let minimum survival rate A_{min} be $1-U^{max}$ and survival rate A_t be $1-U_t$:

$$(12) \qquad A_t = 1 - \frac{C_t}{B_t} \qquad \text{for } \frac{C_t}{B_t} \leq U^{max}$$

$$(13) \qquad A_t = 0.5 A_{min}\left[1+\left(3-\cfrac{2\left(1-\cfrac{C_t}{B_t}\right)}{A_{min}}\right)^{-1}\right] \qquad \text{for } \frac{C_t}{B_t} > U^{max}$$

The penalty invoked when the exploitation rate exceeds U^{max} is:

$$(14) \qquad 1000000\left(A_{min} - \left(1 - \frac{C_t}{B_t}\right)\right)^2$$

This prevents the model from exploring parameter combinations that give unrealistically high exploitation rates. Survival from fishing is calculated as:

$$(15) \qquad SF_{k,t} = 1 - \left(1 - A_t\right) P_{k,t}$$

or

$$(16) \qquad SF_{k,t} = 1 - \left(1 - A_t\right) V_k^s$$

The vector of numbers-at-length in year t is calculated from numbers in the previous year:

$$(17) \qquad \mathbf{N_t} = \left(\left(\mathbf{SF_{t-1}} \otimes \mathbf{N_{t-1}}\right) e^{-M}\right) \bullet \mathbf{G} + \mathbf{R_t}$$

where $\otimes$ denotes the element-by-element vector product. The vector of recruitment, $\mathbf{R_t}$, is determined from $R0$, estimated recruitment deviations, and the stock-recruitment relationship:

$$(18) \qquad R_{k,t} = 0.2 R0 e^{\left(\varepsilon_t - 0.5\sigma_t^2\right)} \frac{B_{t-1+0.5}}{B_0} \bigg/ \left(1 - \frac{5H-1}{4H}\left(1 - \frac{B_{t-1+0.5}}{B_0}\right)\right) \qquad \text{for } 1 \leq k \leq 5$$

$$(19) \qquad R_{k,t} = 0 \qquad \text{for } k > 5$$

The recruitment deviation parameters ε_t were estimated for all years from 1980. The recruitment deviations were constrained to have a mean of 1 in arithmetic space.

The model predicts CPUE in year t from mid-season recruited biomass, the scaling coefficient, and the shape parameter:

$$(20) \qquad \hat{I}_t = q^I \left(B_{t+0.5} \right)^h$$

Available biomass $B_{t+0.5}$ is the mid-season vulnerable biomass after half the catch has been removed (no natural mortality is applied, because the time over which half the catch is removed might be short). It is calculated as in equation (9), but using the mid-year numbers, $N_{k,t+0.5}$:

$$(21) \qquad N_{k,t+0.5}^{vuln} = N_{k,t} \left(1 - \frac{(1-A_t)}{2} V_k^s \right).$$

Similarly,

$$(22) \qquad \hat{I2}_t = q^{I2} \left(B_{t+0.5} \right)^h = X q^I \left(B_{t+0.5} \right)^h$$

The same shape parameter h is used for both the early and recent CPUE series: experimentation outside the model showed that this was appropriate despite the different units of measurement for the two series. The predicted research diver survey index is calculated from mid-season model numbers in bins greater than 89 mm length, taking into account research diver selectivity-at-length:

$$(23) \qquad N_{k,t+0.5}^{res} = N_{k,t} \left(1 - \frac{(1-A_t)}{2} V_k^r \right)$$

$$(24) \qquad \hat{J}_t = q^J \sum_{k=11}^{55} N_{k,t+0.5}^{res}$$

where the scalar is estimated and the research diver selectivity V_k^r is calculated from:

$$(25) \qquad V_k^r = \frac{1}{1 + 19^{-\left((l_k - T_{50}) / T_{95-50} \right)}}$$

The model predicts proportions-at-length for the RDLF from numbers in each length class for lengths greater than 89 mm:

$$(26) \qquad \hat{p}_{k,t}^r = \frac{N_{k,t+0.5}^{res}}{\sum_{k=11}^{51} N_{k,t+0.5}^{res}} \qquad \text{for } 11 \leq k < 51$$

Predicted proportions-at-length for CSLF are similar:

$$(27) \quad \hat{p}_{k,t}^{s} = \frac{N_{k,t+0.5}^{vuln}}{\displaystyle\sum_{k=23}^{51} N_{k,t+0.5}^{vuln}} \qquad \text{for } 23 \le k < 51$$

The predicted increment for the jth tag-recapture record, using the linear model, is:

$$(28) \quad \hat{d}_{j} = \left(\frac{\beta g_{\alpha} - \alpha g_{\beta}}{g_{\alpha} - g_{\beta}} - L_{j} \right) \left[1 - \left(1 + \frac{g_{\alpha} - g_{\beta}}{\alpha - \beta} \right)^{\Delta t_{j}} \right]$$

where Δt_{j} is in years. For the exponential model (used in the base case) the expected increment is

$$(29) \quad \hat{d}_{j} = \Delta t_{j} g_{\alpha} \left(g_{\beta} / g_{\alpha} \right)^{(L_{j} - \alpha)/(\beta - \alpha)}$$

The error around an expected increment is:

$$(30) \quad \sigma_{j}^{d} = \left(\hat{d}_{j} \phi - \sigma_{MIN} \right) \left(\frac{1}{\pi} \tan^{-1} \left(10^{6} \left(\hat{d}_{j} \phi - \sigma_{MIN} \right) \right) + 0.5 \right) + \sigma_{MIN}$$

Predicted maturity-at-length is:

$$(31) \quad \hat{p}_{k}^{mat} = \frac{1}{1 + 19^{-\left((l_{k} - L_{50}) / L_{95-50} \right)}}$$

2.2.8 Fitting

2.2.8.1 Likelihoods

The distribution of CPUE is assumed to be normal-log and the negative log-likelihood is:

$$(32) \quad -\ln(\mathbf{L})\left(\hat{I}_{t} \mid \theta \right) = \frac{\left(\ln(I_{t}) - \ln(\hat{I}_{t}) \right)^{2}}{2\left(\sigma_{t}^{I} \tilde{\sigma} / \varpi^{I} \right)^{2}} + \ln\left(\sigma_{t}^{I} \tilde{\sigma} / \varpi^{I} \right) + 0.5 \ln(2\pi)$$

Where

$$(33) \quad \sigma_{t}^{I} = \sqrt{\log((cv_{t}^{I})^{2} + 1)}$$

and similarly for PCPUE:

$$(34) \quad -\ln(\mathbf{L})\left(\hat{I2}_{t} \mid \theta \right) = \frac{\left(\ln(I2_{t}) - \ln(\hat{I2}_{t}) \right)^{2}}{2\left(\sigma_{t}^{I2} \tilde{\sigma} / \varpi^{I2} \right)^{2}} + \ln\left(\sigma_{t}^{I2} \tilde{\sigma} / \varpi^{I2} \right) + 0.5 \ln(2\pi)$$

Where

(35) $\sigma_t^{I2} = \sqrt{\log((cv_t^{I2})^2 + 1)}$

The distribution of the RDSI is also assumed to be normal-log and the negative log-likelihood is:

(36) $-\ln(\mathbf{L})\left(\hat{J}_t \mid \theta\right) = \dfrac{\left(\ln\left(J_t\right) - \ln\left(\hat{J}_t\right)\right)^2}{2\left(\sigma_t^J\tilde{\sigma}\Big/\varpi^J\right)^2} + \ln\left(\sigma_t^J\tilde{\sigma}\Big/\varpi^J\right) + 0.5\ln\left(2\pi\right)$

Where

(37) $\sigma_t^J = \sqrt{\log((cv_t^J)^2 + 1)}$

The proportions-at-length from CSLF data are assumed to follow a multinomial distribution, with a standard deviation that depends on the effective sample size (see Section 2.2.9.3) and the weight assigned to the data:

(38) $\sigma_{k,t}^s = \dfrac{\tilde{\sigma}}{\varpi^s n_t^s}$

The negative log-likelihood is:

(39) $-\ln(\mathrm{L})\left(\hat{p}_{k,t}^s \mid \theta\right) = \dfrac{p_{s,t}^s}{\sigma_{k,t}^s}\left(\ln\left(p_{k,t}^s + 0.01\right) - \ln\left(\hat{p}_{k,t}^s + 0.01\right)\right)$

The likelihood for research diver sampling is analogous. Errors in the tag-recapture dataset were also assumed to be normal. For the jth record, the total error is a function of the predicted standard deviation (equation (30)), observation error, and weight assigned to the data:

(40) $\sigma_j^{tag} = \tilde{\sigma}/\varpi^{tag}\sqrt{\sigma_{obs}^2 + \left(\sigma_j^d\right)^2}$

and the negative log-likelihood is:

(41) $-\ln(\mathbf{L})\left(\hat{d}_j \mid \theta\right) = \dfrac{\left(d_j - \hat{d}_j\right)^2}{2\left(\sigma_j^{tag}\right)^2} + \ln\left(\sigma_j^{tag}\right) + 0.5\ln\left(2\pi\right)$

The proportion mature-at-length was assumed to be normally distributed, with standard deviation analogous to proportions-at-length:

(42) $\sigma_k^{mat} = \dfrac{\tilde{\sigma}}{\varpi^{mat}\sqrt{p_k^{mat} + 0.1}}$

The negative log-likelihood is:

$$(43) \quad -\ln(\mathbf{L})\left(\hat{p}_k^{mat} \mid \theta\right) = \frac{\left(p_k^{mat} - \hat{p}_k^{mat}\right)^2}{2\left(\sigma_k^{mat}\right)^2} + \ln\left(\sigma_k^{mat}\right) + 0.5\ln\left(2\pi\right)$$

2.2.8.2 Normalised residuals

These are calculated as the residual divided by the relevant σ term used in the likelihood. For CPUE, the normalised residual is

$$(44) \quad \frac{\ln\left(I_t\right) - \ln\left(\hat{I}_t\right)}{\left(\sigma_t^I \tilde{\sigma} \Big/ \varpi^I\right)}$$

and similarly for PCPUE and RDSI. For the CSLF proportions-at-length, the residual is:

$$(45) \quad \frac{p_{k,t}^s - \hat{p}_{k,t}^s}{\sigma_{k,t}^s}$$

and similarly for proportions-at-length from the RDLFs. Because the vectors of observed proportions contain many empty bins, the residuals for proportions-at-length include large numbers of small residuals, which distort the frequency distribution of residuals. When presenting normalised residuals from proportions-at-length, we arbitrarily ignore normalised residuals less than 0.05.

For tag-recapture data, the residual is:

$$(46) \quad \frac{d_j - \hat{d}_j}{\sigma_j^{tag}}$$

and for the maturity-at-length data the residual is:

$$(47) \quad \frac{p_k^{mat} - \hat{p}_k^{mat}}{\sigma_k^{mat}}$$

2.2.8.3 Dataset weights

Proportions at length (CSLF and RDLF) were included in the model with a multinomial likelihood. The length frequency distributions for individual years were assigned relative weights (effective sample size), based on a sample size that represented the best least squares fit of log(cv_i)~log(P_i), where cv_i was the bootstrap CV for the ith proportion, P_i. (See Figure A1, Appendix A, for a plot of this relationship). The weights for individual years (n_t^s for CSLF and n_t^r for RDLF) were multiplied by the weight assigned to the dataset (ϖ_s for CSLF and ϖ_r for RDLF) to obtain the model weights for the observations.

In previous assessments, the weight of the dataset was determined iteratively so that the standardised deviation of the normalised residuals (SDNRs) was close to one. In this assessment, we used an alternative weighting scheme following Francis (2011) for the base case model, where the weight for the CSLF dataset was determined as

(48) $\quad \varpi^s = 1/\text{var}_t\left[\left(\overline{O}_t^s - \overline{E}_t^s\right)/\left(v_t^s/n_t^s\right)^{0.5}\right]$ (Method TA1.8, table A1 in Francis 2011)

Where

(49) $\quad \overline{O}_t^s = \sum_k p_{k,t}^s l_k$

(50) $\quad \overline{E}_t^s = \sum_k \hat{p}_{k,t}^s l_k$

(51) $\quad v_t^s = \sum_k \left(l_k\right)^2 \hat{p}_{k,t}^s - \left(\overline{E}_t^s\right)^2$

The weight for the RDLF dataset was calculated similarly. This weighting method allows for the possibility of substantial correlations within a dataset, and generally produces relatively smaller sample sizes, thus down-weighting the composition data (Francis 2011). The actual and estimated sample sizes for the commercial catches at length are given in Table 1.

The relative abundance indices (CPUE and RDSI) were included in the model with a lognormal likelihood. The weights for individual years were determined by the CV calculated in the standardisation and were then scaled by the weight assigned to the dataset to obtain the model weights for the observations. In previous assessments, the weight of the dataset was determined iteratively so that the standardised deviation of the normalised residuals was close to one. In this assessment, we used an alternative weighting scheme recommended by Francis (2011). With this approach, a series of lowess lines of various degrees of smoothing were fitted to the abundance indices (this is carried out outside the assessment model), and the CV of the residuals from the lowess line which is considered to have the "appropriate" smoothness is used. The CV was applied to all years in the time series and remained constant in the stock assessment model. The choice of the "appropriate" fit is based on visual examination of the lowess lines. This is equivalent to saying that we expect the stock assessment model to fit these data as well as the smoother does.

2.2.8.4 Priors and bounds

Bayesian priors were established for all estimated parameters (Table 2). Most were incorporated simply as uniform distributions with upper and lower bounds set arbitrarily wide so as not to constrain the estimation. The prior probability density for M was a normal-log distribution with mean μ_M and standard deviation σ_M. The contribution to the objective function of estimated $M = x$ is:

(52) $\quad -\ln(\mathbf{L})(x \mid \mu_M, \sigma_M) = \dfrac{\left(\ln(M) - \ln(\mu_M)\right)^2}{2\sigma_M^{\ 2}} + \ln\left(\sigma_M \sqrt{2\pi}\right)$

The prior probability density for the vector of estimated recruitment deviations ε, was assumed to be normal with a mean of zero and a standard deviation of 0.4. The contribution to the objective function for the whole vector is:

(53) $\quad -\ln(\mathbf{L})(\varepsilon \mid \mu_\varepsilon, \sigma_\varepsilon) = \dfrac{\displaystyle\sum_{i=1}^{n_\varepsilon}\left(\varepsilon_i\right)^2}{2\sigma_\varepsilon^{\ 2}} + \ln\left(\sigma_\varepsilon\right) + 0.5\ln\left(2\pi\right).$

Constant parameters are given in Table 3

2.2.8.5 Penalty

A penalty is applied to exploitation rates higher than the assumed maximum (Equation 13); it is added to the objective function after being multiplied by an arbitrary weight (1000000) determined by experiment.

AD Model Builder™ also has internal penalties that keep estimated parameters within their specified bounds, but these should have no effect on the final outcome, because choice of a base case excludes the situations where parameters are estimated at or near a bound.

2.2.9 Fishery indicators

The assessment calculates the following quantities from their posterior distributions: the model's mid-season spawning and recruited biomass for 2014 ($B_{current}$ and $B_{current}^r$) and for the projection period (B_{proj} and B_{proj}^r).

Simulations were carried out to calculate deterministic MSY: maximum constant annual catch that can be sustained under deterministic recruitment. A single simulation run was done by starting from an unfished equilibrium state, and running under a constant exploitation rate until the catch and spawning stock biomass stabilised. For each simulation run with exploitation rate U, the equilibrium total annual catch and spawning stock biomass were calculated. The exploitation rate U that maximizes the annual catch is U_{msy}. The corresponding catch is MSY, and the corresponding SSB is B_{msy}. Together with B_o, B_{msy}, $U_{current}$, $U_{\%40B0}$ and U_{msy} the current and projected stock status are reported in relation to the following indicators:

$\%B_0$ current and projected spawning biomass as a percent of B_0

$\%B_{msy}$ current and projected spawning biomass as a percent of B_{msy}

$\Pr(> B_{current})$ Probability that projected spawning biomass is greater than $B_{current}$

$\Pr(> B_{msy})$ Probability that current and projected spawning biomass is greater than B_{msy}

$\%B_0^r$ current and projected recruited biomass as a percent of B_0^r

$\%B_{msy}^r$ current and projected recruited biomass as a percent of B_{msy}^r

$\Pr(> B_{msy}^r)$ Probability that current and projected recruit-sized biomass is greater than B_{msy}^r

$\Pr(> B_{current}^r)$ Probability that projected recruit-sized biomass is greater than $B_{current}^r$

$\Pr(B_{proj} > 40\%B_0)$ Probability that current and projected spawning biomass is greater than 40% B_0

$\Pr(B_{proj} < 20\%B_{msy})$ Probability that current and projected spawning biomass is less than 20% B_0

$\Pr(B_{proj} < 10\%B_{msy})$ Probability that current and projected spawning biomass is less than 10% B_0

$\Pr(U_{proj} > U_{40\%B0})$ Probability that current and projected exploitation rate is greater than $U_{40\%B0}$

2.2.10 Markov chain-Monte Carlo (MCMC) procedures

AD Model Builder™ uses the Metropolis-Hastings algorithm. The step size is based on the standard errors of the parameters and their covariance relationships, estimated from the Hessian matrix.

For the MCMCs in this assessment single long chains were run, starting at the MPD estimate. The base case was 5 million simulations long and samples were saved, regularly spaced by 5000. The value of $\tilde{\sigma}$ was fixed to that used in the MPD run because it may be inappropriate to let a variance component change during the MCMC.

2.2.11 Development of base case and sensitivity model runs

The 2010 assessment used the commercial catch length frequency data from 2002–2014 and excluded the length frequency data from other years because the sampling coverage in those years was considered to be patchy. However, Haist (2014) suggested that paua commercial fishery length samples may not be representative of the fishery because the sampling programme does not follow a completely random design. The SFWG decided to investigate using all the commercial catch length frequency data in the assessment.

Following discussions of input data by the Shellfish Working Group (SFWG) five initial model runs were done (models 1.0–1.4). These preliminary models investigated a number of weighting methods on observational datasets, the choice of growth models (exponential versus inverse-logistic models), and whether the pre-2002 length frequency data should be included (Table 4). After reviewing the diagnostics and outputs from these models, the Shellfish WG agreed on a base case (model 1.5).

The base case model used the methods recommended by Francis (2011) to determine the weight of the proportion-at-length and abundance data, excluded the pre-2002 commercial length frequency data (1992–1994, 1998, and 2001), and estimated growth using the inverse-logistic model. In the base case, the RDSI and RDLF were excluded, and the CPUE shape parameter was fixed at 1 assuming a linear relationship between CPUE and abundance. The commercial catch history used in the base case was that estimated under "assumption 2" (between 1983–84 and 1995–96, 40%, 53%, and 7% of the catch in Statistical Area 030 was taken from PAU 5A, PAU 5B, and PAU 5D respectively, see Fu et al. (2015)).

The SFWG suggested the following sensitivity runs: Run 1.6 used the SDNRs-based method to determine the weights of the proportion-at-length and abundance data; RUN 1.7 included all the commercial length frequency data; RUN 1.8 used commercial catch history that was estimated under "assumption 1" (between 1984 and 1996, 18%, 75%, and 7% of the catch in Statistical Area 030 was taken from PAU 5A, PAU 5B, and PAU 5D respectively); RUN 1.9 used commercial catch history estimated under "assumption 3" (between 1984 and 1996, 61%, 32%, and 7% of the catch in Statistical Area 030 was taken from PAU 5A, PAU 5B, and PAU 5D respectively); RUN 2.0 included the RDSI and RDLF data. A summary description of the preliminary model runs, base case, and sensitivity models is given in Table 4. The MCMC runs were carried out to models 1.5 (base case), 1.6, and 1.7.
For models that used the Francis (2011) method to determine the weight of the proportion-at-length (e.g. models 1.1, 1.3, 1.5, and 1.7), the effective sample sizes were mostly less than 10% of the actual number of fish measured (see Table 1). This was expected as this method accounted for the potential correlations in the proportion-at-length data and would effectively down-weight the dataset compared to the method based on the SDNRs (e.g. models 1.0, 1.2, and 1.6) which resulted in much larger sample sizes (see Table 1).

Following Francis (2011) a series of lowess lines of various degrees of smoothing were fitted to the CPUE indices. For the early CPUE (1990–2001), the residuals from the lowess line which was considered to have the "appropriate" smoothness had a CV of 0.1 (corresponding to the "f" value of 0.95, which represents the degree of smoothness of the lowess line, see Figure A2–left, Appendix A); for the recent CPUE (2002–2013), a CV of 0.08 was considered to be appropriate (corresponding to the "f" value of 0.95, see Figure A2–right, Appendix A). The CVs for the CPUE indices were fixed at

those values in the assessment (except for models 1.0, 1.2 and 1.6 in which the CVs were determined using SDNR-based weighting method).

3. RESULTS

3.1 Preliminary model runs

Model fits and diagnostics from preliminary models runs (1.0–1.4) are given in Appendix A. Estimates of objective function values (negative log-likelihood) and parameters are summarised in Table 5. MPD 1.0 fitted poorly to the early CPUE series and predicted an opposite trend to the observed indices (Figure A3), but it fitted reasonably well to the commercial catch length distributions including the pre-2002 length distributions (Figure A4). This is because very large effective sample sizes were assigned to the CSLF dataset (see Table 1). In contrast, MPD 1.1 fitted well to both CPUE series (Figure A5), but fitted poorly to the pre-2002 length frequency data (Figure A6), when the CSLF data were downweighted. Both MPD 1.2 and 1.3 fitted CPUE indices and CSLF data reasonably well when only the CSLF for 2002–2014 were included in the model, although there are some noticeable differences in the predicted CPUE trend for the last few years, possibly due to the differences in data weighting (Figure A7 and A8). These results suggested that there were conflicts between the CPUE indices and the pre-2002 commercial length frequency data.

Exponential growth models were used in models 1.0–1.3. The exponential growth model fitted the bulk of the tag-recapture data well (Figure A9), but had negative bias for both small (under 90 mm) and large (over 130 mm) size classes (Figure A10-left). The bias in the residuals appeared to be corrected when the inverse-logistic model was used in MPD 1.4 (Figure A10-right). The negative log likelihood value from the tag-capture data for MPD 1.4 was much less than that for MPD 1.3 (Table 5). The fits to CPUE and CSLF data were very similar between MPD 1.3 and 1.4 (Figure A11 and A12), with only marginal differences in the likelihood values. Biomass estimates were also very similar between the two models (Figure A13).

3.2 MPD base case and sensitivity

Based on the results from the preliminary runs, the SFWG concluded that the pre-2002 length frequency distributions were unlikely to be representative of the fishery, given the small number of samples being collected (n=1 in 1994, 1998, and 2001, n=2 in 1993, and n=3 in 1992), and therefore decided to exclude these data in the base case. It was also decided to use the inverse-logistic model in the base case, as it better represents the observed mean growth, especially for the large size classes. Model estimates of objective function values, parameters, and indicators for the base case and sensitivity models are given in Table 5.

Both the base case (Francis (2011) data weighting) and MPD 1.6 (SDNRs-based data weighting) fitted the two CPUE indices very well (Figure 2), and the QQ plots of the residuals from the fits to the abundance indices show no apparent departure from the normality assumption (Figure 3). MPD 1.6 had noticeably better fits to commercial length frequency data, and MPD 1.5 predicted a broader distribution than the observed LF for a number of years (e.g. 2004, 2005, and 2006, Figure 4). Residuals suggested that the fits to the LF in the 120 to 140 mm size range were less adequate for MPD 1.5 (Figure 5). Francis (2011) suggested using the predicted annual mean length (across length classes) as a diagnostic tool for the proportion-at-length data, because of potential correlations in residuals for individual length classes, and there was a reasonable match between the predicted and observed mean length for MPD 1.5 (Figure 6).

The inverse-logistic growth curves used in both models predicted similar growth increments for the bulk of size classes (Figure 7). However, MPD 1.6 estimated higher growth for the size classes under

90 mm and also above 130 mm (Figure 7). The residual patterns suggested that MPD 1.5 provided a reasonably adequate fit, whereas MPD 1.6 had a negative bias for the small and large size classes (Figure 8).

The fits to maturity data appeared adequate and length at 50% and full maturity were estimated to be about 92 mm and 110 mm respectively (Figure 9–left). The base case model estimated a step change of 4.3 mm in commercial selectivity between 2006 and 2011 (Figure 9–right), which was close to the increase of the voluntary MHS (5 mm). Natural mortality (M) was estimated to be 0.11 for the base case, close to the mean of the prior distribution. A higher M (0.14) was estimated for MPD 1.6 when more weight was assigned to the LF data.

MPD 1.7 included all the commercial length frequency data. Because small sample sizes were assigned to the CSLF data (see Table 1), this model fitted to the CPUE series well (Figure 10), but fitted pre-2002 LF poorly (Figure 11), which corroborated that there were conflicts between the CPUE and the early length frequency data.

The base case estimated $B_{current}$ to be 38% of B_0 (Table 5). Estimated biomass was lower in MPD 1.6 with $B_{current}$ estimated to be 34% of B_0 (Figure 12). Estimated biomass for MPD 1.7 was very similar to the base case.

Biomass estimates were sensitive to the assumptions made in the estimates of the catch history (Figure 13). If 18% of the commercial catch in Statistical Area 030 was assumed to have been taken from PAU 5A between 1984 and 1996 (MPD 1.8), estimated $B_{current}$ was 46% of B_0; if the assumed proportion was 75%, estimated $B_{current}$ was 34% of B_0. Model 2.0 Included RDSI and RDLF (Figure A14 and A15) and it appeared to have little influence on model results, estimated parameters and biomass were very similar to the base case (see Table 5, Figure 14).

3.3   MCMC results

MCMC was conducted for the base case (1.5) to derive the posterior distribution of estimated parameters. The SFWG also suggested additional MCMC runs for model 1.6 in which CSLF data were up-weighted, and model 1.7 which included the pre-2002 length frequency data.

3.4   Marginal posterior distributions and the Bayesian fit

The main diagnostic used for the MCMC was the trace plots of the posterior samples for estimated parameters. For the base case the MCMC simulation started at the values of MPD estimates for model parameters and the traces show good mixing (Figure 15). There is no evidence of non-convergence for estimated biomass indicators (B_0, $B_{current}$, and $B_{current}$ as a percent of B_0) and their posterior distributions are well formed, with posterior medians being reasonably close to the MPD estimates (Figure 16).

The posterior distributions for estimated parameters and biomass indicators for the base case are summarised in Table 6. The estimated posterior of M has a median of 0.108 with a 90% credible interval between 0.095 and 0.123. The range of the posterior distribution was very close to that of the prior (Figure 17). This suggested that the information in the observations about M was consistent with the assumed prior function. However, it might also mean that there wasn't much information in the observations about M, so it didn't move it much from the prior.

The estimates of recruitment deviations showed periods of relatively high recruitment in the mid-1990s and in the 2000s, but in most years, recruitment was close to or below the long term average. (Figure 18–left). Exploitation rates have declined since 2002, but have increased slightly over the last four years (Figure 18 –right). The estimated exploitation rate in 2014 was 0.11 (0.08–0.15).

The MCMC fits to both CPUE indices were adequate: the posterior distribution of the predicted indices were broadly comparable to the observed indices given the error assumed for the observations (Figure 19). The posterior distributions of mean residuals (across all years) of fits to the CSLF data showed some trend between 130 and 140 mm (Figure 20–left), which could be explained by the poor fits to the mode of the distributions for a number of years (see Figure 6). The QQ quantiles of the posterior residuals from the fits to the tag-recapture data showed no evidence of poor fits (Figure 20–right).

The posterior distributions of spawning stock biomass (SSB) for the base case are shown in Figure 21. The SSB decreased through to 2006 but started to increase since then. The SSB was relatively stable between 2011 and 2014. The estimated B_0 was 1381 t (1264–1522 t) and $B_{current}$ was 41% (33–50%) of B_0 (Table 6).

Deterministic B_{msy} was calculated using posterior samples of estimated parameters. The median of B_{msy} was estimated to be about 27% B_0 and the corresponding exploitation rate (U_{msy}) was estimated to be 23% (Table 6). The target exploitation rate ($U_{40\%B_0}$) was estimated to be 13%. Estimated changes in stock size in relation to fishing pressure over time are shown in Figure 22. This was done by plotting the annual spawning biomass and exploitation rate as a ratio of a reference value from 1965 to 2014. Each point on the trajectory represents the estimated annual stock status: the value on the x axis is the mid-season spawning stock biomass as a ratio of either B_0 (Figure 22–left) or B_{msy} (Figure 22–right), the value on the y axis is the corresponding exploitation rate as a ratio of $U_{\%40B_0}$ (Figure 22–left) or U_{msy} (Figure 22–right) for that year. The trajectory started in 1965 when the SSB was close to B_0 and the exploitation rate was close to 0. The model indicated that there was an early phase of the fishery where the exploitation rates were below $U_{\%40B_0}$ and the SSBs were above 40% , B_0 and a development phase where the exploitation rates increased and the SSBs decreased in relation to the target. The current exploitation rate is below $U_{\%40B_0}$ and the current spawning stock biomass is very close to 40% B_0 .

Estimated parameters and biomass indicators for the MCMC 1.6 and MCMC 1.7 are summarised in Table 7 and Table 8 respectively. Diagnostic plots for the two sensitivity runs are given in Appendix B. When the CSLF data were up-weighted (MCMC 1.6), the MCMC chain for the inverse-logistic parameters did not converge and the traces exhibited strong negative correlation among the three parameters (Figure B1). However, this did not appear to have affected the estimates of biomass indicators, which show no evidence of non-convergence (Figure B2–left). There is much less uncertainly in estimated biomass for MCMC 1.6 when large sample sizes were assumed for the CSLF data (see Figure B2–right), and $B_{current}$ was estimated to be 35% (30–41%) of B_0 (Table 7). Model results from MCMC 1.7 were very similar to the base case, and $B_{current}$ was estimated to be 42% (33–52%) of B_0 (Table 8).

3.5 Projections

Projections were made for the base case with a number of alternative future catch scenarios. The three different catch levels assumed for the next three years (projections were made to 2017) were the current catch, a 10% increase of the 2014 catch level, and/or a 20% increase of the 2014 catch level. In the projections, future recruitment deviations were resampled from recent model estimates (2000–2010).

Assuming that the future catch remains at its current level, the projection suggested that the spawning stock abundance will increase to 48% (0.38–0.61) of B_0 over the next three years (Table 9, Figure 23). The projection also indicated that the probability of the spawning biomass being above the target (40% B_0) will increase from 55% in 2014 to 67% in 2017, and that the stock status is very unlikely to be below the soft (20% B_0) or hard limit (10%) in the short term.

Assuming a 10% increase in the catch, the projected biomass will increase slightly over the next three years, and the probability of the spawning stock biomass being above the target (40% B_0) will slightly increase to 63% in 2017 (Table 10). Assuming a 20% increase in catch, the projected biomass will remain relatively stable, and the biomass in 2017 will be similar to $B_{current}$ (Table 11).

4. DISCUSSION

Assessments for New Zealand paua stocks have usually been conducted at the Quota Management Area level, as fishery management measures are usually made at this scale. For PAU 5A, there were concerns about the applicability of the assessment to the entire QMA, although there was general agreement that biomass decline had occurred in the southern region of the QMA over recent years. If changes in abundance have differed between subareas, a QMA-level model assuming a homogenous area is unlikely to be informative of the stock status.

There have been changes in management initiatives in recent years towards fine-scale management of paua stocks. Subarea management zones, based on the research strata, were established in PAU 5A in 2006, with voluntary catch limits and minimum harvest sizes in place for each zone. Therefore, a subarea level assessment is probably more relevant in informing management decisions. In addition, improvement of the collection and reporting of fishery data at finer scale has allowed the development of models to assess the fish stock at a smaller spatial scale.

This report assesses the status of stocks for the southern areas of PAU 5A (Chalky and South coast). Estimates from the base case model suggested that the current spawning stock population ($B_{current}$) was 41% (33–50%) B_0, and recruit-sized stock abundance ($B_{current}^r$) was 32% (24–41%) of initial state (B_r^r). The model suggested that it was very unlikely that the stock will fall below the soft or hard limits. The projection suggested that biomass is likely to increase over the next three years at current catch levels.

The model presented here, whilst fairly representing some of the data, also shows some indications of lack of fit. It is unlikely the estimates of historical stock size are reliable, given assumptions about annual recruitment and the use of the historical catch-effort indices of abundance. Some conflicts between length frequency distributions and CPUE were noticed during the assessment. The early CPUE showed a declining trend, indicating that this was probably a fishing-down period for the fishery, when large fish were removed from the stock, which would most likely result in a decline of mean length in the commercial catch samples. This is not consistent with the observed trend in the

length distributions. A plausible explanation for this contradiction is that the commercial catch samples in the early years were unrepresentative of the fishery due to the small sample sizes.

The assessment considered both exponential and inverse-logistic growth models. The inverse-logistic distribution has been widely used to model the growth of abalone and is considered to be more suitable to describe the growth of small and juvenile paua, which appears to be linear (Haddon et al. 2008). The use of the inverse-logistic model resulted in marked improvement in the fits to the tag-recapture data (particularly for the small and large size classes). However, potential correlations between parameters could lead to poor MCMC performance on some occasions (e.g. MCMC 1.6).

The recent practice in paua stock assessments has been to exclude the research diver survey data (RDSI and RDLF) from the base case (Fu 2013, 2014a). This decision was made by the Shellfish Working Group on the basis of the work by Cordue (2009) and Haist (2010) both of which suggested that the research diver survey indices were unlikely to index stock abundance at the QMA level. The research diver survey using the timed-swim method has been discontinued for all paua stocks and the last survey was conducted in 2005.

CPUE provides information on changes in relative abundance. However, CPUE is generally considered to be a poor index of stock abundance for paua, due to divers' ability to maintain catch rates by moving from area to area despite a decreasing biomass (hyperstability). Breen & Kim (2003) argued that standardised CPUE might be able to relate to the changes of abundance in a fully exploited fishery, and a large decline in the CPUE is most likely to reflect a decline in the fishery. However, for the southern area of PAU 5A, the interpretation of the decline of CPUE in the early 1990s is confounded by the shifting of fishing effort from Stewart Island to South Coast (the CPUE is based on Statistical Area 030). The fishers suggested that the catch rates had declined markedly at Stewart Island during this period, the extent to which the CPUE reflected abundance in Chalky and South Coast is unknown. Attempts to estimate the relationship between CPUE and biomass (through the parameter h) have been made in some of the previous paua stock assessments and on some occasions have suggested evidence of hyperstability (McKenzie & Smith 2009a).

Another source of uncertainty is the catch data. The commercial catch is unknown before 1974 and is estimated with uncertainly before 1995. Although we think that the effect is minor, major differences may exist between the catches we assume and what was actually taken. In addition, non-commercial catch estimates are poorly determined and could be substantially different from what was assumed, although because of its relative inaccessibility, non-commercial catches are most likely to be small in PAU 5A.

There were also uncertainties in the estimated catch history relating to the allocation of the pre-division catch among the three substocks of PAU 5 and between subareas within PAU 5A. Sensitivity trials have used catch estimates made under alternative assumptions. Between the lower-bound and upper-bound catch estimates, model estimates of current spawning stock status ranged from 34 to 46% of B_0. There is little information on the historic catches in Fiordland, but anecdotal evidence suggested that the catch between 1981 and 1984 was about 60–70 tonne annually (Storm Stanley pers. comm.). This suggested that the lower bound estimates are too low, and the upper bound estimates are too high. The general consensus is that there had been a redistribution of catch when the quota was split among the substocks but the extent to which this happened is unknown. However, the lower and upper bound estimates should have encompassed most of the uncertainty in the historic catches.

Heterogeneity in growth can be a problem for this kind of model (Punt 2003). Variation in growth is addressed to some extent by having a stochastic growth transition matrix based on increments observed in several different places; similarly the length frequency data are integrated across samples from many places. One potential effect is that model results could be more optimistic. For instance, if some local stocks are fished very hard and others are not fished, recruitment failure can result because of the depletion of spawners. Spawners must breed close to each other and the dispersal of larvae is unknown and may be limited. Recruitment failure is a common observation in overseas abalone

fisheries, so local processes may decrease recruitment, an effect that the current model cannot account for.

Another source of uncertainty is that fishing may cause spatial contraction of populations (Shepherd & Partington 1995), or that some populations become relatively unproductive after initial fishing (Gorfine & Dixon 2000). If this happens, the model will overestimate productivity in the population as a whole. However, there is no clear evidence in the fishery data to suggest that this has happened or is happening in PAU 5A.

5. ACKNOWLEDGEMENTS

6. REFERENCES

Andrew, N.L.; Breen, P.A.; Naylor, J.R.; Kendrick, T.H.; Gerring, P. (2000). Stock assessment of paua (*Haliotis iris*) in PAU 7 in 1998–99. *New Zealand Fisheries Assessment Report 2000/49*. 40 p.

Breen, P.A.; Andrew, N.L.; Kendrick, T.H. (2000a). Stock assessment of paua (*Haliotis iris*) in PAU 5B and PAU 5D using a new length-based model. *New Zealand Fisheries Assessment Report 2000/33*. 37 p.

Breen, P.A.; Andrew, N.L.; Kendrick, T.H. (2000b). The 2000 stock assessment of paua (*Haliotis iris*) in PAU 5B using an improved Bayesian length-based model. *New Zealand Fisheries Assessment Report 2000/48*. 36 p.

Breen, P.A.; Andrew, N.L.; Kim, S.W. (2001). The 2001 stock assessment of paua (*Haliotis iris*) in PAU 7. *New Zealand Fisheries Assessment Report 2001/55*. 53 p.

Breen, P.A.; Kim, S.W. (2003). The 2003 stock assessment of paua (*Haliotis iris*) in PAU 7. *New Zealand Fisheries Assessment Report 2003/35*. 112 p.

Breen, P.A.; Kim, S.W. (2004a). The 2004 stock assessment of paua (*Haliotis iris*) in PAU 4. *New Zealand Fisheries Assessment Report 2004/55*. 79 p.

Breen, P.A.; Kim, S.W. (2004b). The 2004 stock assessment of paua (*Haliotis iris*) in PAU 5A. *New Zealand Fisheries Assessment Report 2004/40*. 86 p.

Breen, P.A.; Kim, S.W. (2005). The 2005 stock assessment of paua (*Haliotis iris*) in PAU 7. *New Zealand Fisheries Assessment Report 2005/47*. 114 p.

Breen, P.A.; Kim, S.W. (2007). The 2006 stock assessment of paua (*Haliotis iris*) stocks PAU 5A (Fiordland) and PAU 5D (Otago). *New Zealand Fisheries Assessment Report 2007/09*. 164 p.

Breen, P.A.; Kim, S.W.; Andrew, N.L. (2003). A length-based Bayesian stock assessment model for abalone. *Marine and Freshwater Research 54(5): 619–634*.

Breen, P.A.; Smith, A.N.H. (2008a). The 2007 assessment for paua *(Haliotis iris)* stock PAU 5B (Stewart Island). *New Zealand Fisheries Assessment Report 2008/05*.

Breen, P.A.; Smith, A.N.H. (2008b). Data used in the 2007 assessment for paua (*Haliotis iris*) stock PAU 5B (Stewart Island). *New Zealand Fishery Assessment Report 2008/6*. 45 p.

Bull, B.; Francis, R.I.C.C.; Dunn, A.; McKenzie, A.; Gilbert, D.J.; Smith, M.H.; Bian, R. (2012). CASAL (C++ algorithmic stock assessment laboratory): CASAL User Manual v2.30-2012/03/21. *NIWA Technical Report 135*.

Cordue, P.L. (2009). Analysis of PAU5A dive survey data and PCELR catch and effort data. Final report for SeaFIC and PauaMAC5. (Unpublished report held by SeaFIC.)

Francis, R.I.C.C. (2011). Data weighting in statistical fisheries stock assessment models. *Canadian Journal of Fisheries and Aquatic Sciences 68: 15*.

Fu, D. (2012). The 2011 stock assessment of paua (*Haliotis iris*) for PAU 7. *New Zealand Fisheries Assessment Report 2012/27.* 56 p.

Fu, D. (2013). The 2012 stock assessment of paua (*Haliotis iris*) for PAU 5D. *New Zealand Fisheries Assessment Report 2013/57.* 56 p.

Fu, D. (2014a). The 2013 stock assessment of paua (*Haliotis iris*) for PAU 5B. *New Zealand Fisheries Assessment Report* 2014/45. 51 p.

Fu, D. (2014b). The 2013 stock assessment of paua (*Haliotis iris*) for PAU 3. *New Zealand Fisheries Assessment Report* 2014/44. 33 p.

Fu, D.; McKenzie, A. (2010a). The 2010 stock assessment of paua (*Haliotis iris*) for Chalky and South Coast in PAU 5A. *New Zealand Fisheries Assessment Report 2010/36.* 63 p.

Fu, D.; McKenzie, A. (2010b). The 2010 stock assessment of paua (*Haliotis iris*) for Milford, George, Central, and Dusky in PAU 5A. *New Zealand Fisheries Assessment Report 2010/46.* 55 p.

Fu, D.; McKenzie. A; Naylor, R. (2010). Summary of input data for the 2010 PAU 5A stock assessment. *New Zealand Fisheries Assessment Report 2010/35.* 58 p.

Fu, D.; McKenzie, A.; Naylor, J.R. (2012). Summary of input data for the 2011 PAU 7 stock assessment. *New Zealand Fisheries Assessment Report* 2012/26. 46 p.

Fu, D.; McKenzie, A; Naylor, R. (2013). Summary of input data for the 2012 PAU 5D stock assessment. *New Zealand Fisheries Assessment Report* 2013/56. 47 p.

Fu, D.; McKenzie, A; Naylor, R. (2014a). Summary of input data for the 2013 PAU 5B stock assessment. *New Zealand Fisheries Assessment Report* 2014/43. 61 p.

Fu, D.; McKenzie, A; Naylor, R. (2014b). Summary of input data for the 2013 PAU 3 stock assessment. *New Zealand Fisheries Assessment Report* 2014/42. 45 p.

Fu, D.; McKenzie, A; Naylor, R. (2015). Summary of input data for the 2014 PAU 5A stock assessment. *New Zealand Fisheries Assessment Report 2015/xx.* xx p

Gorfine, H.K.; Dixon, C.D. (2000). A behavioural rather than resource-focused approach may be needed to ensure sustainability of quota managed abalone fisheries. *Journal of Shellfish Research* 19: 515–516.

Haddon, M.; Mundy, C.; Tarbath, D. (2008). Using an inverse-logistic model to describe growth increments of blacklip abalone (Haliotis rubra) in Tasmania. *Fishery Bulletin 106(1)*: 58.

Haist, V. (2010). Paua research diver survey: review of data collected and simulation study of survey method. *New Zealand Fisheries Assessment Report 2010/38.* 54 p.

Haist, V. (2014). Review of paua commercial catch length frequency sampling programme. Final Research Report to the Ministry for Primary Industries. 2014/7. 66 p.

Kim, S.W.; Bentley, N.; Starr, P.J.; Breen, P.A. (2004). Assessment of red rock lobsters (*Jasus edwardsii*) in CRA 4 and CRA 5 in 2003. *New Zealand Fisheries Assessment Report 2004/8.* 165 p.

McKenzie, A.; Smith, A.N.H. (2009a). The 2008 stock assessment of paua (*Haliotis iris*) in PAU 7. *New Zealand Fisheries Assessment Report 2009/34.* 84 p.

McKenzie, A.; Smith, A.N.H. (2009b). Data inputs for the PAU 7 stock assessment in 2008. *New Zealand Fisheries Assessment Report 2009/33.* 34 p.

McShane, P.E.; Mercer, S.F.; Naylor, J.R. (1994). Spatial variation and commercial fishing of the New Zealand paua (*Haliotis iris* and *H. australis*). *New Zealand Journal of Marine and Freshwater Research* 28: 345–355.

McShane, P.E.; Mercer, S.; Naylor, J.R.; Notman, P.R. (1996). Paua (*Haliotis iris*) fishery assessment in PAU 5, 6, and 7. New Zealand Fisheries Assessment Research Document 96/11. 35 p. (Unpublished report held in NIWA library, Wellington.)

Punt, A.E. (2003). The performance of a size-structured stock assessment method in the face of spatial heterogeneity in growth. *Fisheries Research 65:* 391–409.

Schiel, D.R. (1989). Paua fishery assessment 1989. New Zealand Fisheries Assessment Research Document 89/9: 20 p. (Unpublished report held in NIWA library, Wellington, New Zealand.)

Schiel, D.R. (1992). The paua (abalone) fishery of New Zealand. *In:* Abalone of the world: Biology, fisheries and culture. Shepherd, S.A.; Tegner, M.J.; Guzman del Proo, S. (eds.) pp. 427–437. Blackwell Scientific, Oxford.

Schiel, D.R.; Breen, P.A. (1991). Population structure, ageing and fishing mortality of the New Zealand abalone *Haliotis iris*. *Fishery Bulletin 89*: 681–691.

Shepherd, S.A.; Breen, P.A. (1992). Mortality in abalone: its estimation, variability and causes. *In*: Abalone of the World: Biology, Fisheries and Culture. S.A. Shepherd, S.A.; Tegner, M.J. Guzman del Proo, S. (eds.) pp. 276–304. Blackwell Scientific: Oxford.

Shepherd, S.A.; Partington, D. (1995). Studies on Southern Australian abalone (genus Haliotis). XVI. Recruitment, habitat and stock relations. *Marine and Freshwater Research 46*: 669–680.

Shepherd, S.A.; Rodda, K.R.; Vargas, K.M. (2001). A chronicle of collapse in two abalone stocks with proposals for precautionary management. *Journal of Shellfish Research 20:* 843–856.

Table 1: Actual sample sizes, initial sample sizes determined for the multinomial likelihood, and model weighted sample sizes for the PAU 5A south commercial catch sampling length frequency data from selected model runs. A descriptions of the runs are summarised in Table 4. Models 1.1, 1.3, 1.5, and 1.7 used the method of Francis (2011) for data weighting, and Models 1.0, 1.2, and 1.6 used the SDNRs-based method.

Fishing year	Actual sample size	Initial sample size	Model run							
			1.0	1.1	1.2	1.3	1.5	1.6	1.7
1992	1 347	261	257	6	−	−	−	−	5
1993	441	331	326	7	−	−	−	−	6
1994	930	356	351	8	−	−	−	−	6
1998	1 324	157	155	3	−	−	−	−	3
2001	1 469	122	120	3	−	−	−	−	2
2002	967	501	493	11	521	20	16	509	9
2003	831	539	531	12	561	21	17	547	10
2004	348	532	524	12	553	21	17	540	10
2005	157	339	334	7	353	13	11	344	6
2006	120	191	188	4	199	8	6	194	3
2007	1 823	508	500	11	528	20	16	516	9
2008	3 278	176	173	4	183	7	6	179	3
2009	2 010	192	189	4	200	8	6	195	3
2010	1 569	347	342	8	361	14	11	352	6
2011	1 126	256	252	6	266	10	8	260	5
2012	2 018	217	214	5	226	9	7	220	4
2013	431	396	390	9	412	16	12	402	7
2014	540	370	364	8	385	15	12	376	7

Table 2: Base case model specifications: for estimated parameters, the phase of estimation, type of prior, (U, uniform; N, normal; LN, lognormal), mean and CV of the prior, lower bound and upper bound.

Parameter	Phase	Prior	μ	CV	Lower	Upper
$\ln(R0)$	1	U	−	−	5	50
M	3	LN	0.1	0.35	0.01	0.5
g_{max}	2	U	−	−	1	50
$g_{50\%}$	2	U	−	−	0.01	150
$g_{50-95\%}$	2	U			0.01	150
φ	2	U	−	−	0.001	1
$Ln(q^I)$	1	U	−	−	-30	0
$Ln(q^J)$	1	U	−	−	-30	0
$Ln(q^k)$	1	U	−	−	-30	0
L_{50}	1	U	−	−	70	145
L_{95-50}	1	U	−	−	1	50
T_{50}	2	U	−	−	70	125
T_{95-50}	2	U	−	−	0.001	50
D_{50}	2	U	−	−	70	145
D_{95-50}	2	U	−	−	0.01	50
ε	1	N	0	0.4	-2.3	2.3
D_s	1	U	−	−	0.01	10

Table 3: Values for fixed quantities in base case model.

Variable	Value
L_1	75
L_2	120
a	2.99E-08
b	3.303
U^{max}	0/80
σ_{min}	1
σ_{obs}	0.25
$\widetilde{\sigma}$	0.2
H	0.75

Table 4: Summary descriptions for MPD base case and sensitivity runs. The "low", "median", and "high" refer to catch estimates made under assumption 1, 2, 3 in table 4 of Fu et al. (2015), respectively.

Model	Data weighting	Growth model	CSLF	Catch estimates	RDSI and RDLF
1.0	SDNR	exponential	1992–2014	median	No
1.1	TA 1.8 method	exponential	1992–2014	median	No
1.2	SDNR	exponential	2002–2014	median	No
1.3	TA 1.8 method	exponential	2002–2014	median	No
1.4	1.3 weights	inverse-logistic	2002–2014	median	No
1.5	TA 1.8 method	inverse-logistic	2002–2014	median	No
1.6	SDNR	inverse-logistic	2002–2014	median	No
1.7	TA 1.8 method	inverse-logistic	1992–2014	median	No
1.8	TA 1.8 method	inverse-logistic	2002–2014	low	No
1.9	TA 1.8 method	inverse-logistic	2002–2014	high	No
2.0	TA 1.8 method	inverse-logistic	2002–2014	median	Yes

Table 5: MPD estimates for base case and sensitivity trials. "–" indicates parameter fixed and likelihood contributions not used when datasets were removed. SDNRs for CSLF were calculated from mean length.

											Model runs
	1.0	1.1	1.2	1.3	1.4	1.5	1.6	1.7	1.8	1.9	2.0
Likelihoods											
CPUE	4.5	-12.7	-16.0	-12.4	-11.9	-12.0	-14.8	-12.1	-9.6	-13.0	-12.3
PCPUE	-10.8	-14.6	-11.2	-14.8	-14.9	-14.9	-11.9	-14.8	-14.8	-14.8	-14.7
RDSI	–	–	–	–	–	–	–	–	–	–	1.2
CSLF	399.9	17.6	274.2	13.2	14.2	11.6	267.9	15.4	11.9	11.6	11.1
RDLF	–	–	–	–	–	–	–	–	–	–	9.1
Tags	860.3	852.3	856.6	852.3	834.7	834.6	848.7	834.6	834.6	834.7	834.8
Maturity	-50.2	-50.2	-50.2	-50.2	-50.2	-50.2	-50.2	-50.2	-50.2	-50.2	-50.2
Prior on M	28.3	0.8	1.5	0.2	-1.1	-1.1	3.7	-0.6	-0.3	-1.3	-0.7
Prior on ε	21.1	2.2	11.3	2.0	1.5	1.4	8.9	1.4	3.0	0.7	1.7
U penalty	0.0	0.0	0.0	0.0	0.0	0.0	0.0	0.0	0.0	0.0	0.0
ε penalty	0.0	0.0	0.0	0.0	0.0	0.0	0.0	0.0	0.0	0.0	0.0
Total	1253.1	795.3	1066.2	790.4	772.2	769.3	1052.3	773.5	774.5	767.6	779.9
Parameters											
$\ln(R_0)$	13.4	12.9	12.9	12.9	12.9	12.9	13.0	13.0	12.9	13.0	12.9
M	0.216	0.123	0.127	0.120	0.108	0.108	0.137	0.113	0.116	0.103	0.112
T_{50}	91.8	91.9	91.9	91.9	91.9	91.9	91.9	91.9	91.9	91.9	91.9
T_{95-50}	18.7	18.7	18.7	18.7	18.7	18.7	18.7	18.7	18.7	18.7	18.7
D_{50}	125.8	125.0	126.1	125.8	124.7	124.7	125.9	124.0	124.9	124.9	124.9
D_{95-50}	5.0	4.6	4.7	4.5	4.2	4.2	4.6	4.3	4.1	4.2	4.2
D^s	0.9	0.9	0.8	0.8	0.9	0.9	0.8	1.0	0.8	0.8	0.8
L_{50}	–	–	–	–	–	–	–	–	–	–	102.5
L_{95-50}	–	–	–	–	–	–	–	–	–	–	16.1
$\ln(q^I)$	-12.4	-12.8	-12.5	-12.9	-13.1	-13.1	-12.7	-13.0	-13.3	-13.0	-13.0
$\ln(q^{I2})$	-12.3	-12.4	-12.2	-12.5	-12.7	-12.7	-12.3	-12.6	-12.8	-12.7	-12.6
$\ln(q^J)$	–	–	–	–	–	–	–	–	–	–	-14.2
g_α	22.9	25.6	23.5	25.6	–	–	–	–	–	–	–
g_β	7.9	7.0	7.7	7.0	–	–	–	–	–	–	–
φ	0.39	0.41	0.40	0.41	0.38	0.37	0.40	0.37	0.37	0.38	0.38
g_{max}	–	–	–	–	22.1	21.8	42.5	21.6	21.3	22.2	22.5
$g_{50\%}$	–	–	–	–	108.3	108.9	74.1	109.3	110.0	108.1	107.4
$g_{50-95\%}$	–	–	–	–	52.7	51.8	90.6	51.2	50.1	53.1	53.9

Table 5 continued.

	1.0	1.1	1.2	1.3	1.4	1.5	1.6	1.7	1.8	1.9	2.0
Indicators											
B_0	871	1209	1128	1243	1338	1344	1097	1291	1194	1520	1301
Bcurrent	425	434	342	442	512	518	371	499	552	520	498
Bcurrent/B_0	0.49	0.36	0.30	0.36	0.38	0.38	0.34	0.39	0.46	0.34	0.38
rB_0	673	1057	990	1093	1190	1196	946	1140	1050	1361	1150
rBcurrent	222	266	208	277	346	351	224	329	382	347	329
rBcurrent/rB_0	0.33	0.25	0.21	0.25	0.29	0.29	0.24	0.29	0.36	0.26	0.29
Ucurrent	0.19	0.16	0.20	0.15	0.12	0.12	0.18	0.13	0.11	0.12	0.13
Weights											
CPUE	0.046	0.2	0.253	0.2	0.2	0.2	0.23	0.2	0.2	0.2	0.2
PCPUE	0.16	0.2	0.164	0.2	0.2	0.2	0.17	0.2	0.2	0.2	0.2
RDSI	–	–	–	–	–	–	–	–	–	–	0.208
CSLF	0.197	0.004	0.208	0.008	0.008	0.006	0.20	0.004	0.006	0.006	0.006
RDLF	–	–	–	–	–	–	–	–	–	–	0.01
Tags	0.2	0.2	0.2	0.2	0.2	0.2	0.20	0.2	0.2	0.2	0.2
Maturity	3.508	3.508	3.508	3.508	3.508	3.508	3.51	3.508	3.508	3.508	3.508
SDNRs											
CPUE	1.00	0.80	1.00	0.84	0.88	0.88	0.99	0.86	1.08	0.77	0.85
PCPUE	1.01	0.72	1.00	0.70	0.69	0.69	1.00	0.70	0.70	0.70	0.71
RDSI	–	–	–	–	–	–	–	–	–	–	0.86
CSLF	1.00	0.22	1.00	0.22	0.23	0.21	0.99	0.21	0.21	0.21	0.20
CSLF (mean)	4.18	1.00	4.39	1.00	1.11	1.00	4.41	1.00	1.00	1.00	1.00
RDLF	–	–	–	–	–	–	–	–	–	–	1.00
Tags	1.05	1.08	1.05	1.08	1.12	1.12	1.05	1.12	1.12	1.12	1.12
Maturity	1.00	1.00	1.00	1.00	1.00	1.00	1.00	1.00	1.00	1.00	1.00

Table 6: Summary of the marginal posterior distributions from the MCMC chain from the base case (1.5). The columns show the minimum values observed in the 1000 samples, the maxima, the 5th and 95th percentiles, and the medians. Biomass is in tonnes.

	Min	5%	Median	95%	Max
Parameters					
f	774.0	779.7	786.2	794.4	806.9
$\ln(R0)$	12.6	12.8	13.0	*13.1*	13.4
M	0.081	0.095	0.108	*0.123*	0.140
D_{50}	114.7	122.0	124.5	*126.6*	130.1
D_{95-50}	1.6	2.9	4.8	*7.6*	14.3
D^s	0.0	0.4	0.9	1.4	2.7
L_{50}	88.4	90.5	91.8	92.9	94.2
L_{95-50}	13.3	16.2	18.9	*21.8*	25.5
$\ln(q^I)$	-13.6	-13.4	-13.2	*-13.0*	-12.8
$\ln(q^{II})$	-13.5	-13.1	-12.8	*-12.5*	-12.3
φ	0.31	0.35	0.38	*0.42*	0.47
g_{max}	16.7	19.4	22.4	*27.0*	29.9
$g_{50\%}$	92.4	99.7	107.7	113.4	118.1
$g_{50-95\%}$	39.8	46.4	53.2	61.3	71.4
	Min	5%	Median	95%	Max
B_0	1135	1264	1381	1522	1765
B_{msy}	310	341	373	411	482
$B_{current}$	311	433	561	745	1153
$B_{current}/B_0$	0.25	0.33	0.41	0.50	0.68
$B_{current}/B_{msy}$	0.89	1.22	1.51	1.87	2.57
B_{msy}/B_0	0.26	0.26	0.27	0.28	0.28
B_0^r	975	1108	1228	1366	1559
B_{msy}^r	142	176	211	250	298
$B_{current}^r$	190	283	385	531	839
$B_{current}^r/B_0^r$	0.17	0.24	0.32	0.41	0.57
$B_{current}^r/B_{msy}^r$	0.87	1.34	1.83	2.53	3.95
B_{msy}^r/B_0^r	0.13	0.15	0.17	0.19	0.21
MSY	47	52	57	65	86
U_{msy}	0.15	0.19	0.23	0.30	0.40
$U_{\%40B_0}$	0.09	0.11	0.13	0.16	0.20
$U_{current}$	0.05	0.08	0.11	0.15	0.21

Table 7: Summary of the marginal posterior distributions from the MCMC chain from model 1.6. The columns show the minimum values observed in the 1000 samples, the maxima, the 5th and 95th percentiles, and the medians. Biomass is in tonnes.

	Min	5%	Median	95%	Max
Parameters					
f	1059.1	1064.8	1071.3	1079.5	1094.5
$\ln(R0)$	12.8	12.9	13.0	13.1	13.3
M	0.116	0.126	0.137	0.150	0.178
D_{50}	124.9	125.4	125.9	126.2	126.8
D_{95-50}	3.9	4.2	4.6	5.0	5.4
D^s	0.6	0.7	0.8	0.9	1.0
L_{50}	88.9	90.5	91.8	92.9	94.2
L_{95-50}	13.8	16.3	18.9	21.8	26.2
$\ln(q^I)$	-13.1	-12.9	-12.7	-12.6	-12.5
$\ln(q^{II})$	-12.7	-12.5	-12.3	-12.2	-12.0
φ	0.34	0.38	0.41	0.45	0.49
g_{max}	22.0	27.9	42.2	57.1	60.0
$g_{50\%}$	54.5	59.2	74.5	94.1	104.8
$g_{50-95\%}$	65.5	77.7	89.1	97.8	100.0
Indicators					
B_0	974	1056	1111	1175	1268
B_{msy}	275.4	300	315	331	353
$B_{current}$	277	329	388	463	580
$B_{current}/B_0$	0.2	0.30	0.35	0.41	0.50
$B_{current}/B_{msy}$	0.88	1.05	1.23	1.46	1.80
B_{msy}/B_0	0.27	0.28	0.28	0.29	0.29
B_0^r	801	898	955	1018	1106
B_{msy}^r	99	133	155	175	195
$B_{current}^r$	153	194	237	294	380
$B_{current}^r/B_0^r$	0.2	0.21	0.25	0.30	0.39
$B_{current}^r/B_{msy}^r$	0.9	1.19	1.54	2.04	2.98
B_{msy}^r/B_0^r	0.1	0.14	0.16	0.18	0.19
MSY	50	53	55	59	67
U_{msy}	0.23	0.26	0.30	0.36	0.49
$U_{\%40B0}$	0.14	0.16	0.18	0.20	0.26
$U_{current}$	0.11	0.14	0.18	0.21	0.26

Table 8: Summary of the marginal posterior distributions from the MCMC chain from model 1.7. The columns show the minimum values observed in the 1000 samples, the maxima, the 5th and 95th percentiles, and the medians. Biomass is in tonnes.

	Min	5%	Median	95%	Max
Parameters					
f	779.3	785.6	792.5	801.2	813.9
$\ln(R0)$	12.7	12.8	13.0	13.2	13.5
M	0.087	0.099	0.113	0.129	0.156
D_{50}	116.9	120.9	123.6	126.0	128.5
D_{95-50}	1.4	2.8	5.0	8.4	16.4
D^s	0.0	0.4	1.0	1.6	2.8
L_{50}	89.0	90.6	91.8	93.0	94.2
L_{95-50}	13.9	16.2	18.8	21.7	25.5
$\ln(q^I)$	-13.7	-13.4	-13.1	-12.9	-12.6
$\ln(q^{II})$	-13.6	-13.1	-12.8	-12.5	-12.1
φ	0.32	0.35	0.38	0.42	0.46
g_{max}	16.2	19.1	22.2	26.9	30.0
$g_{50\%}$	94.0	100.0	108.0	113.8	120.2
$g_{50-95\%}$	37.2	45.5	52.5	60.6	67.4
Indicators					
B_0	1087	1218	1341	1502	1894
B_{msy}	294.0	328	361	405	503
$B_{current}$	303	421	555	757	1194
$B_{current}/B_0$	0.2	0.33	0.42	0.52	0.69
$B_{current}/B_{msy}$	0.92	1.22	1.54	1.92	2.51
B_{msy}/B_0	0.26	0.26	0.27	0.27	0.28
B_0^r	940	1060	1184	1334	1675
B_{msy}^r	102	160	197	237	298
$B_{current}^r$	167	268	373	534	916
$B_{current}^r/B_0^r$	0.2	0.24	0.32	0.41	0.59
$B_{current}^r/B_{msy}^r$	0.8	1.36	1.91	2.68	4.19
B_{msy}^r/B_0^r	0.1	0.15	0.17	0.18	0.20
MSY	48	52	58	67	88
U_{msy}	0.15	0.20	0.25	0.32	0.52
$U_{\%40B_0}$	0.09	0.11	0.14	0.17	0.25
$U_{current}$	0.05	0.08	0.11	0.15	0.23

Table 9: Summary of key indicators from the projection for the base case (1.5) MCMC with future commercial catch assumed to be the same the current catch: projected biomass as a percentage of the virgin and current stock status, for spawning stock and recruit-sized biomass. Numbers in the bracket gives the 90% credible interval.

				Year
	2014	2015	2016	2017
$B_{proj}\%B_0$	0.41 (0.32–0.53)	0.41 (0.32–0.54)	0.42 (0.32–0.55)	0.43 (0.32–0.56)
$B_{proj}\%B_{msy}$	1.51 (1.17–1.95)	1.53 (1.18–1.98)	1.56 (1.19–2.03)	1.58 (1.19–2.07)
$\Pr(>B_{msy})$	1.00	1.00	1.00	1.00
$\Pr(>B_{current})$	0.00	0.84	0.81	0.81
$\Pr(>40\%B_0)$	0.55	0.60	0.64	0.67
$\Pr(<20\%B_0)$	0.00	0.00	0.00	0.00
$\Pr(<10\%B_0)$	0.00	0.00	0.00	0.00
$\%B_0^r$	0.32(0.23–0.43)	0.32 (0.23–0.44)	0.33 (0.24–0.44)	0.33 (0.24–0.45)
$\%B_{msy}^r$	1.83 (1.27–2.70)	1.86 (1.27–2.77)	1.89 (1.28–2.82)	1.92 (1.30–2.85)
$\Pr(>B_{msy}^r)$	1.00	1.00	1.00	1.00
$\Pr(>B_{current}^r)$	0.00	0.72	0.80	0.90
$\Pr(U_{proj}>U_{40\%B0})$	0.14	0.08	0.04	0.02

Table 10: Summary of key indicators from the projection for MCMC 1.5 with future commercial catch assumed to be 10% higher than current commercial catch: projected biomass as a percentage of the virgin and current stock status, for spawning stock and recruit-sized biomass. Numbers in the bracket gives the 90% credible interval.

				Year
	2014	2015	2016	2017
$B_{proj}\%B_0$	0.41 (0.32–0.52)	0.41 (0.32–0.53)	0.42 (0.32–0.54)	0.42 (0.32–0.54)
$B_{proj}\%B_{msy}$	1.5 (1.2–2.0)	1.5 (1.2–2.0)	1.5 (1.2–2.0)	1.6 (1.2–2.0)
$\Pr(>B_{msy})$	1.00	1.00	1.00	1.00
$\Pr(>B_{current})$	0.00	0.99	0.85	0.76
$\Pr(>40\%B_0)$	0.55	0.58	0.60	0.62
$\Pr(<20\%B_0)$	0.00	0.00	0.00	0.00
$\Pr(<10\%B_0)$	0	0	0	0
$\%B_0^r$	0.32 (0.23–0.43)	0.32 (0.23–0.44)	0.32 (0.23–0.44)	0.32 (0.23–0.44)
$\%B_{msy}^r$	1.8 (1.3–2.7)	1.9 (1.3–2.8)	1.9 (1.3–2.8)	1.9 (1.3–2.8)
$\Pr(>B_{msy}^r)$	1.00	1.00	1.00	1.00
$\Pr(>B_{current}^r)$	0.00	0.64	0.65	0.71
$\Pr(U_{proj}>U_{40\%B0})$	0.22	0.32	0.31	0.31

Table 11: Summary of key indicators from the projection for MCMC 1.5 with future commercial catch assumed to be the 20% higher than the current commercial catch: projected biomass as a percentage of the virgin and current stock status, for spawning stock and recruit-sized biomass. Numbers in the bracket gives the 90% credible interval.

	Year			
	2014	2015	2016	2017
$B_{proj} \% B_0$	0.41 (0.32–0.52)	0.41 (0.32–0.53)	0.41 (0.31–0.53)	0.41 (0.31–0.54)
$B_{proj} \% B_{msy}$	1.5 (1.2–2.0)	1.5 (1.2–2.0)	1.5 (1.2–2.0)	1.5 (1.1–2.0)
$\Pr(> B_{msy})$	1.00	1.00	1.00	1.00
$\Pr(> B_{current})$	0.00	0.91	0.63	0.594
$\Pr(> 40\% B_0)$	0.55	0.57	0.57	0.58
$\Pr(< 20\% B_0)$	0.00	0.00	0.00	0.00
$\Pr(< 10\% B_0)$	0.00	0.00	0.00	0.00
$\% B_0^r$	0.32 (0.23–0.43)	0.32 (0.23–0.43)	0.32 (0.23–0.44)	0.32 (0.22–0.44)
$\% B_{msy}^r$	1.8 (1.3–2.7)	1.8 (1.3–2.7)	1.8 (1.2–2.8)	1.8 (1.2–2.8)
$\Pr(> B_{msy}^r)$	1.00	1.00	1.00	1.00
$\Pr(> B_{current}^r)$	0.00	0.57	0.50	0.47
$\Pr(U_{proj} > U_{40\% B0})$	0.22	0.45	0.45	0.45
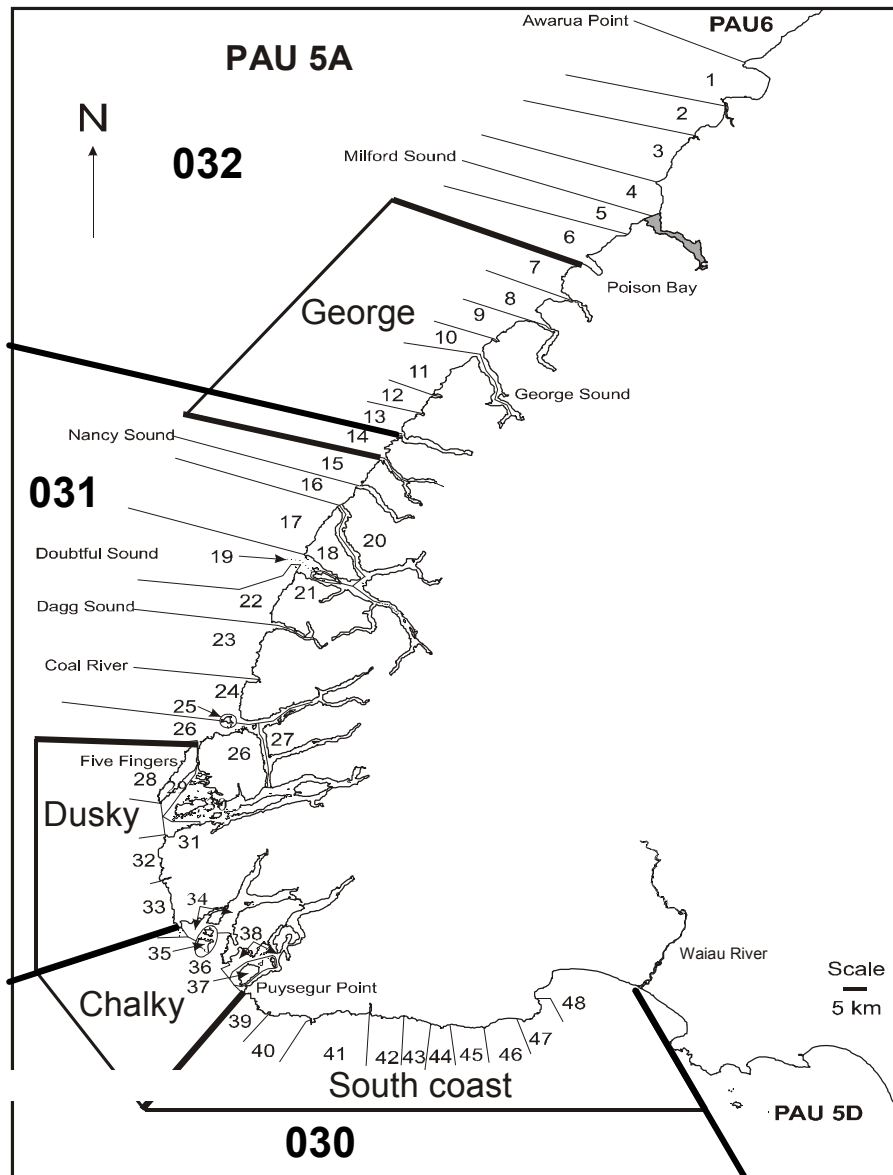
Figure 1: Map of research strata for PAU 5A.
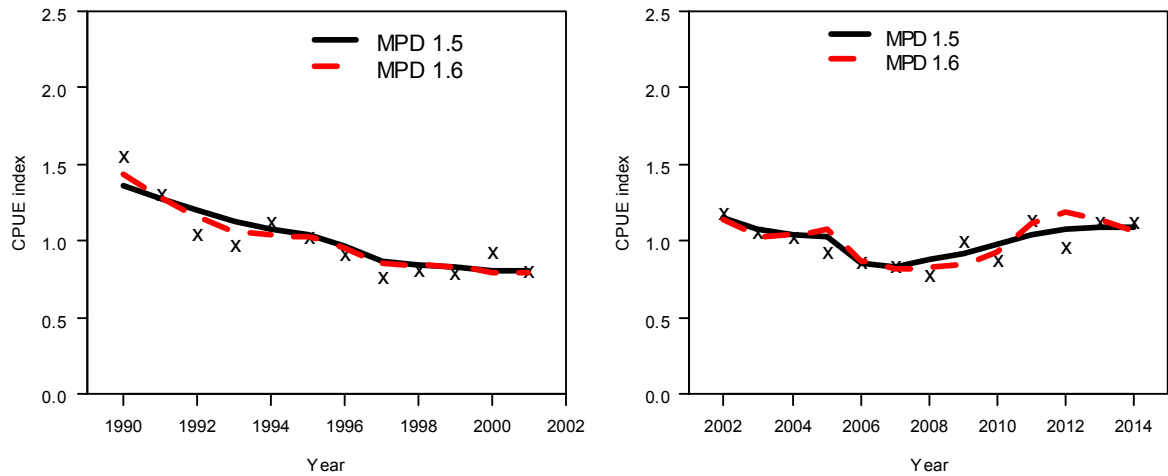
Figure 2: Fits to the CPUE indices 1990–2001 (left) and 2002–2014 indices (right), for MPD 1.5 (base case) and MPD 1.6.

MPD 1.5
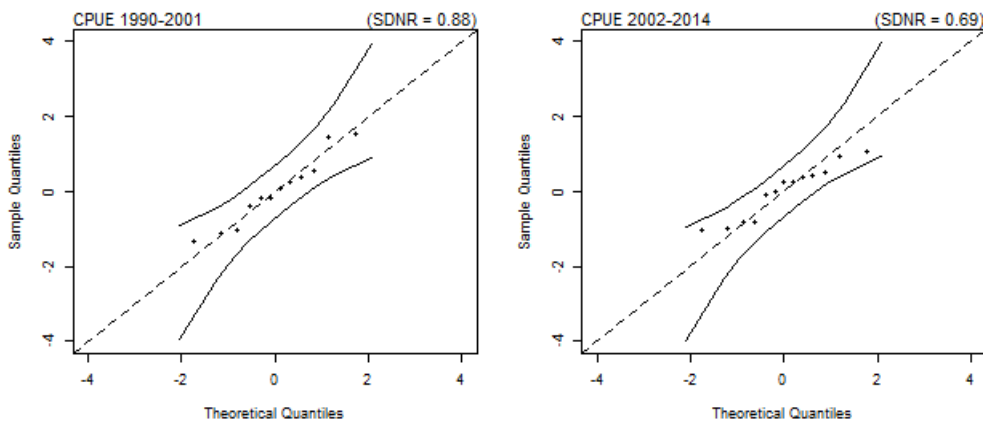
MPD 1.6
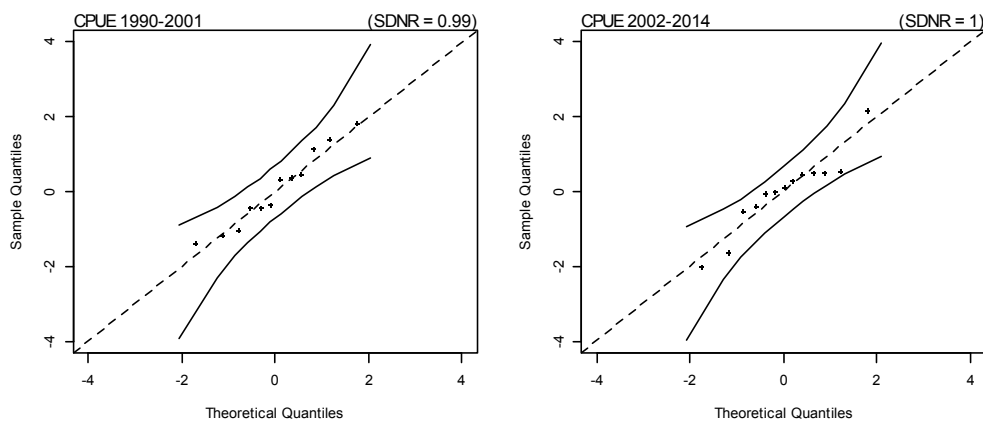
Figure 3: Normal Q-Q plots for residuals from fits to the two CPUE datasets for MPD 1.5 (base case) and MPD 1.6.
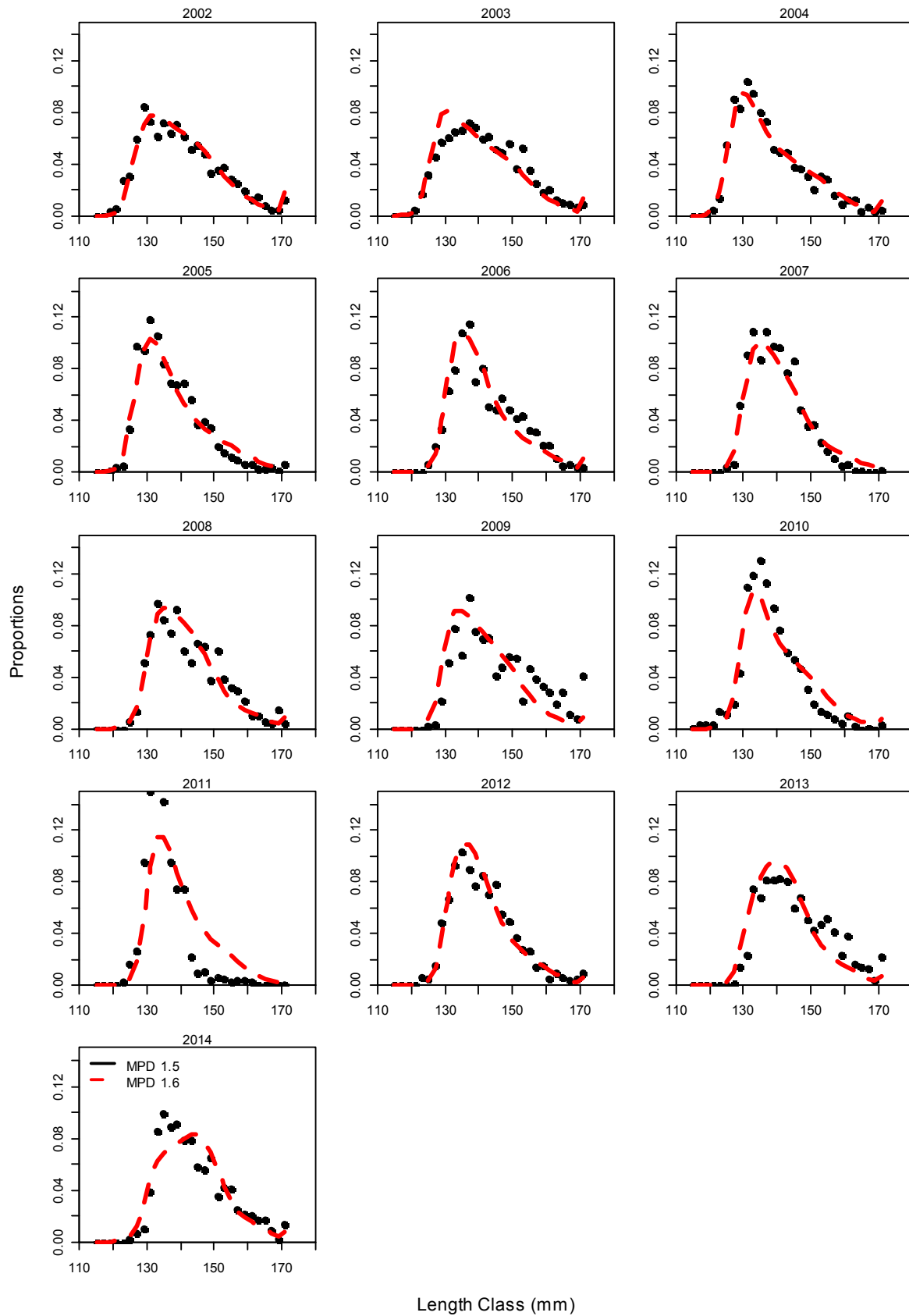
Figure 4: Fits to the CSLF data 2002–2014 for MPD 1.5 (base case) and MPD 1.6.

The 2014 stock assessment of paua (*Haliotis iris*) for Chalky and South Coast in PAU 5A • 37
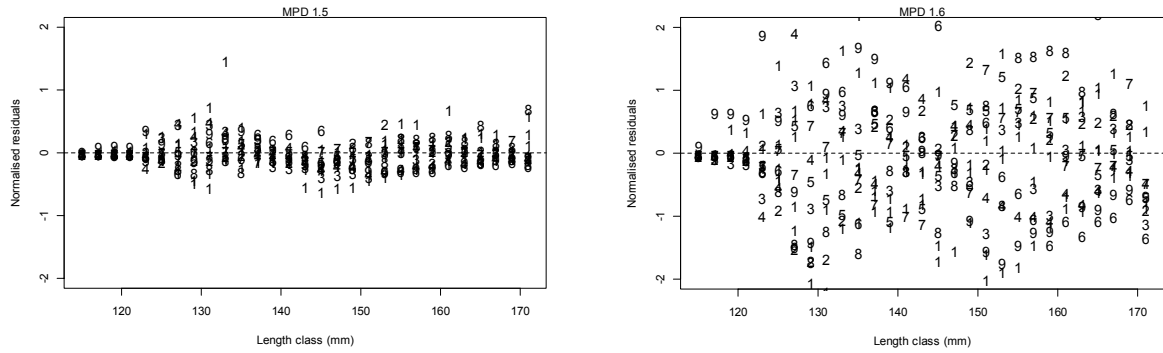
Figure 5: Normalised residuals from fits to the CSLF data for MPD 1.5 (base case) and MPD 1.6. The number indicates the year of the CSLF sample, e.g. "1" indicates the first year, and so on.
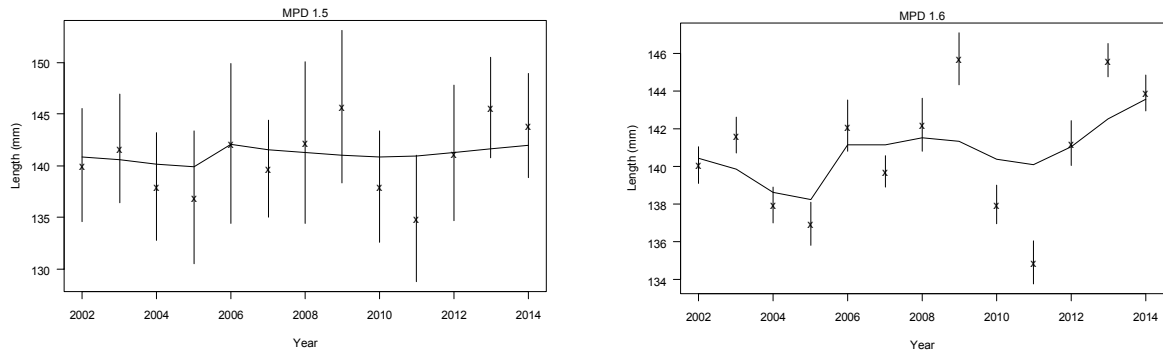
Figure 6: Observed and predicted mean length by year for the CSLF datasets for MPD 1.5 (base case) and MPD 1.6. The vertical lines are confidence intervals for the mean length.
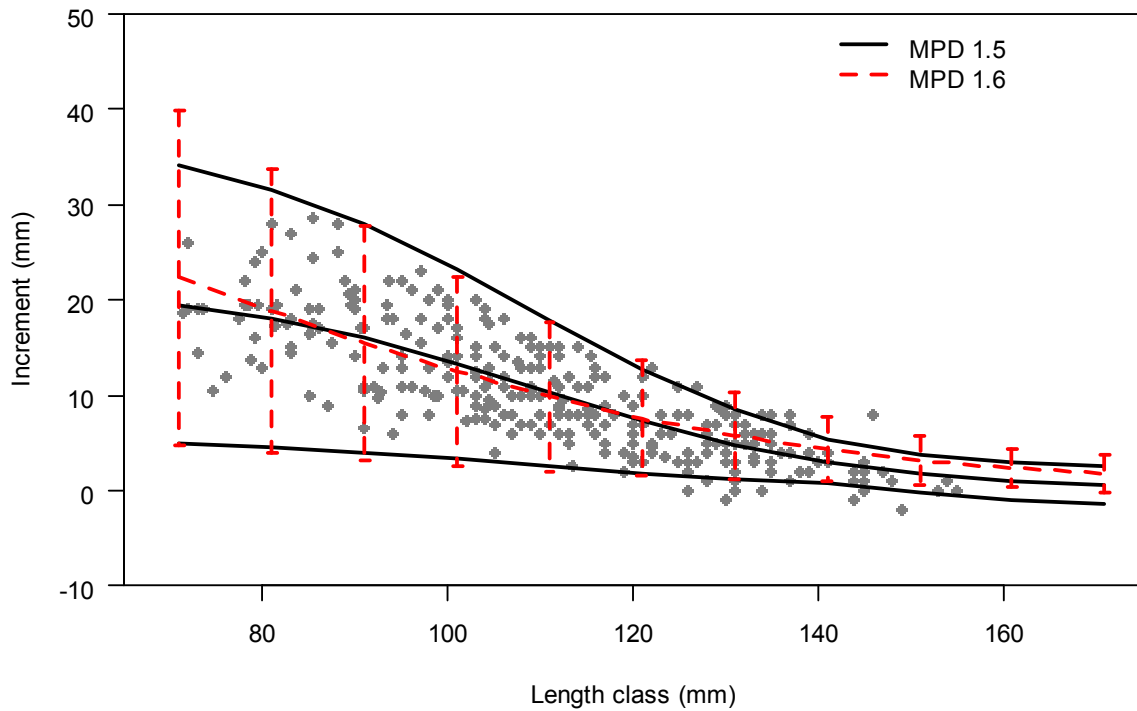
Figure 7: Fits to the tag-recapture data for MPD 1.5 (base case) and MPD 1.6: the dots are observed mean annual increments; the lines are the fitted growth curve with 95% confidence intervals at selected sizes.

MPD 1.5
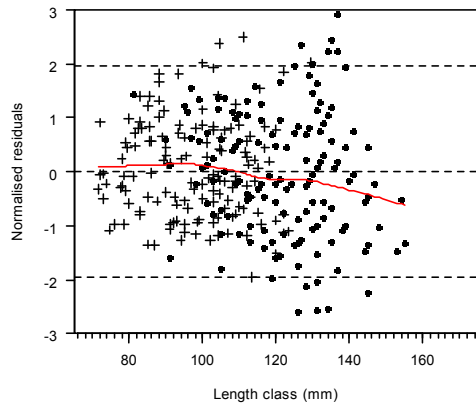
MPD 1.6
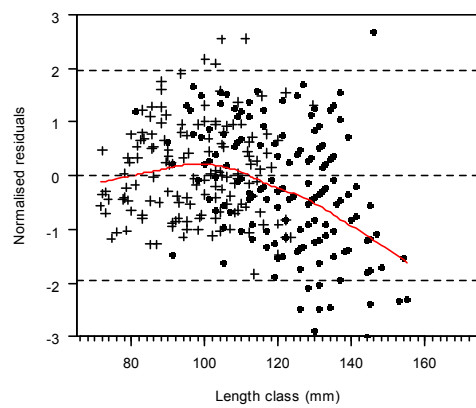
Figure 8: Normalised residuals by length class from fits to growth data for MPD 1.5 (base case) and MPD 1.6. The crosses represent isotopic data and dots represent tag-recapture data. The red line is a fitted smoother through the residuals.
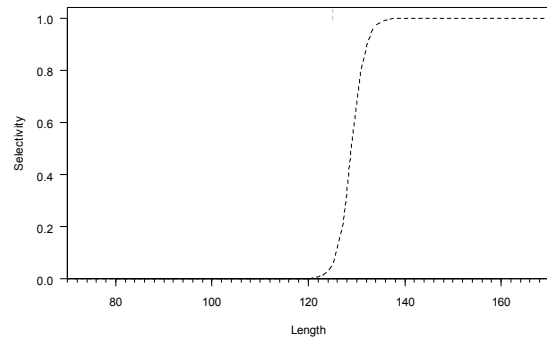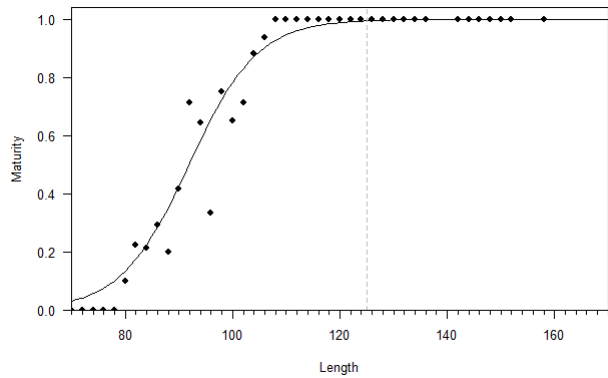
Figure 9: MPD fits to the maturity data (left: dots are observed proportion mature at length with confidence interval; the line is predicted proportion of maturity at length) and estimated selectivity for commercial catch (right: the selectivity is shifted to the right by an estimated 4 mm due to the increase of MHS since 2007) for MPD 1.5
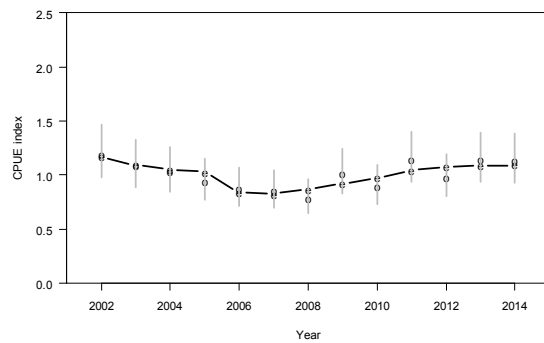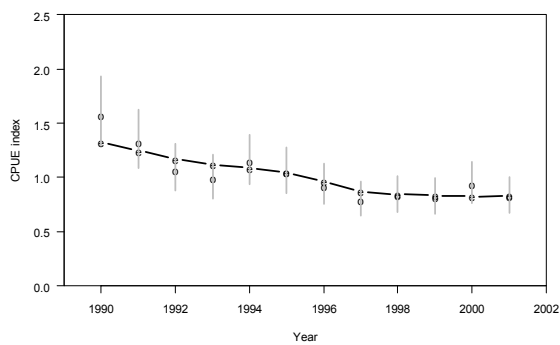
Figure 10: Fits to the CPUE indices for 1990–2001 (left) and 2002–2014 for MPD 1.7.
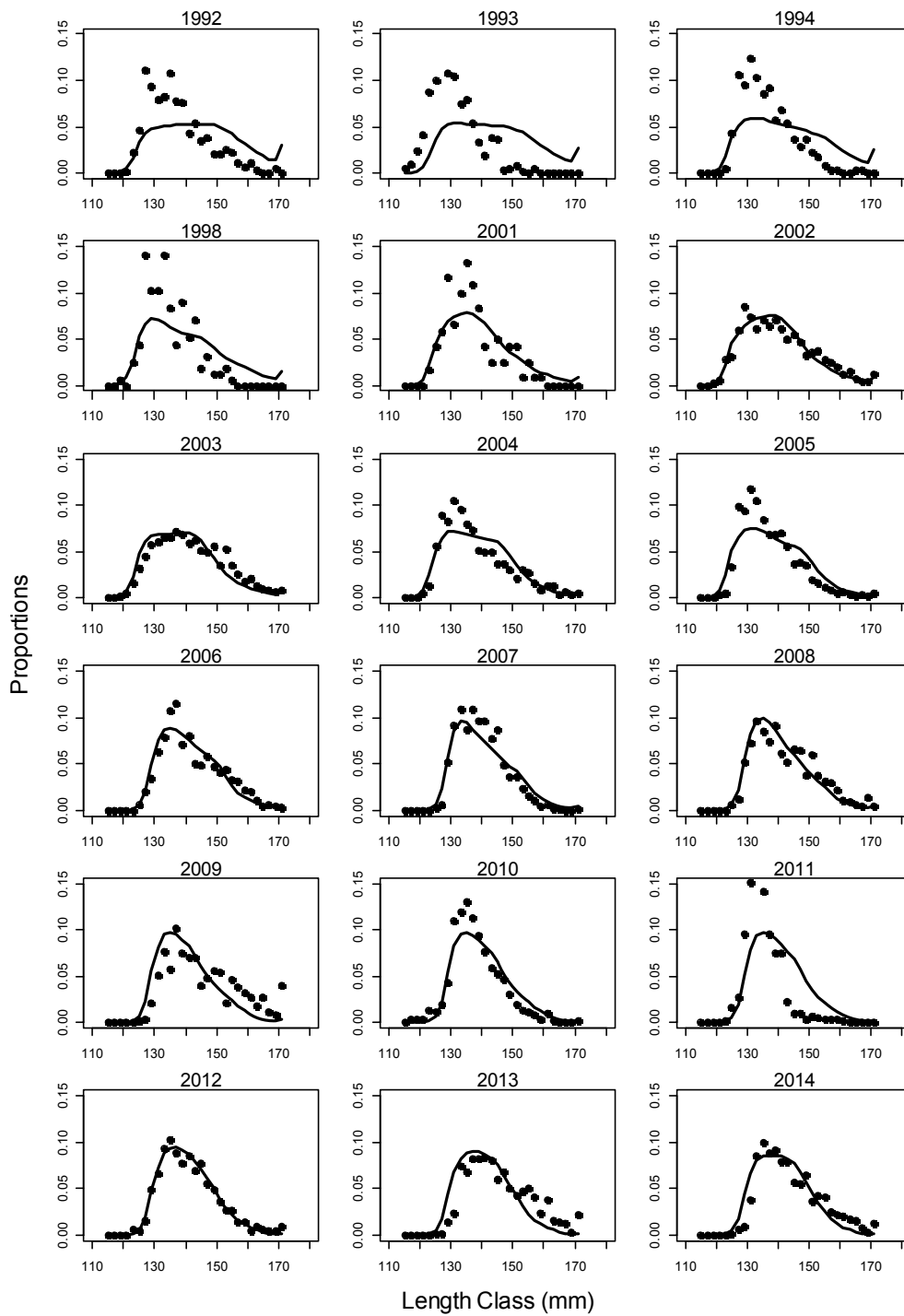
Figure 11: Fits to the CSLF data 1992–2014 for MPD 1.7.
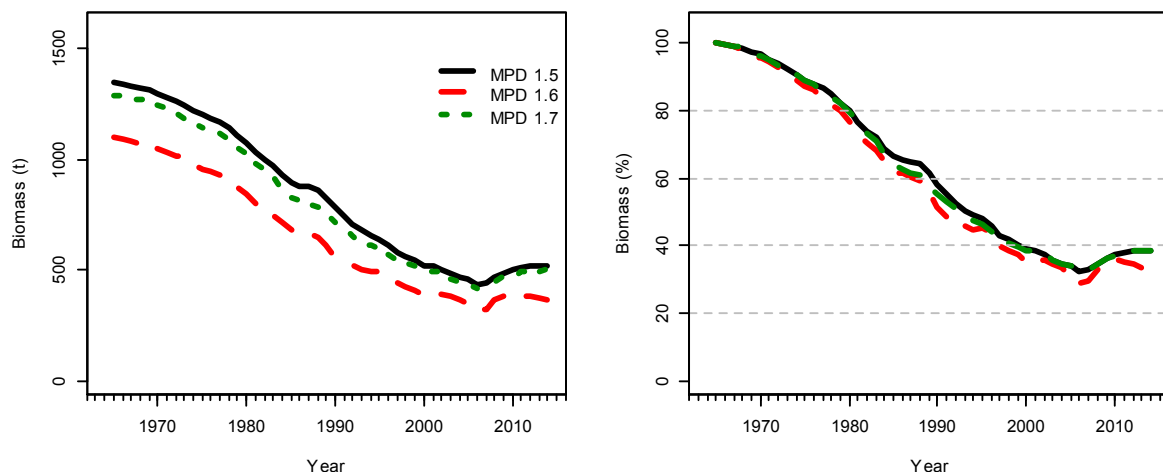
Figure 12: Comparison of estimated spawning biomass (left) and spawning biomass as a percent of B$_0$ for MPD 1.5, MPD 1.6, and MPD 1.7.
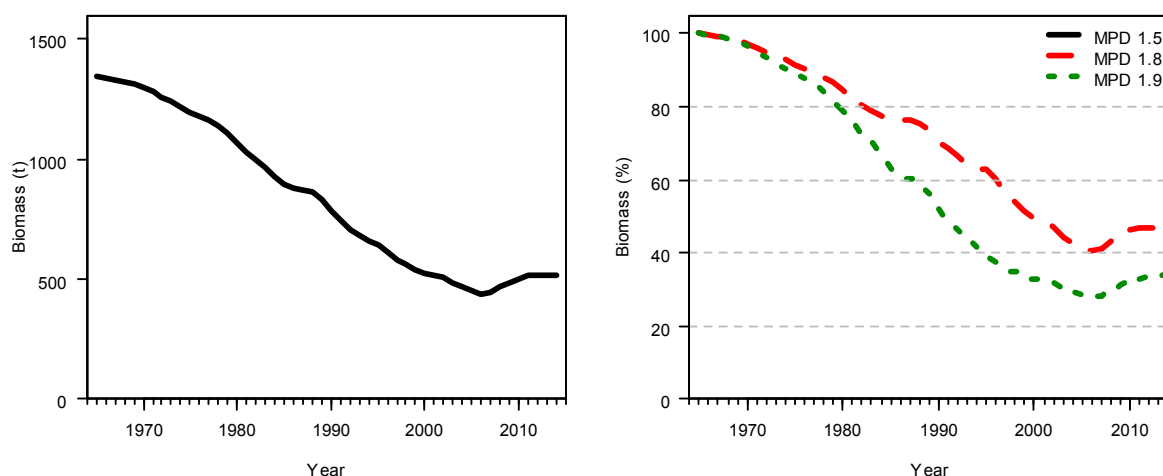
Figure 13: Comparison of estimated spawning biomass (left) and spawning biomass as a percent of B$_0$ for MPD 1.5, MPD 1.8, and MPD 1.9.
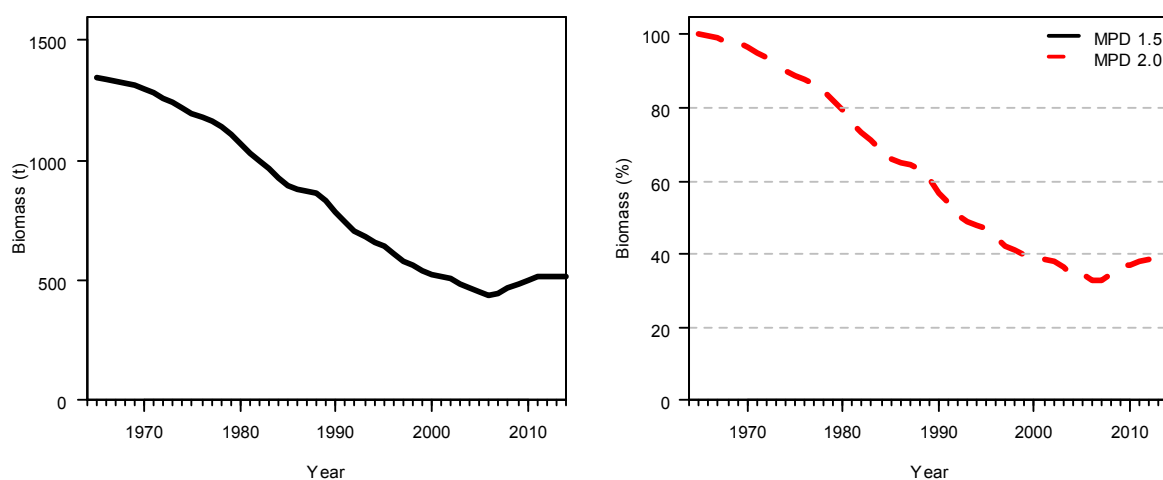
Figure 14: Comparison of estimated spawning biomass (left) and spawning biomass as a percent of B$_0$ to the CSLF 2002–2014 for MPD 1.5 and MPD 2.0.
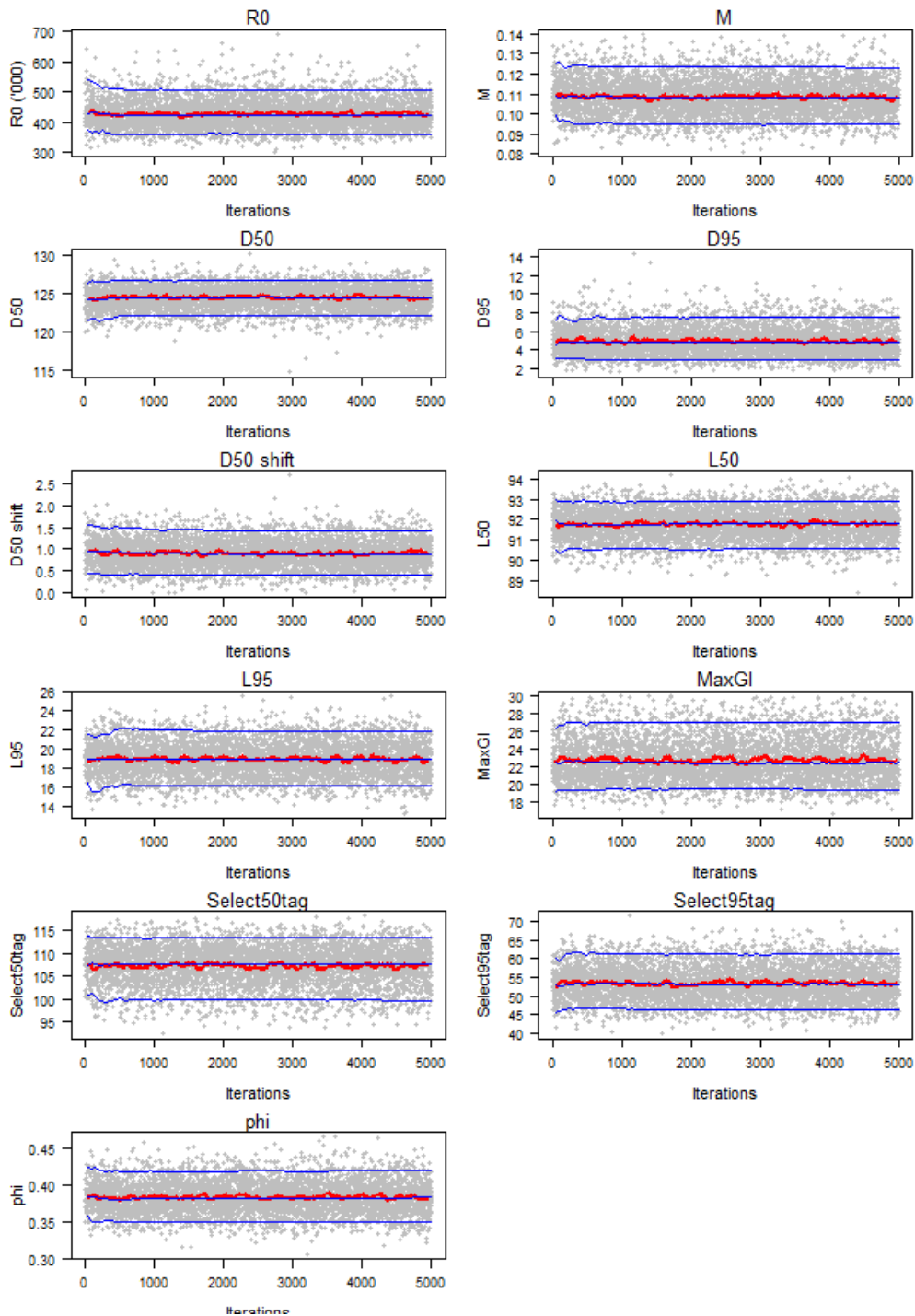
Figure 15: Traces of estimated parameters (left) and biomass indicators (right) for MCMC 1.5 (base case). Blue lines are running 5, 50, and 95% quantiles of the chain and red lines are the moving average of the chain.
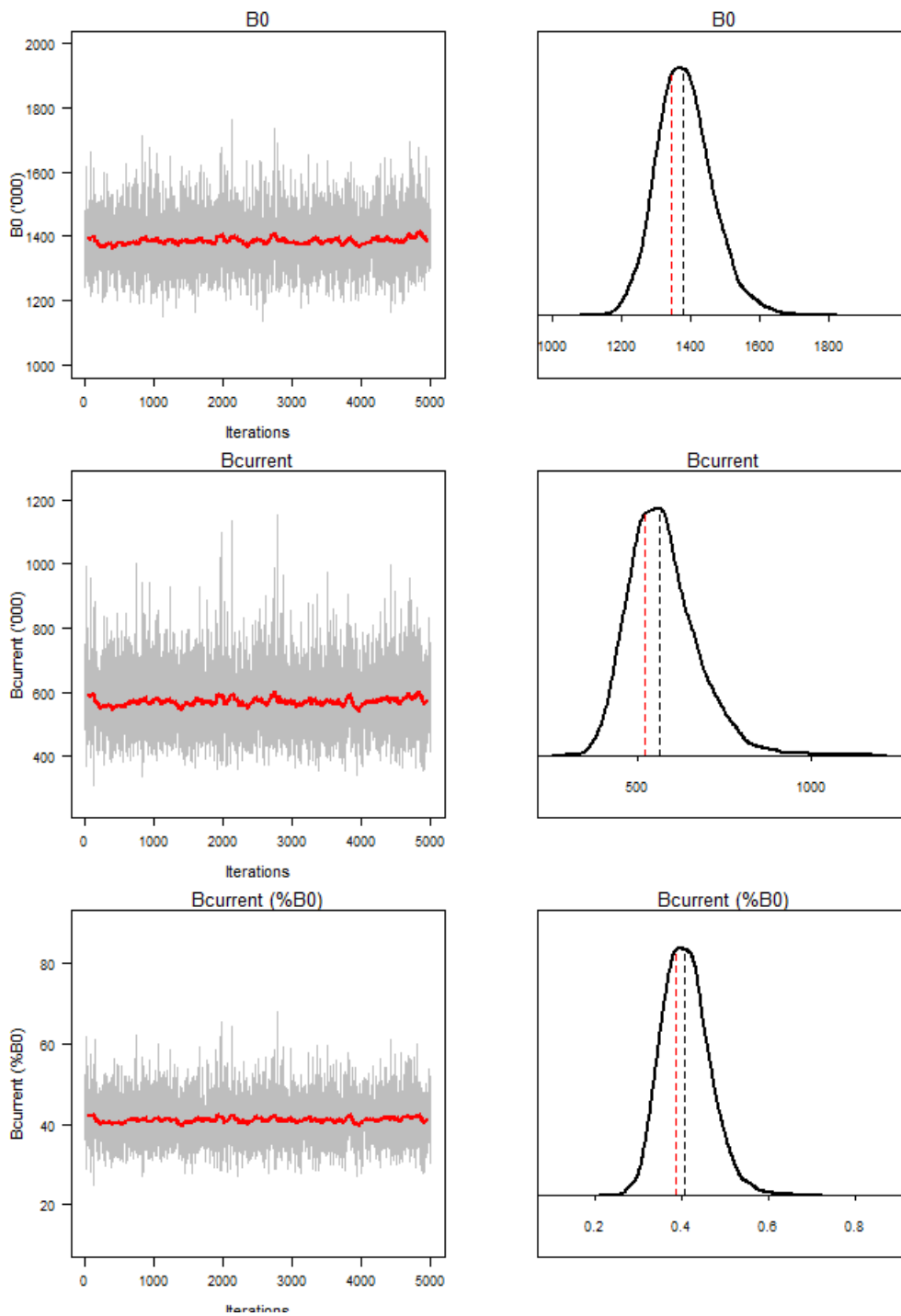
Figure 16: Traces (left) and posterior density (right) of estimated B₀, Bcurrent, and Bcurrent as a percent of B₀ for MCMC 1.5 (base case). The red lines are the moving average of the chain; black dashed lines indicate median of the posterior distribution and red dashed lines indicate the MPD estimate.
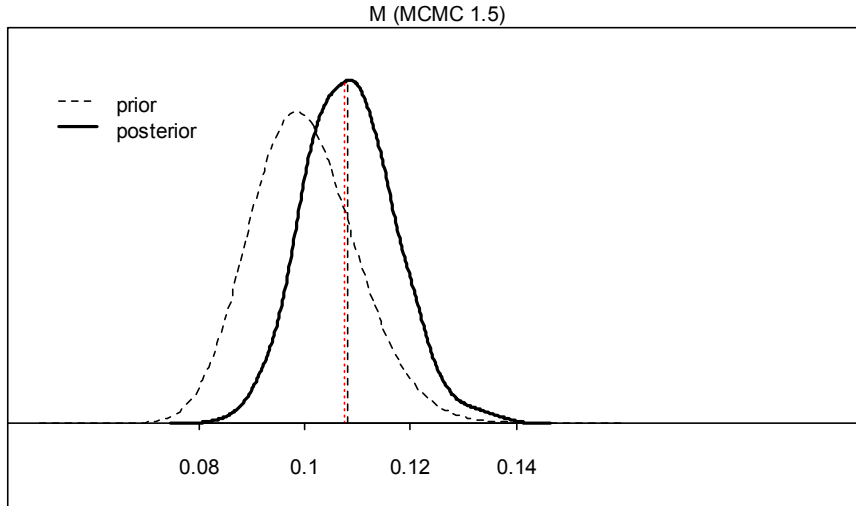
Figure 17: Posterior and prior distributions of estimated natural mortality (M) for MCMC 1.5 (base case). The black dashed vertical line is the posterior median and the red dashed vertical line is the MPD estimates.
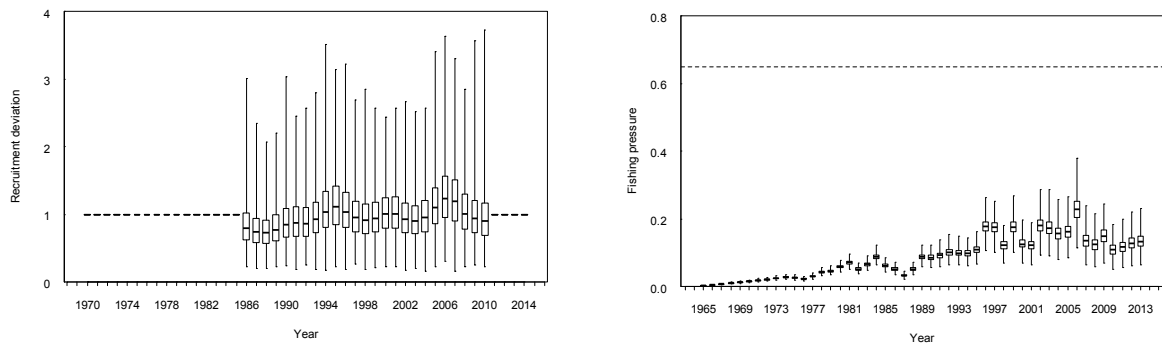
Figure 18: Posterior distributions of recruitment deviations (left), and exploitation rates (right) for MCMC 1.5. The box shows the median of the posterior distribution (horizontal bar), the 25th and 75th percentiles (box), with the whiskers representing the full range of the distribution. Recruitment deviations were estimated for 1980–2008, and fixed at 1 for other years.
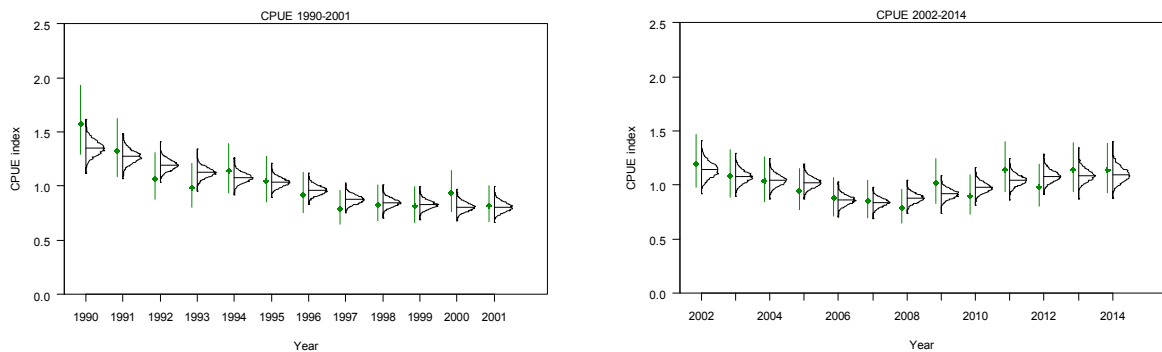
Figure 19: Posterior distributions of model predicted CPUE indices for 1990–2001 (left) and 2002–2012 (right) for MCMC 1.5 (Medians are shown as horizontal lines). Dots are observed CPUE indices and vertical lines are 95% confidence intervals.
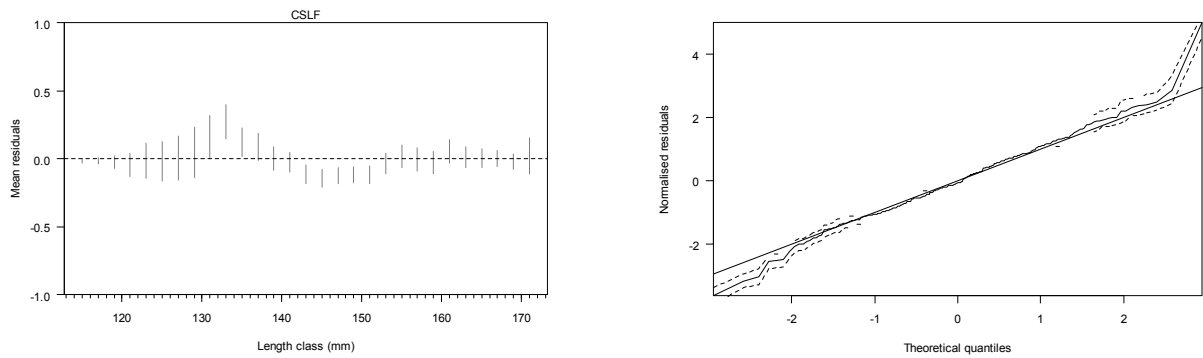
Figure 20: 95% credible intervals of the posterior distributions of mean residuals (across all years) of fits to the CSLF data (left) and the QQ quantiles of posterior distributions of residuals of fits to the tag recapture data (right) from MCMC 1.5.
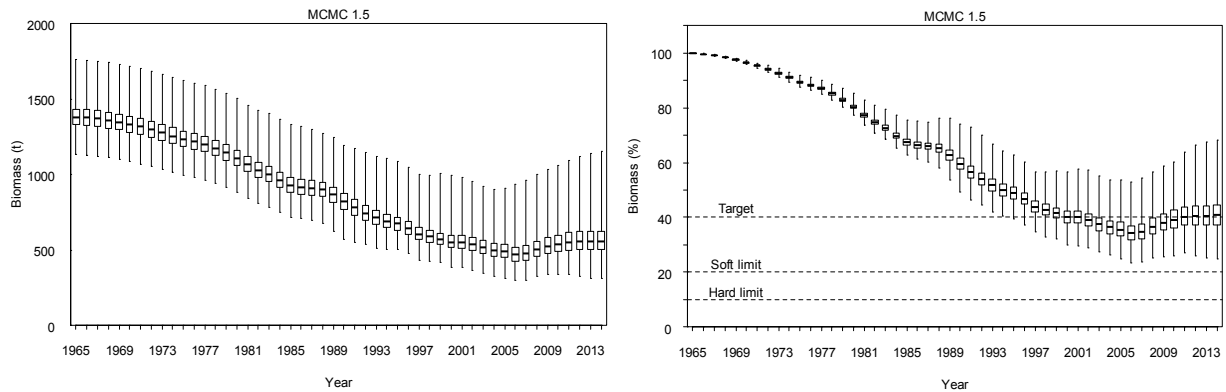
Figure 21: Posterior distributions of spawning stock biomass and spawning stock biomass as a percentage of virgin level from MCMC 1.5. The box shows the median of the posterior distribution (horizontal bar), the 25th and 75th percentiles (box), with the whiskers representing the full range of the distribution.
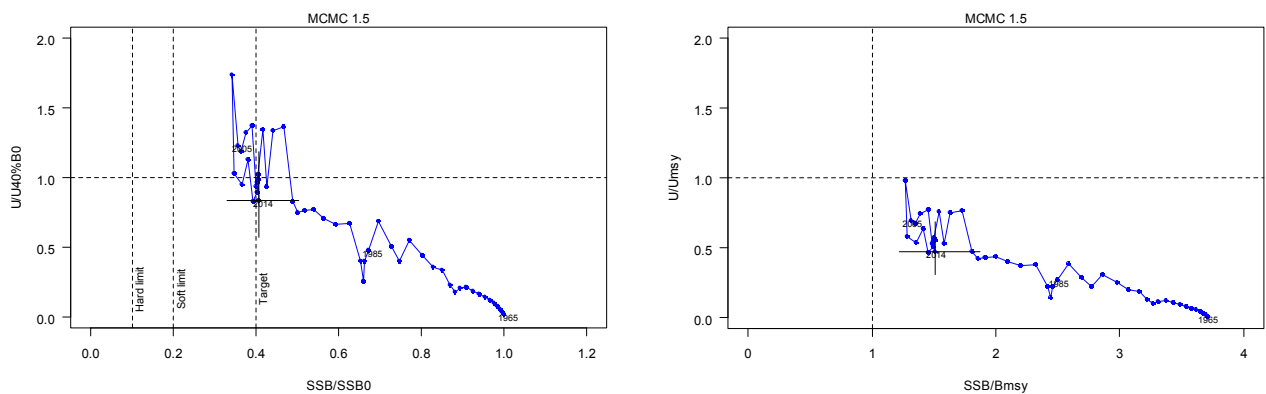
Figure 22: Trajectory of exploitation rate as a ratio of $U_{\%40B0}$ and spawning stock biomass as a ratio of B_0 (left), and exploitation rate as a ratio of U_{msy} and spawning stock biomass as a ratio of B_{msy} from the start of assessment period 1965 to 2014 for MCMC 1.5 (base case). The vertical lines at 10%, 20% and 40% B_0 represent the soft limit, the hard limit, and the target. Estimates are based on MCMC median and the 2014 90% CI is shown by the cross line.
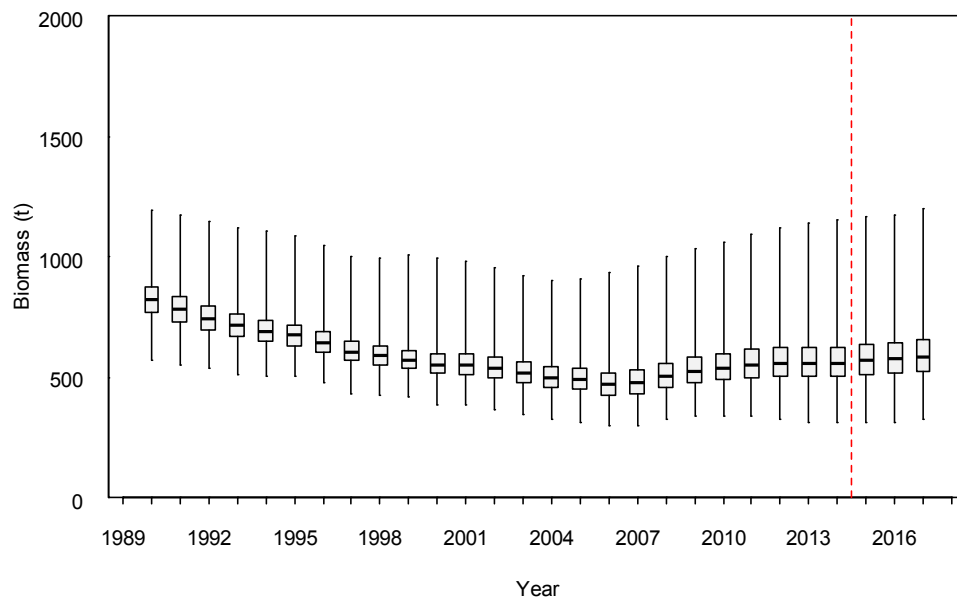
Figure 23: Posterior distributions of projected spawning stock biomass with future commercial catch set to be the same as current catch for MCMC 1.5 (base case). The box shows the median of the posterior distribution (horizontal bar), the 25th and 75th percentiles (box), with the whiskers representing the full range of the distribution.

APPENDIX A: SUMMARY OF RESULTS FOR MPD SENSITIVITY
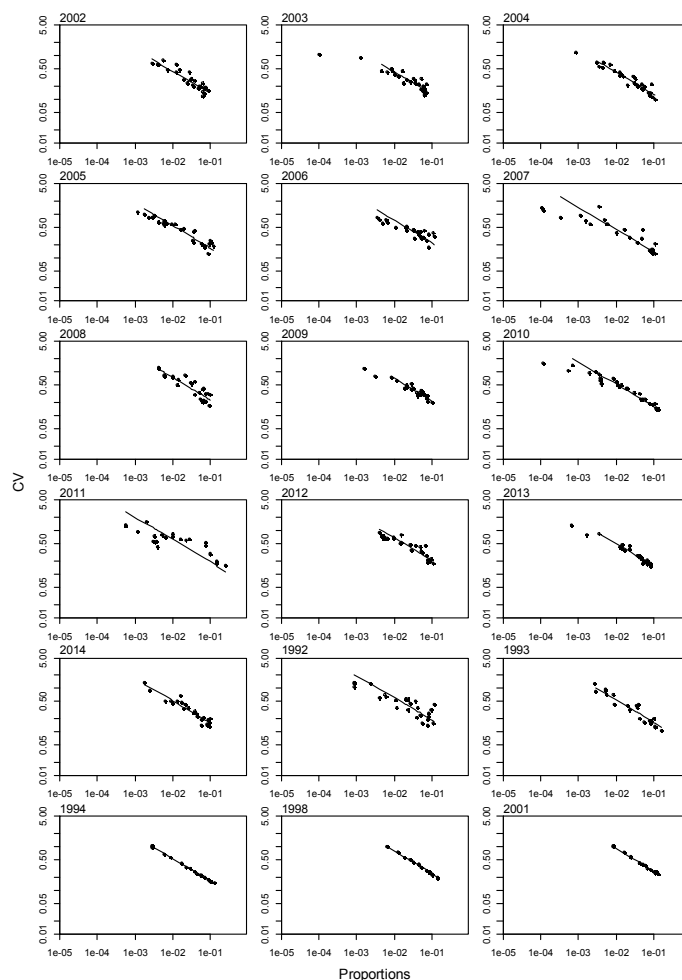
Figure A1: Estimated proportions versus CVs for the commercial catch length frequency distributions for PAU 5A south. Lines indicate the best least squares fit for the effective sample size of the multinomial distribution. Length frequency data for 2002–2012 were included in the base case model.
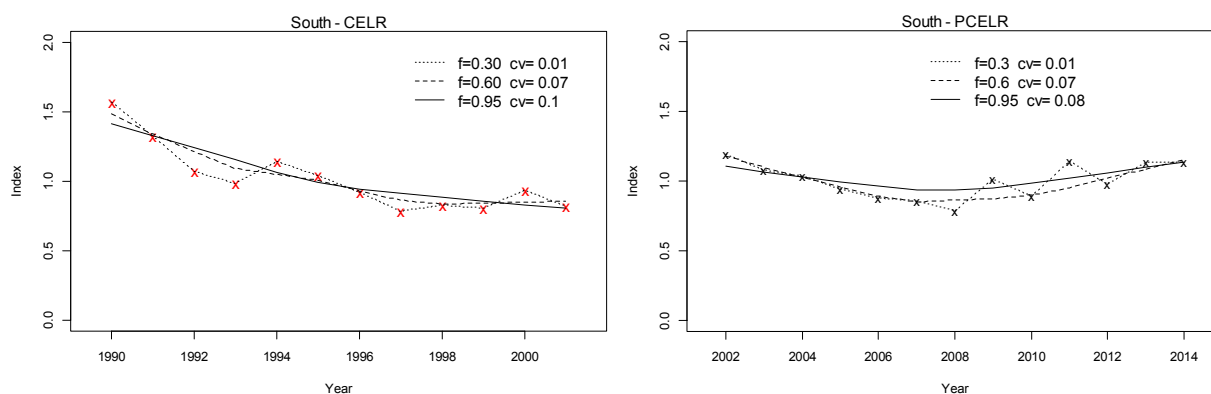
Figure A2: A series of lowess lines of various degrees of freedom (f) fitted to the PAU 5A south standardised CPUE indices for 1990–2001 (left) and for 2002–2014 (right). CVs are calculated from residuals for each of the fitted lowess line. The CV of the residuals from the "appropriate" fit will be used as the CV in the stock assessment model. What is "appropriate" is judged by visual examination of lines with different degrees of smoothing.
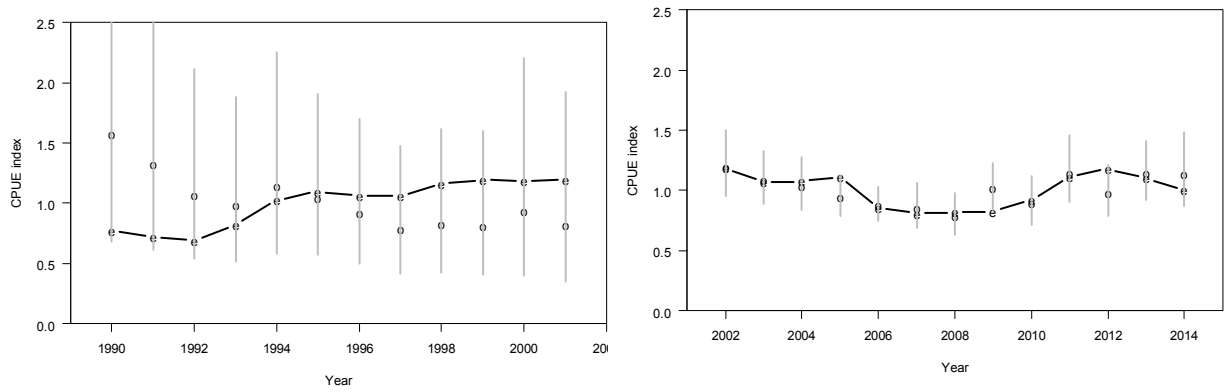
Figure A3: Fits to the CPUE 1990–2001 (left) and 2002–2014 (right) from MPD 1.0. Vertical lines represent 95% confidence interval of observed CPUE.
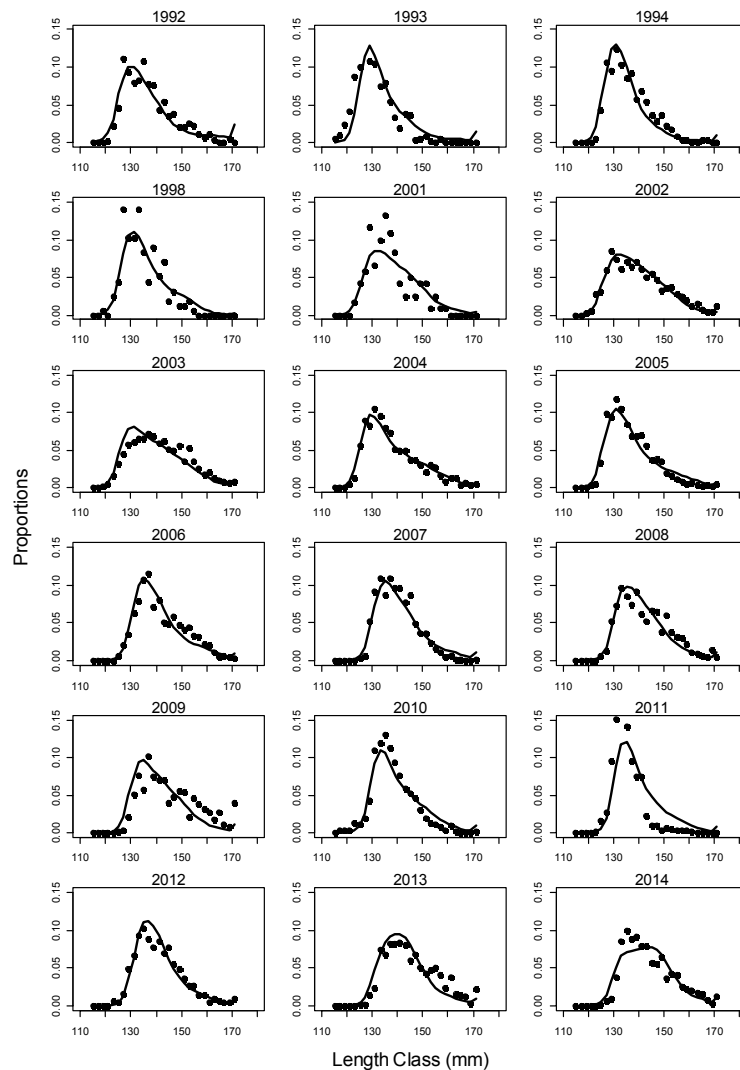
Figure A4: Fits to the CSLF 1992–2014 for MPD 1.0. Lines are predicted values and dots are observed values.
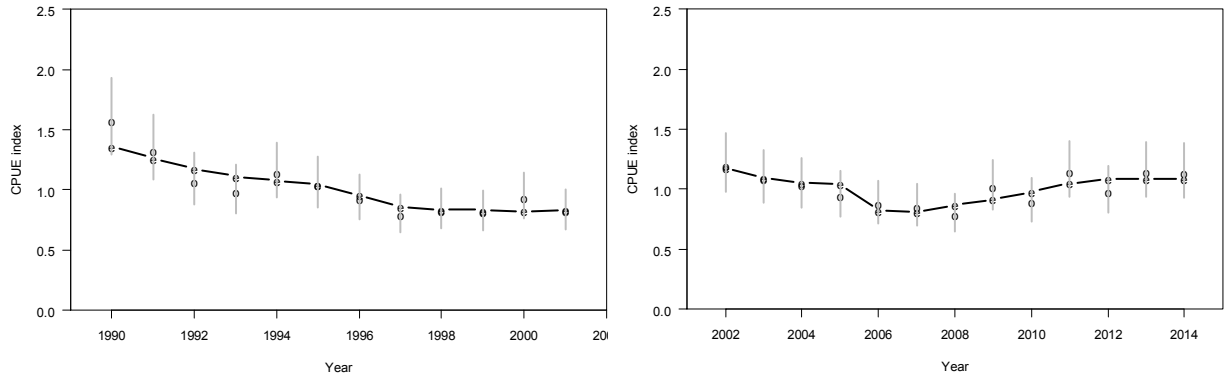
Figure A5: Fits to the CPUE 1990–2001 (left) and 2002–2014 (right) from MPD 1.1. Vertical lines represent 95% confidence interval of observed CPUE.
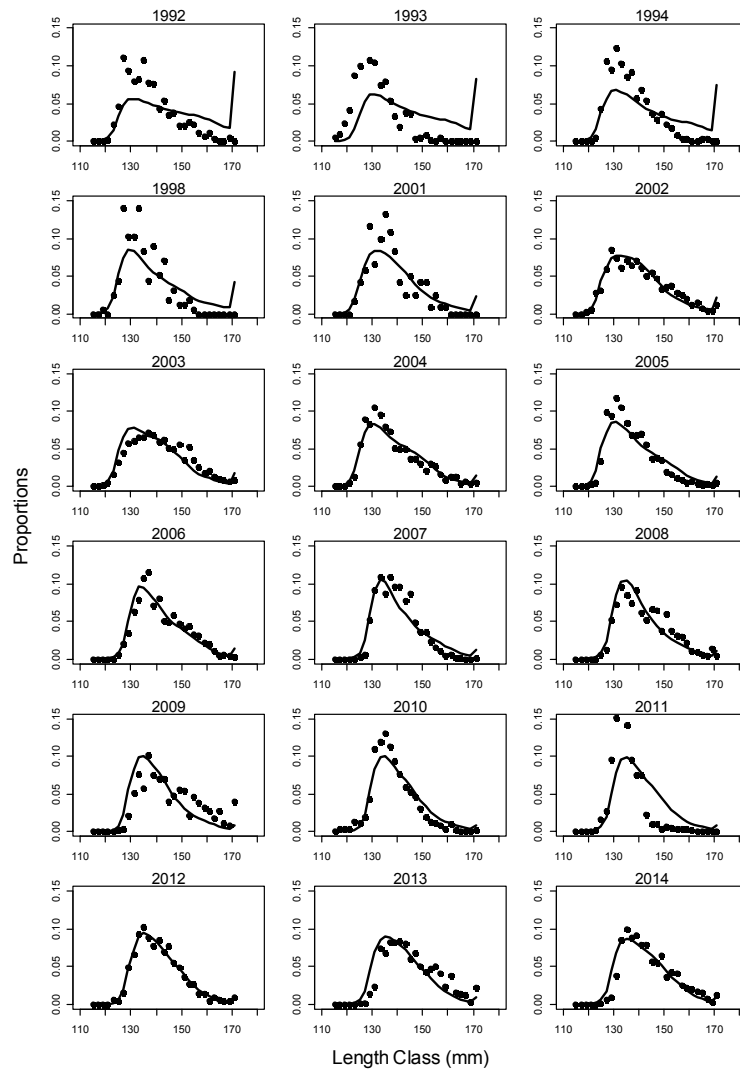
Figure A6: Fits to the CSLF 1992–2014 for MPD 1.1. Lines are predicted values and dots are observed values.
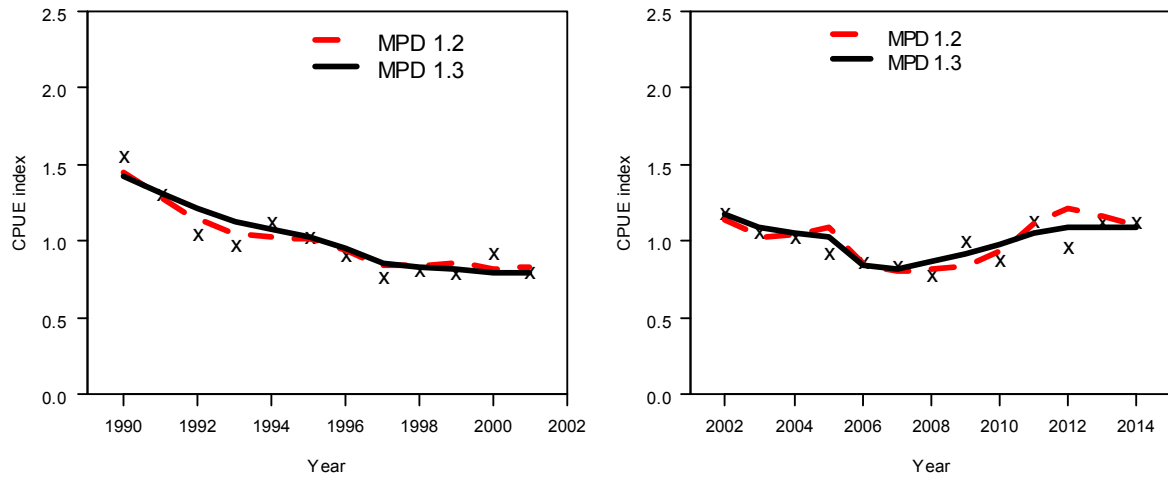
Figure A7: Comparison of fits to the CPUE 1990–2001 (left) and 2002–2014 for MPD 1.2 and MPD 1.3.
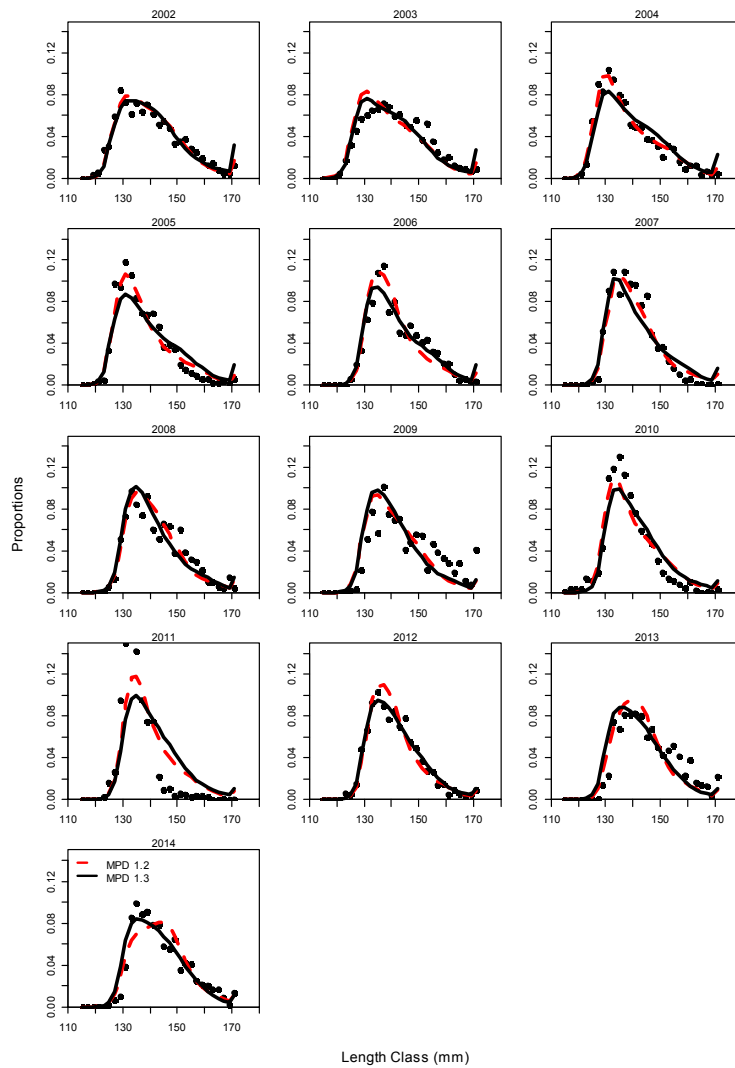
Figure A8: Comparison of fits to the CSLF 2002–2014 for MPD 1.2 and MPD 1.3.
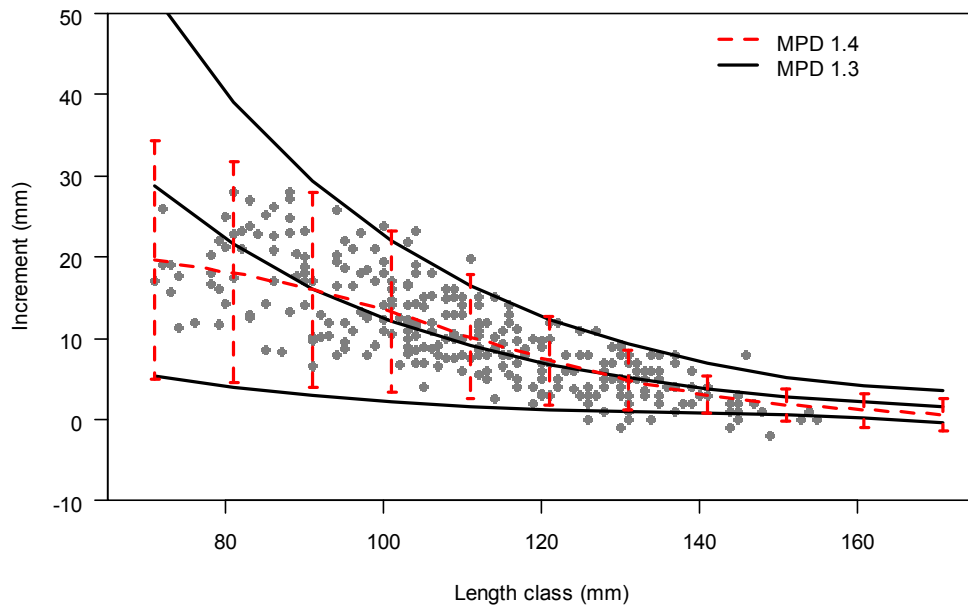
Figure A9: Comparison of estimated growth curve with confidence intervals for MPD 1.3 (exponential growth model) and MPD 1.4 (inverse-logistic growth model).
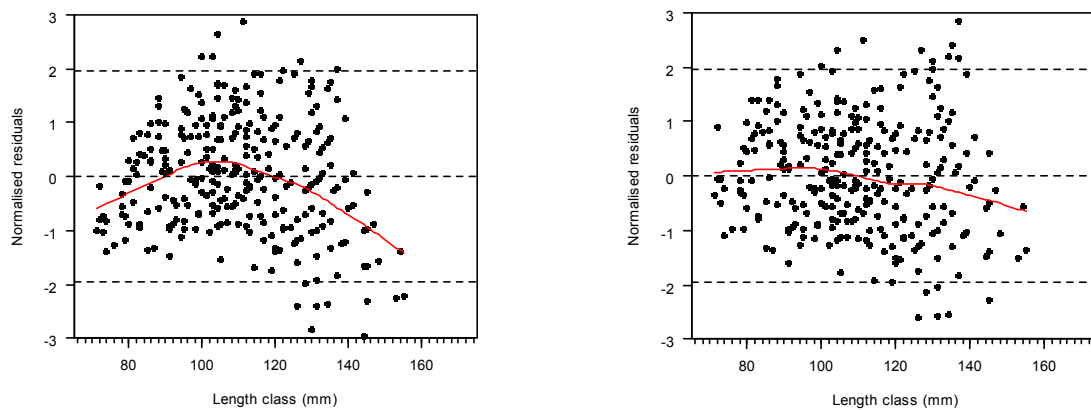
Figure A10: Comparison of residuals from fits to growth data for MPD 1.3 (exponential growth model) and MPD 1.4 (inverse-logistic growth model).
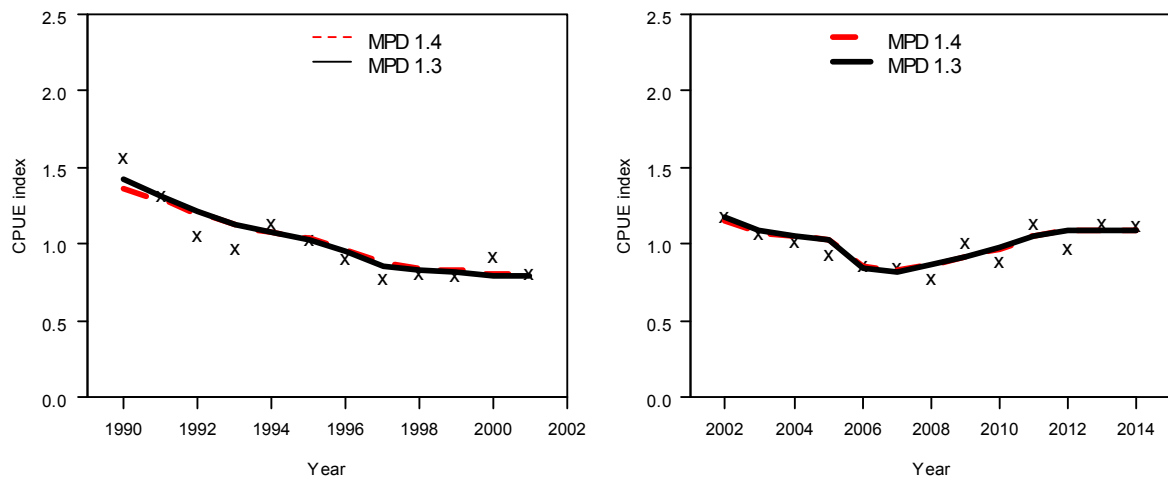
Figure A11: Comparison of fits to the CPUE 1990–2001 (left) and 2002–2014 for MPD 1.3 and MPD 1.4.
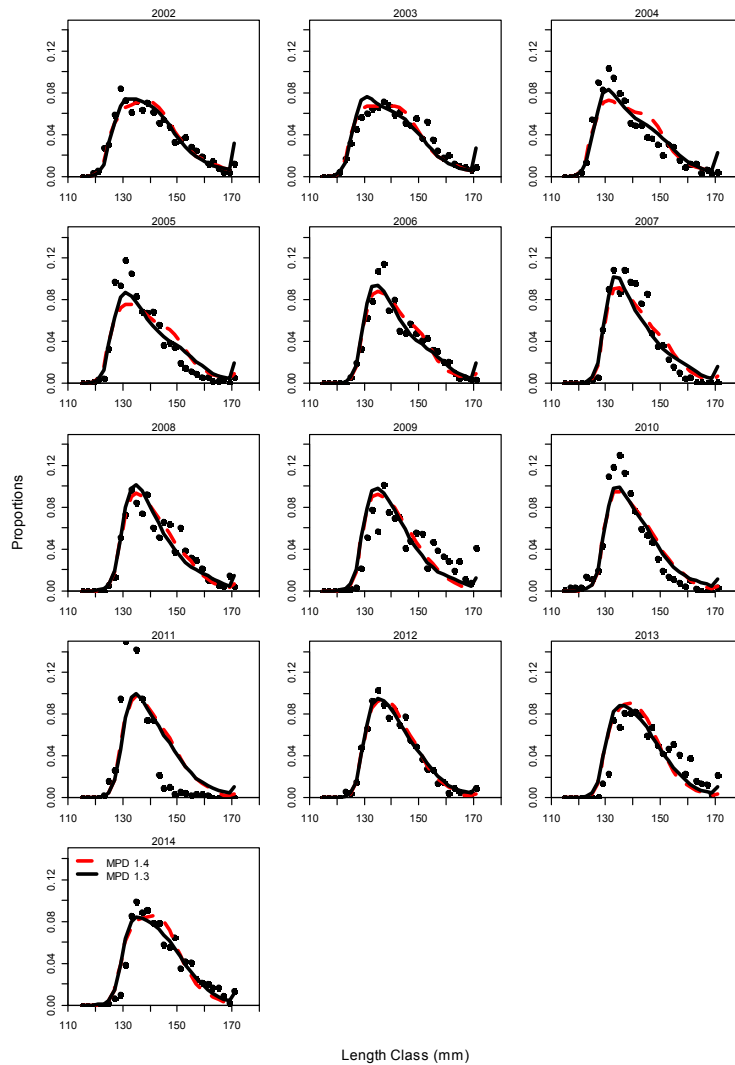
Figure A12: Comparison of fits to the CSLF 2002–2014 for MPD 1.3 and MPD 1.4.
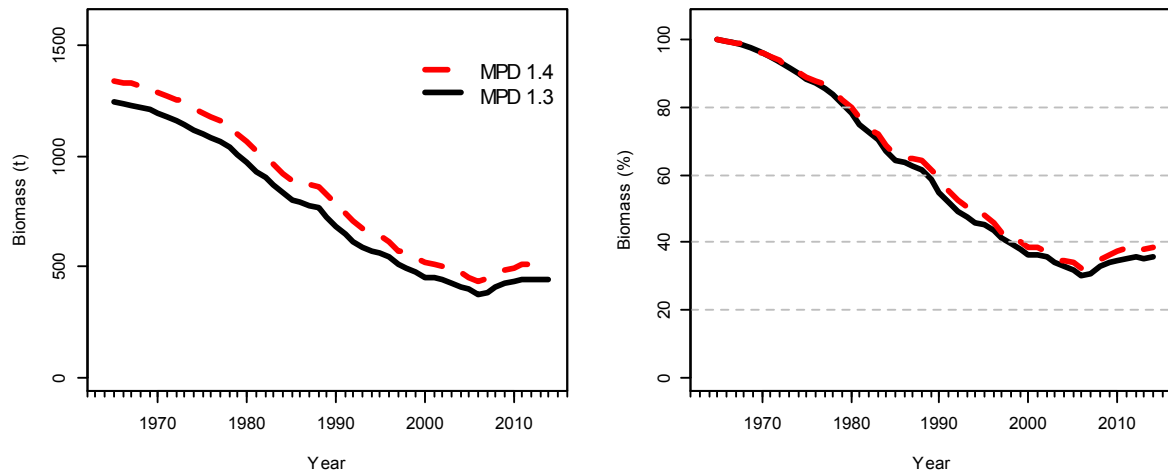
Figure A13: Comparison of estimated spawning biomass (left) and spawning biomass as a percent of B$_0$ to the CSLF 2002–2014 for MPD 1.3 and MPD 1.4.
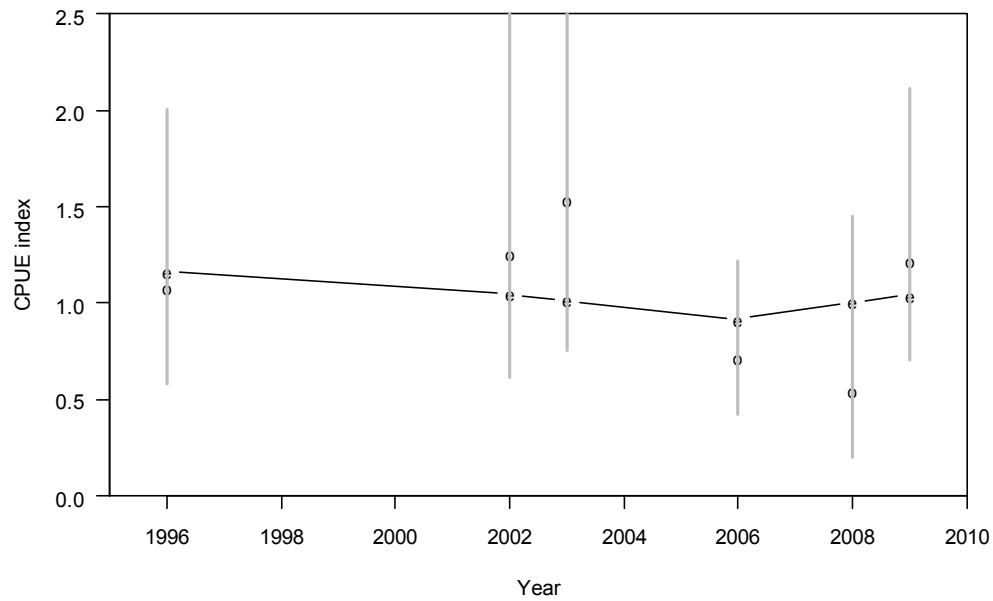
Figure A14: Fits to the RDSI from MPD 2.0. Vertical lines represent 95% confidence interval of observed RDSI.
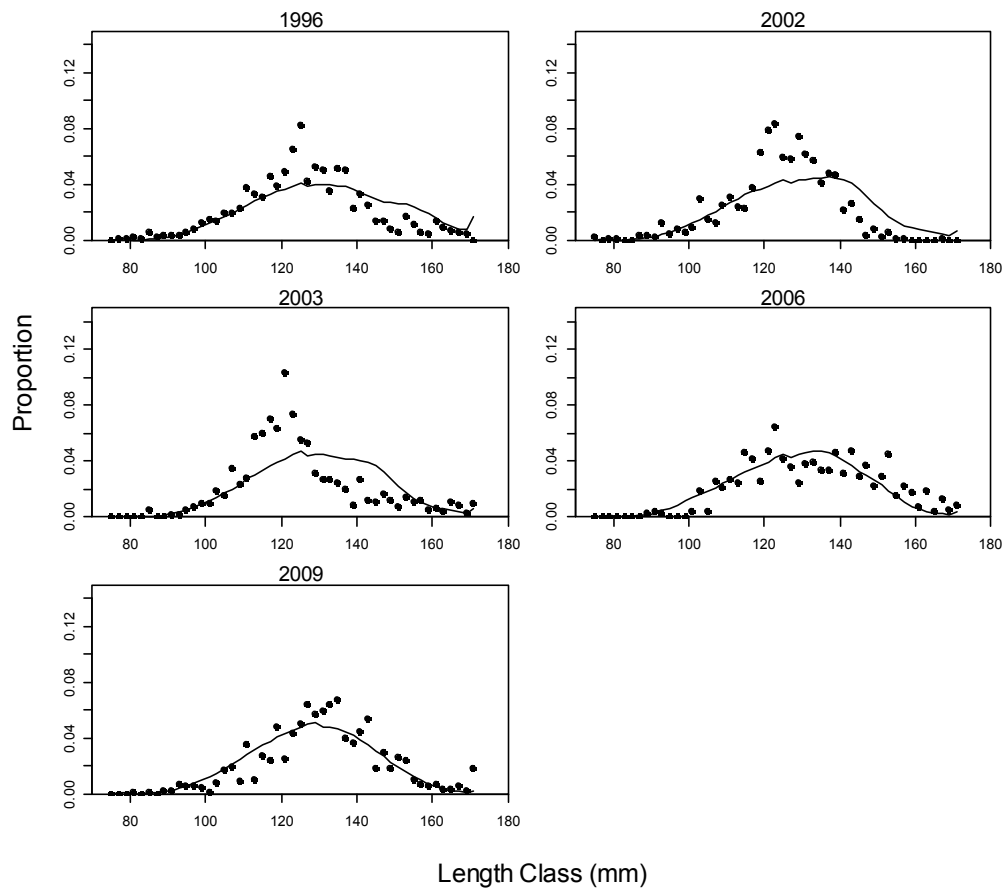
Figure A15: Fits to the RDLF from MPD 2.0. Lines represent predicted values and dots represent observed values.

APPENDIX B: SUMMARY OF RESULTS FOR MCMC SENSITIVITY
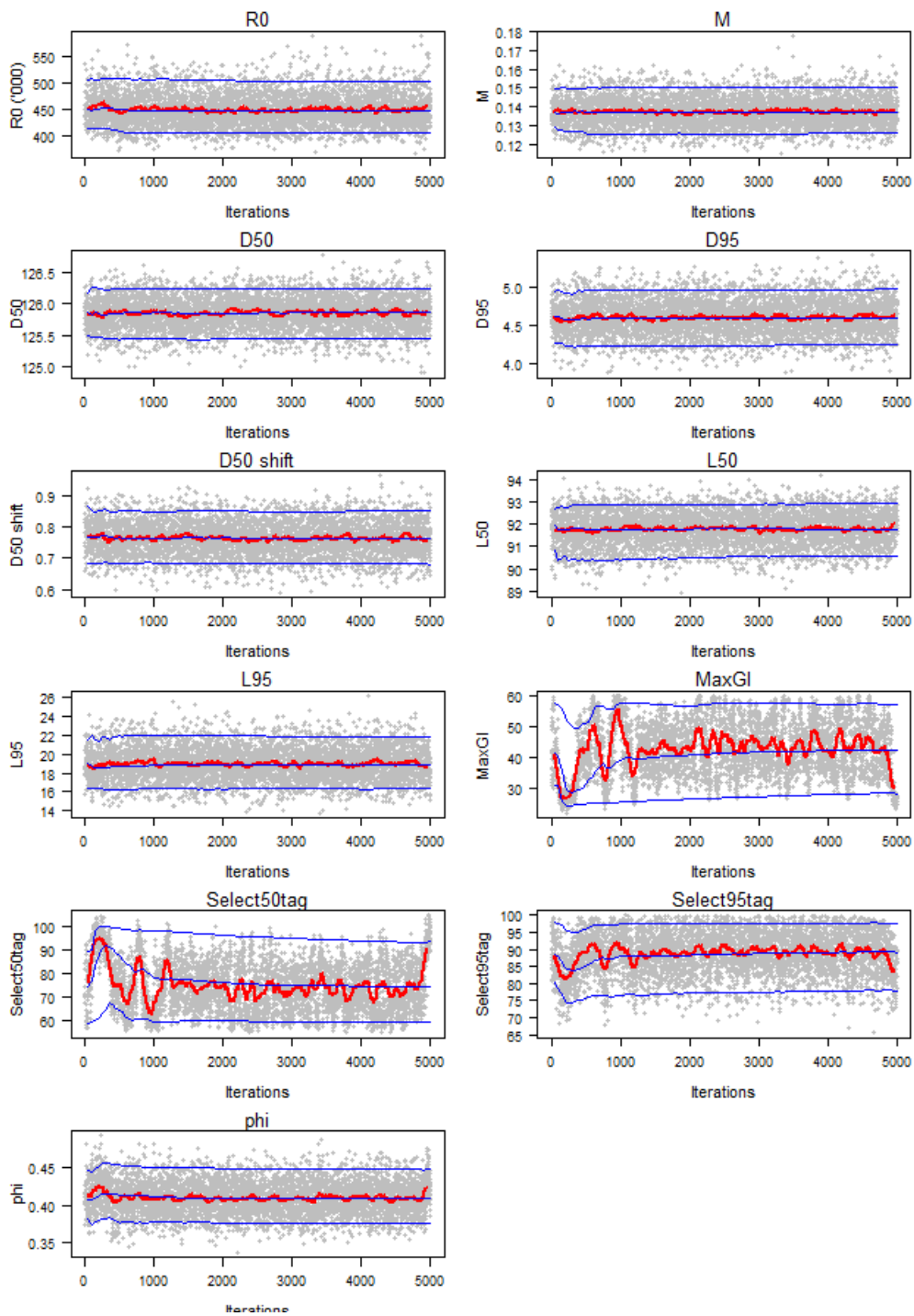
Figure B1: Traces of estimated parameters (left) and biomass indicators (right) for base case MCMC 1.6. Blue lines are running 5, 50, and 95% quantiles of the chain and red lines are the moving average of the chain.
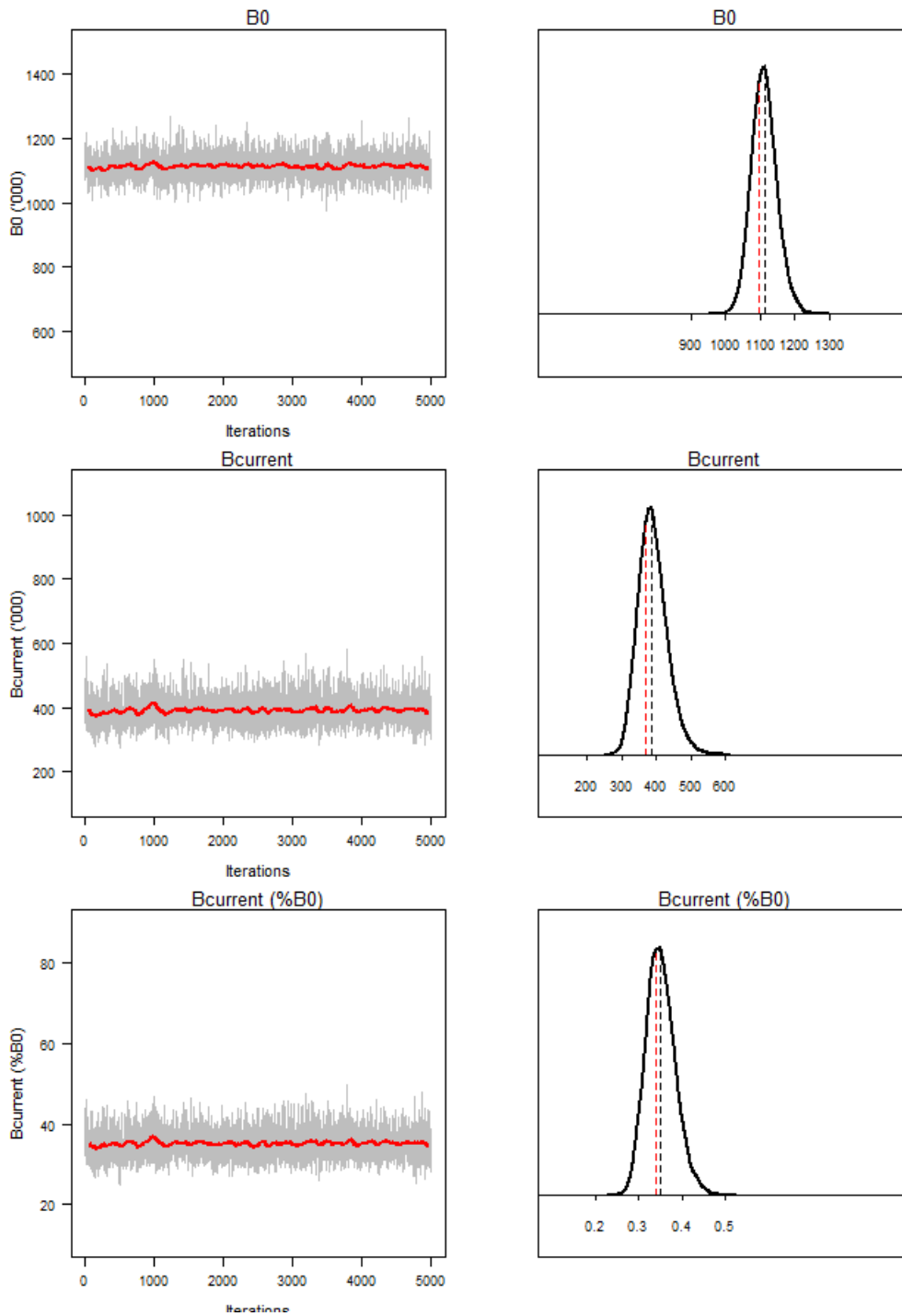
Figure B2: Traces (left) and posterior density (right) of estimated B_0, $B_{current}$, and $B_{current}$ as a percent of B_0 for MCMC 1.6 . The red lines are the moving average of the chain; black dashed lines indicate median of the posterior distribution and red dashed lines indicate the MPD estimate.
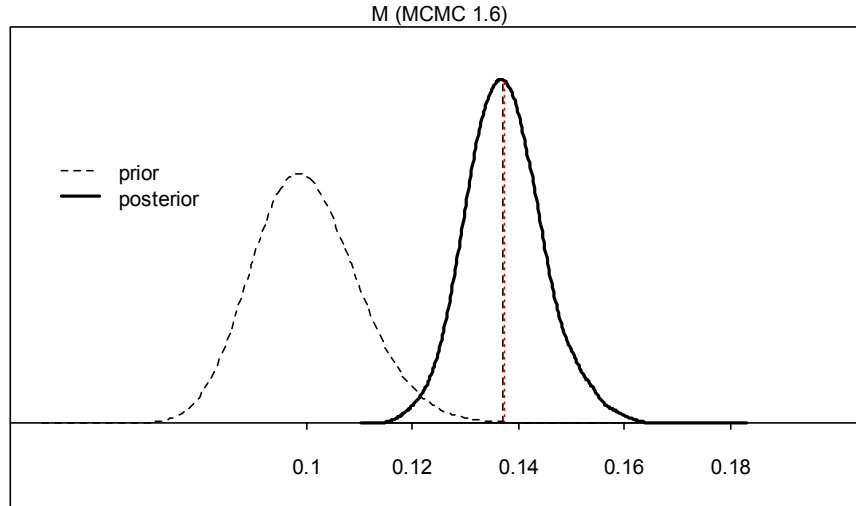
Figure B3: Posterior and prior distributions of estimated natural mortality (M) for MCMC 1.6. The black dashed vertical line is the posterior median and the red dashed vertical line is the MPD estimate.
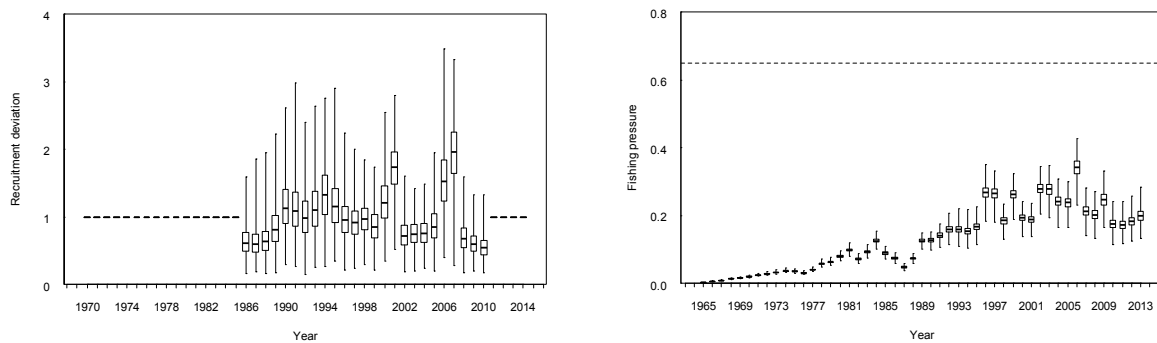
Figure B4: Posterior distributions of recruitment deviations (left), and exploitation rates (right) for MCMC 1.6. The box shows the median of the posterior distribution (horizontal bar), the 25th and 75th percentiles (box), with the whiskers representing the full range of the distribution. Recruitment deviations were estimated for 1986–2008, and fixed at 1 for other years.
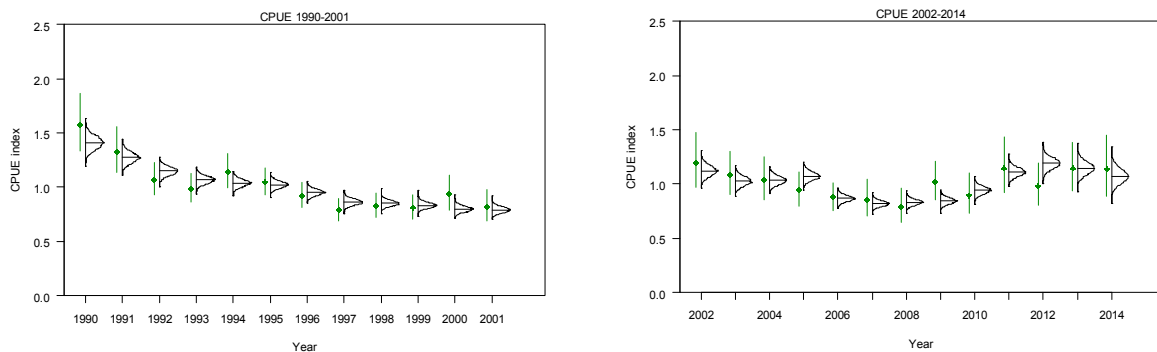
Figure B5: Posterior distributions of model predicted CPUE indices for 1990–2001 (left) and 2002–2012 (right) for MCMC 1.6 (medians are shown as horizontal lines). Dots are observed CPUE indices and vertical lines are 95% confidence intervals.
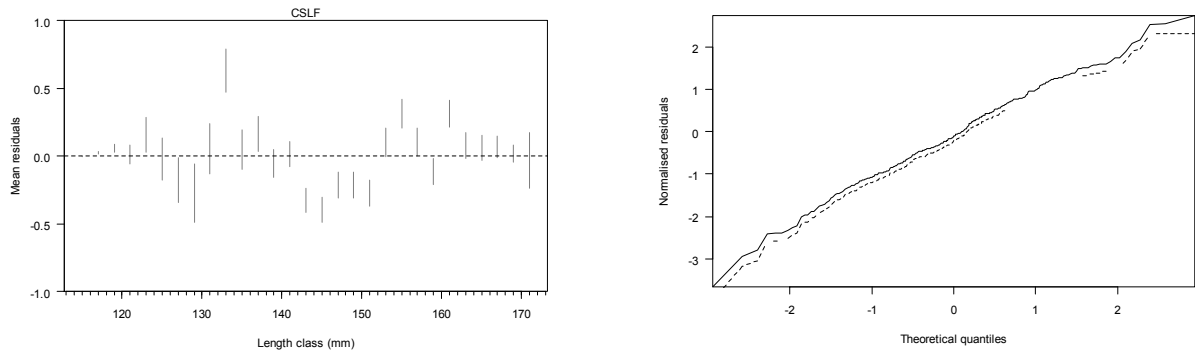
Figure B6: 95% credible intervals of the posterior distributions of mean residuals (across all years) of fits to the CSLF data (left) and the QQ quantiles of posterior distributions of residuals of fits to the tag recapture data (right) from MCMC 1.6.
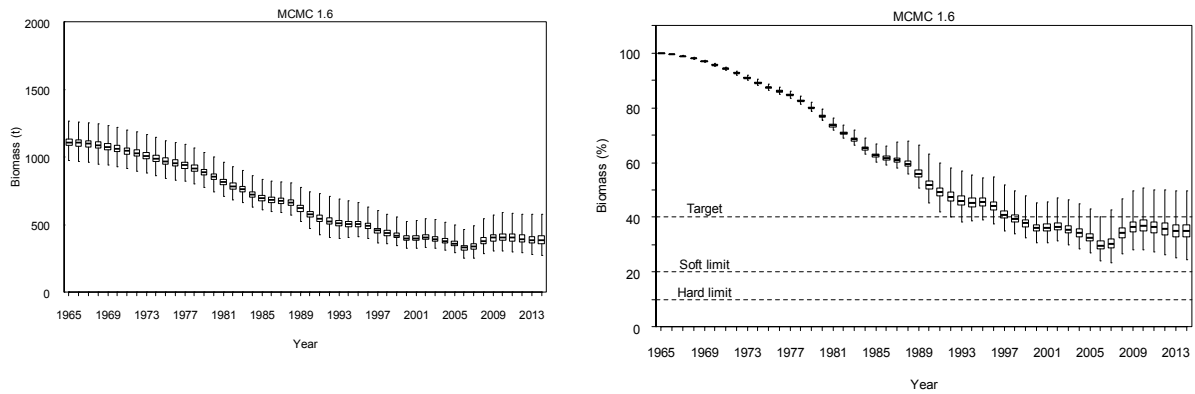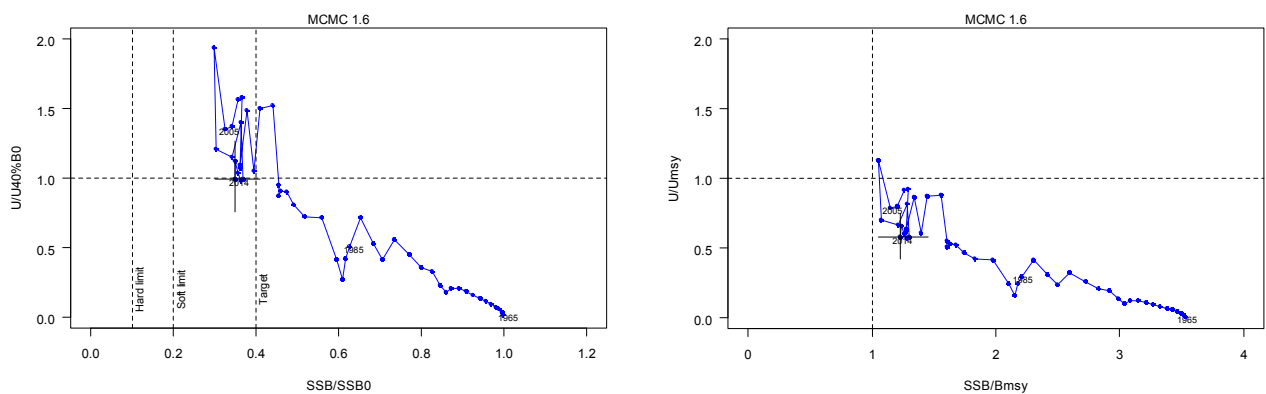

Figure B7: Posterior distributions of spawning stock biomass and spawning stock biomass as a percentage of virgin level from MCMC 1.6. The box shows the median of the posterior distribution (horizontal bar), the 25th and 75th percentiles (box), with the whiskers representing the full range of the distribution.

Figure B8: Trajectory of exploitation rate as a ratio of $U_{\%40B0}$ and spawning stock biomass as a ratio of B_0 (left), and exploitation rate as a ratio of U_{msy} and spawning stock biomass as a ratio of B_{msy} from the start of assessment period 1965 to 2014 for MCMC 1.6. The vertical lines at 10%, 20% and 40% B_0 represent the soft limit, the hard limit, and the target. Estimates are based on MCMC median and the 2014 90% CI is shown by the cross line.
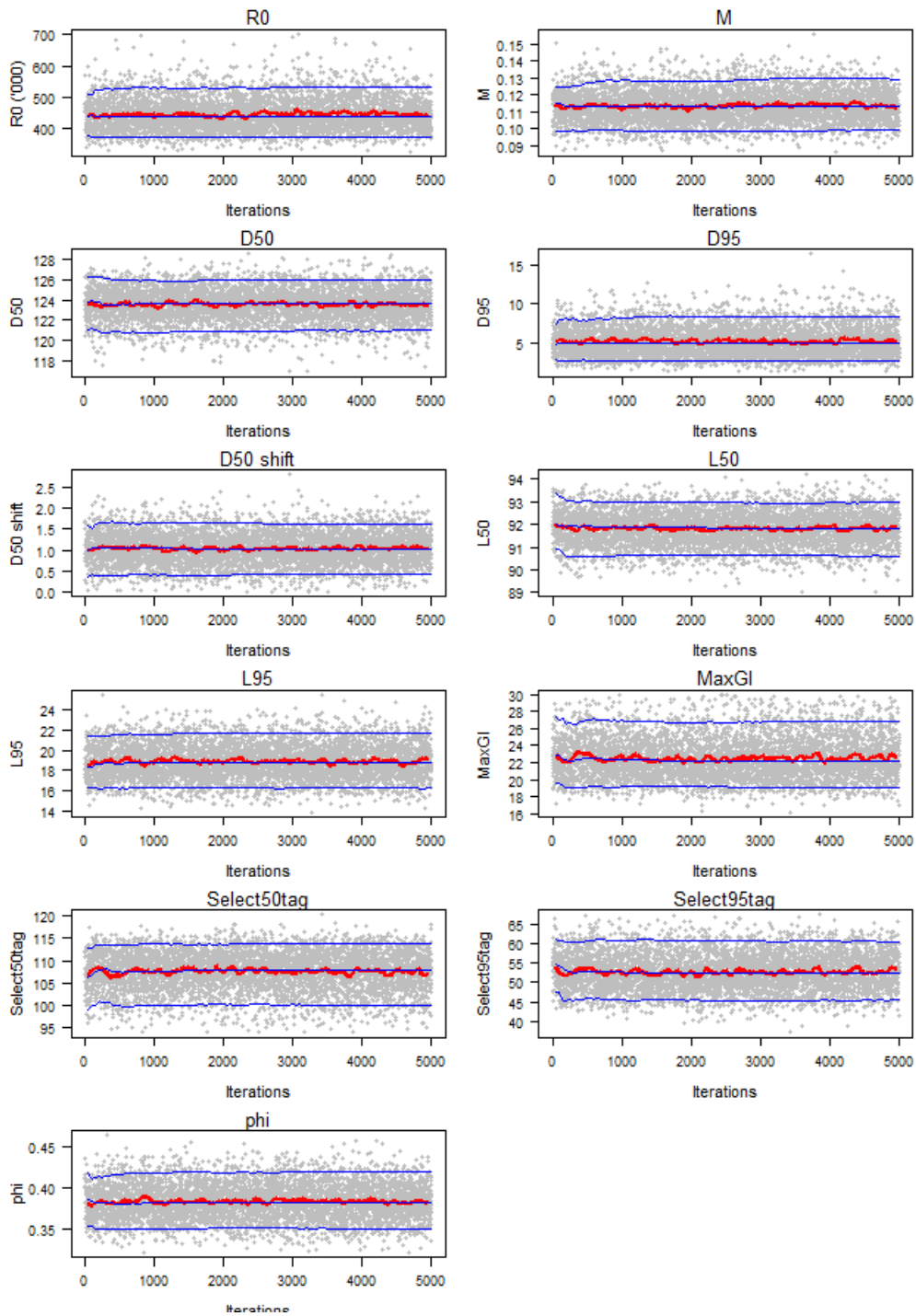
Figure B9: Traces of estimated parameters (left) and biomass indicators (right) for base case MCMC 1.7. Blues lines are running 5, 50, and 95% quantiles of the chain and red lines are the moving average of the chain.
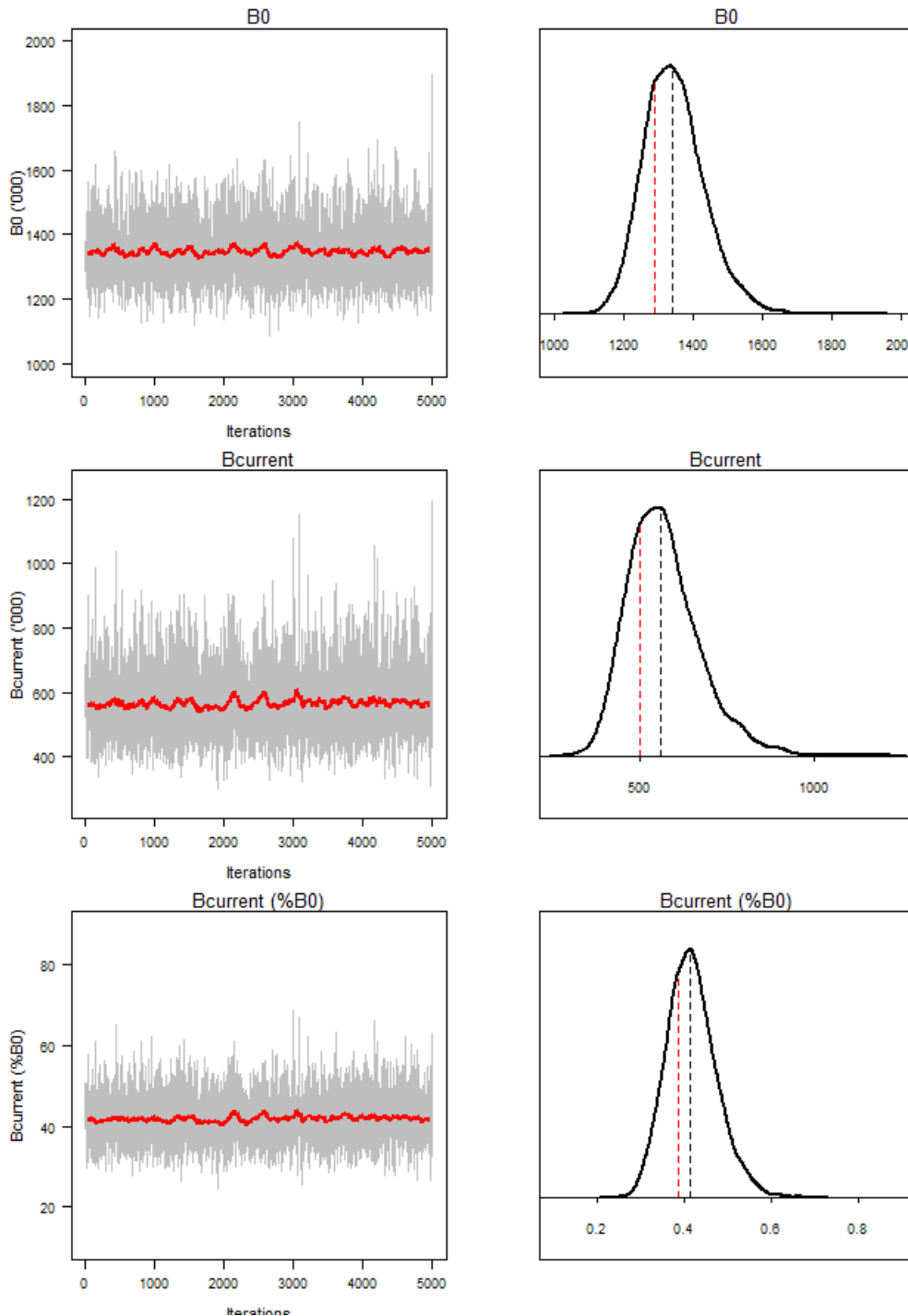
Figure B10: Traces (left) and posterior density (right) of estimated B₀, B_current, and B_current as a percent of B₀ for MCMC 1.7 . The red lines are the moving average of the chain; black dashed lines indicate median of the posterior distribution and red dashed lines indicate the MPD estimate.
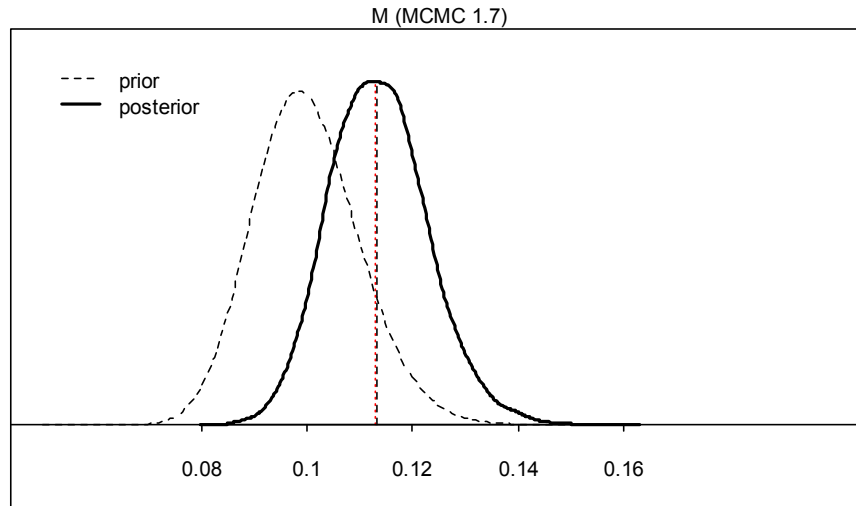
Figure B11: Posterior and prior distributions of estimated natural mortality (M) for MCMC 1.7. The black dashed vertical line is the posterior median and the red dashed vertical line is the MPD estimate.
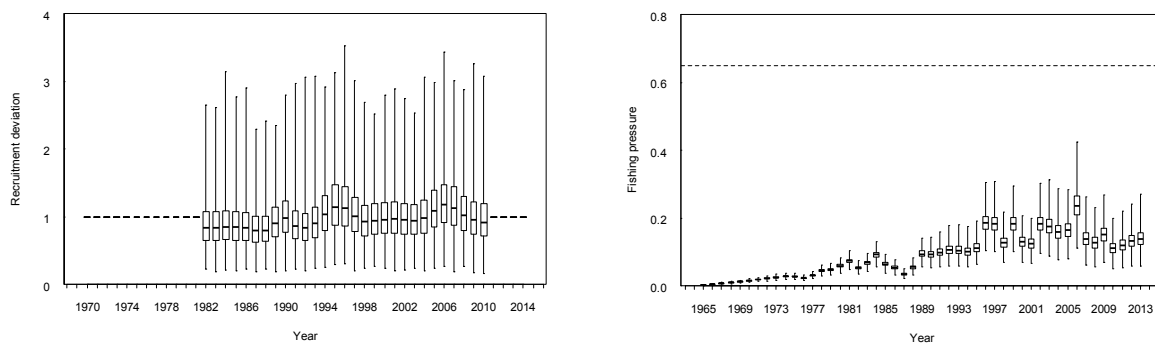

Figure B12: Posterior distributions of recruitment deviations (left), and exploitation rates (right) for MCMC 1.7. The box shows the median of the posterior distribution (horizontal bar), the 25th and 75th percentiles (box), with the whiskers representing the full range of the distribution. Recruitment deviations were estimated for 1986–2008, and fixed at 1 for other years.
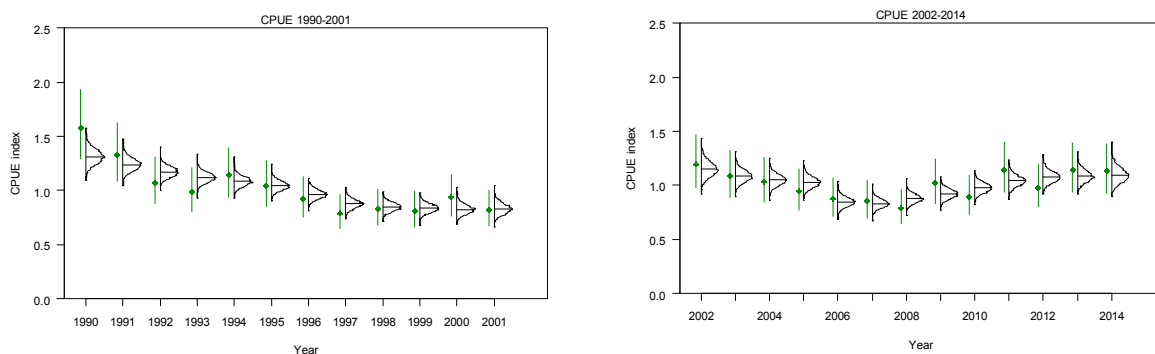

Figure B13: Posterior distributions of model predicted CPUE indices for 1990–2001 (left) and 2002–2012 (right) for MCMC 1.7 (medians are shown as horizontal lines). Dots are observed CPUE indices and vertical lines are 95% confidence intervals.
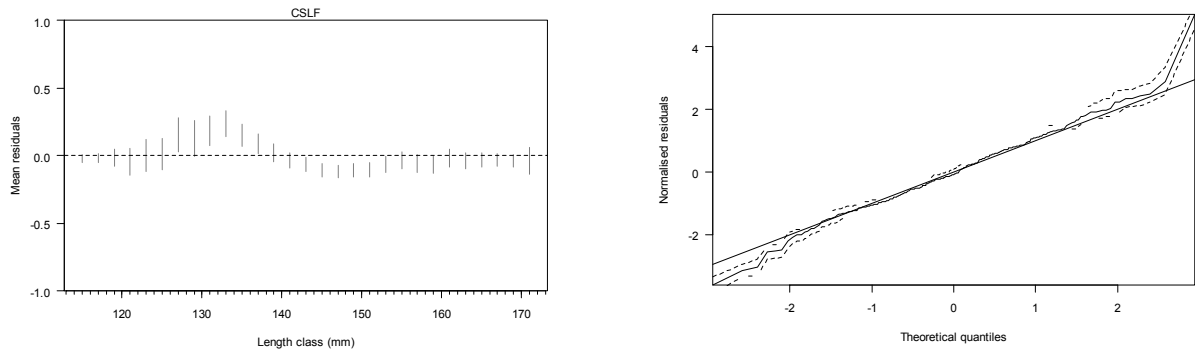
Figure B14: 95% credible intervals of the posterior distributions of mean residuals (across all years) of fits to the CSLF data (left) and the QQ quantiles of posterior distributions of residuals of fits to the tag recapture data (right) from MCMC 1.7.
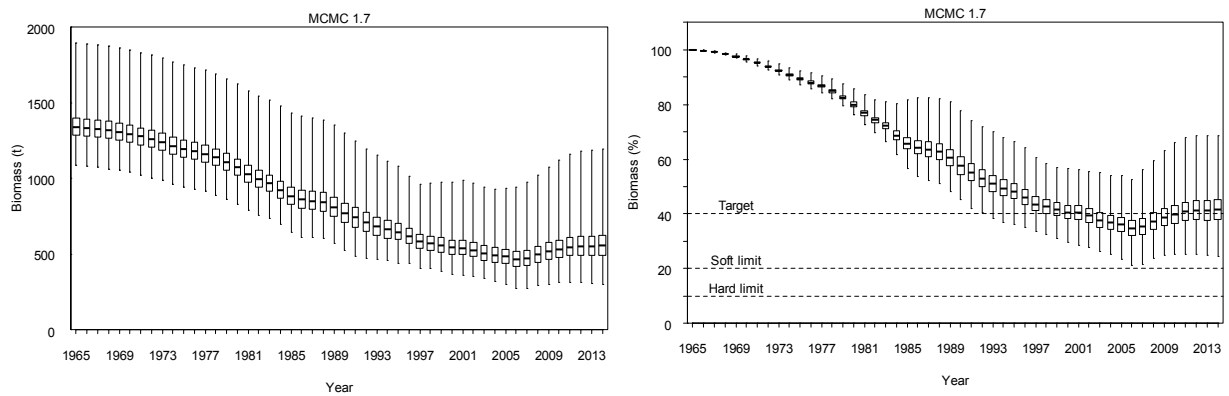

Figure B15: Posterior distributions of spawning stock biomass and spawning stock biomass as a percentage of virgin level from MCMC 1.6. The box shows the median of the posterior distribution (horizontal bar), the 25th and 75th percentiles (box), with the whiskers representing the full range of the distribution.
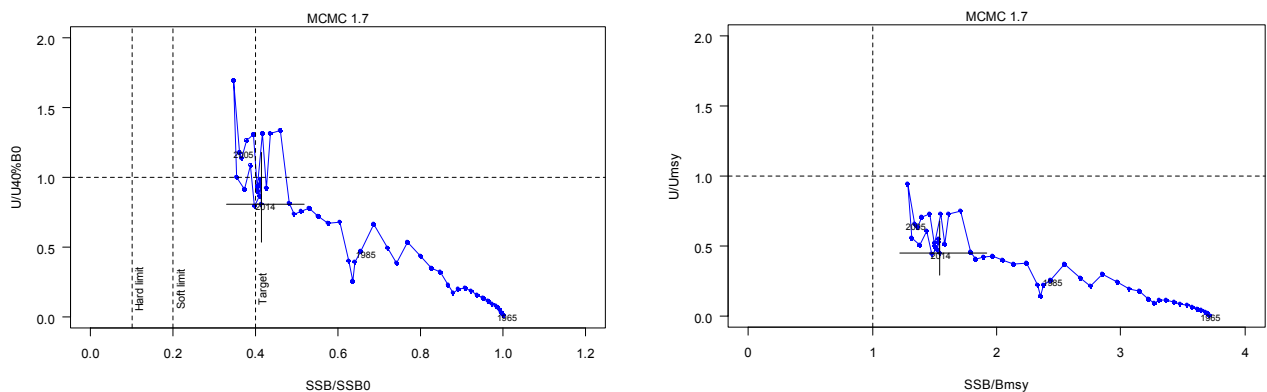

Figure B16: Trajectory of exploitation rate as a ratio of $U_{\%40B0}$ and spawning stock biomass as a ratio of B_0 (left), and exploitation rate as a ratio of U_{msy} and spawning stock biomass as a ratio of B_{msy} from the start of assessment period 1965 to 2014 for MCMC 1.7. The vertical lines at 10%, 20% and 40% B_0 represent the soft limit, the hard limit, and the target. Estimates are based on MCMC median and the 2014 90% CI is shown by the cross line.

APPENDIX C: SUMMARY OF PROJECTIONS FOR MCMC SENSITIVITY

Table C1: Summary of key indicators from the projection for MCMC 1.6 with future commercial catch assumed to be the same the current catch: projected biomass as a percentage of the virgin and current stock status, for spawning stock and recruit-sized biomass.

				Year
	2014	2015	2016	2017
$B_{proj} \% B_0$	0.35 (0.29 –0.42)	0.35 (0.30 –0.43)	0.36 (0.30 –0.44)	0.37 (0.29 –0.48)
$B_{proj} \% B_{msy}$	1.23 (1.03 –1.50)	1.25 (1.04 –1.53)	1.27 (1.04 –1.58)	1.29 (1.03 –1.66)
$Pr(> B_{msy})$	0.99	0.99	0.99	0.98
$Pr(> B_{current})$	0.00	1.00	0.87	0.71
$Pr(> 40\% B_0)$	0.08	0.11	0.16	0.24
$Pr(< 20\% B_0)$	0.00	0.00	0.00	0.00
$Pr(< 10\% B_0)$	0.00	0.00	0.00	0.00
$\% B_0^r$	0.25 (0.120 –0.31)	0.24 (0.19 –0.31)	0.24 (0.19 –0.31)	0.25 (0.19 –0.32)
$\% B_{msy}^r$	1.54 (1.14 –2.17)	1.49 (1.09 –2.13)	1.51 (1.10 –2.15)	1.54 (1.12 –2.20)
$Pr(> B_{msy}^r)$	1.00	0.99	0.99	1.00
$Pr(> B_{current}^r)$	0.00	0.06	0.21	0.59
$Pr(U_{proj} > U_{40\% B0})$	0.48	0.55	0.53	0.47

Table C2: Summary of key indicators from the projection for MCMC 1.7 with future commercial catch assumed to be the same the current catch: projected biomass as a percentage of the virgin and current stock status, for spawning stock and recruit-sized biomass.

				Year
	2014	2015	2016	2017
$B_{proj} \% B_0$	0.42 (0.32 –0.54)	0.42 (0.32 –0.55)	0.43 (0.32 –0.56)	0.43 (0.32 –0.57)
$B_{proj} \% B_{msy}$	1.54 (1.17 –2.01)	1.56 (1.18 –2.04)	1.58 (1.19 –2.07)	1.61 (1.20 –2.12)
$Pr(> B_{msy})$	1.00	1.00	1.00	1.00
$Pr(> B_{current})$	0.00	1.00	0.98	0.90
$Pr(> 40\% B_0)$	0.61	0.65	0.68	0.72
$Pr(< 20\% B_0)$	0.00	0.00	0.00	0.00
$Pr(< 10\% B_0)$	0.00	0.00	0.00	0.00
$\% B_0^r$	0.32 (0.23 –0.44)	0.32 (0.23 –0.45)	0.33 (0.23 –0.46)	0.33 (0.23 –0.46)
$\% B_{msy}^r$	1.91 (1.28 –2.91)	1.95 (1.29 –2.98)	1.98 (1.30 –3.01)	2.02 (1.32 –3.05)
$Pr(> B_{msy}^r)$	1.00	1.00	1.00	1.00
$Pr(> B_{current}^r)$	0.00	0.74	0.83	0.93
$Pr(U_{proj} > U_{40\% B0})$	0.18	0.16	0.15	0.14